Titre: Title:	Méthode des éléments finis hybride appliquée aux vibrations des coques sphériques
Auteur: Author:	Mohamed Menaa
Date:	2013
Type:	Mémoire ou thèse / Dissertation or Thesis
Référence: Citation:	Menaa, M. (2013). Méthode des éléments finis hybride appliquée aux vibrations des coques sphériques [Ph.D. thesis, École Polytechnique de Montréal]. PolyPublie. https://publications.polymtl.ca/1222/

UNIVERSITÉ DE MONTRÉAL

MÉTHODE DES ÉLÉMENTS FINIS HYBRIDE APPLIQUÉE AUX VIBRATIONS DES COQUES SPHÉRIQUES

MOHAMED MENAA

DÉPARTEMENT DE GÉNIE MÉCANIQUE

ÉCOLE POLYTECHNIQUE DE MONTRÉAL

THÈSE PRÉSENTÉE EN VUE DE L'OBTENTION

DU DIPLÔME DE PHILOSOPHIAE DOCTOR

(GÉNIE MÉCANIQUE)

AOÛT 2013

UNIVERSITÉ DE MONTRÉAL

ÉCOLE POLYTECHNIQUE DE MONTRÉAL

Cette thèse intitulée:

MÉTHODE DES ÉLÉMENTS FINIS HYBRIDE APPLIQUÉE AUX VIBRATIONS DES COQUES SPHÉRIQUES

présentée par : MENAA Mohamed

en vue de l'obtention du diplôme de : Philosophiae Doctor

a été dûment acceptée par le jury d'examen constitué de :

M. BALAZINSKI Marek, Doct., président

M. LAKIS Aouni A., Ph.D., membre et directeur de recherche

M. MAYER René, Ph.D., membre

M. NEJAD ENSAN Manouchehr, Ph.D., membre

DÉDICACE

À mes chers parents

À ma sœur

À ma chère femme

REMERCIEMENTS

Je tiens à présenter mes profonds remerciements et ma gratitude à mon directeur de recherche, Dr Aouni Lakis, pour sa précieuse orientation, ses encouragements et conseils tout au long de la période pendant laquelle il m'a accueilli dans son laboratoire pour mener à terme mes recherches à dessein d'obtenir mon diplôme de doctorat au sein de l'École Polytechnique de Montréal.

Qui plus est, je voudrais exprimer sincères mes remerciements aux membres du jury de ma thèse :

Dr. Marek Balazinski

Dr. Aouni A. Lakis

Dr. Manouchehr Nejad Ensan

Dr. René Mayer

pour le temps consacré à l'évaluation de mon travail de recherche et aussi à leurs suggestions.

Je saisis cette occasion pour remercier chaleureusement ma femme pour son soutien tout au long du processus de préparation de ce travail de recherche.

RÉSUMÉ

L'analyse des coques sphériques remplies de fluide et soumises à un écoulement supersonique a été l'objet de peu de recherches. Un nombre limité de travaux a été consacré à l'analyse des coques sphériques remplies de fluide ou sous l'effet du flottement supersonique. Dans cette thèse, nous élaborons un modèle capable d'analyser le comportement dynamique des coques sphériques à vide, partiellement remplies de liquide ou soumises à un écoulement supersonique.

La méthode développée est une combinaison de la méthode des éléments finis, de la théorie des coques minces, de la théorie potentielle du fluide et de la théorie aérodynamique du fluide. Différents paramètres seront considérés dans l'étude.

Dans la première partie de l'étude, l'analyse vibratoire des coques sphériques a été menée. Le modèle structural est basé sur une combinaison de la théorie des coques minces sphériques et de la méthode des éléments finis classique. Les équations de mouvement utilisant la méthode des éléments finis hybride ont été dérivées et résolues numériquement. Les résultats ont été validés en utilisant les données numériques et théoriques disponibles dans la littérature. L'analyse a été accomplie pour des coques sphériques de différentes géométries, différentes conditions aux rives et plusieurs rapports rayon-épaisseur. La méthode des éléments finis hybride peut être utilisée efficacement pour la conception et l'analyse des coques sphériques utilisées dans les structures des aéronefs à haute vitesse.

Dans la seconde partie de cette étude, une méthode des éléments finis hybride a été appliquée pour l'étude des vibrations libres des coques sphériques remplies de liquide. Le modèle structural est basé sur une combinaison de la théorie des coques minces et de la méthode des éléments finis classique. Nous supposons un fluide incompressible. Les fréquences naturelles pour différentes taux de remplissage sont obtenues et comparées aux données théoriques et expérimentales qui existent dans la littérature. Le comportement dynamique pour différentes géométries, taux de remplissage et conditions aux limites avec différents rapports rayon-épaisseur a été élucidé. Cette méthode des éléments finis hybride peut être utilisée efficacement dans l'analyse du comportement dynamique des structures aérospatiales avec un moindre effort de calcul et de meilleures précisions que les logiciels commerciaux utilisant la méthode des éléments finis classique.

Dans la troisième partie de l'étude, l'analyse aéroélastique d'une coque sphérique soumise à un écoulement supersonique externe a été entreprise. Le modèle structural est basé sur une combinaison de la théorie linéaire des coques sphériques et la méthode des éléments finis classique. Dans cette méthode des éléments finis hybride, les déplacements nodaux ont été trouvés à partir de la solution exacte des équations de la coque sphérique plutôt que des fonctions polynomiales. La théorie potentielle du piston du premier ordre, avec effet de correction de courbure, a été couplée avec le modèle structural pour tenir compte de la pression sur la coque. Les matrices linéaires de masse, de rigidité et d'amortissement ont été formulées à partir de la méthode des éléments finis hybride. Les équations aéroélastiques ont été déduites et résolues numériquement. Les résultats obtenus ont été validés à l'aide des données théoriques et numériques, disponibles dans la littérature. Cette analyse a été accomplie pour des coques sphériques de différentes conditions aux limites, géométries, paramètres d'écoulement et différents rapports rayon-épaisseur de la coque. Les résultats montrent que la coque perd sa stabilité dynamique à travers un flottement avec modes couplés. Cette méthode des éléments finis hybride peut être utilisée efficacement pour l'analyse et la conception de coques sphériques employées dans les structures des aéronefs à haute vitesse.

ABSTRACT

The analysis of spherical shells filled with fluid and subjected to supersonic flow has been the subject of few research. Most of these studies treat the dynamic behaviour of empty shells. Few works have investigated spherical shells filled with fluid or subjected to supersonic flutter.

In this thesis, we propose to develop a model to analyse the vibratory behaviour of both empty spherical shells and partially filled with fluid. This model is also applicable to study of the dynamic stability of spherical shells subjected to supersonic flow.

The model developed is a combination of finite element method, thin shell theory, potential fluid theory and aerodynamic fluid theory. Different parameters are considered here in this study.

In the first part of this study, free vibration analysis of spherical shell is carried out. The structural model is based on a combination of thin shell theory and the classical finite element method. Free vibration equations using the hybrid finite element formulation are derived and solved numerically. The results are validated using numerical and theoretical data available in the literature. The analysis is accomplished for spherical shells of different geometries, boundary conditions and radius to thickness ratios. This proposed hybrid finite element method can be used efficiently for design and analysis of spherical shells employed in high speed aircraft structures.

In the second part of the present study, a hybrid finite element method is applied to investigate the free vibration of spherical shell filled with fluid. The structural model is based on a combination of thin shell theory and the classical finite element method. It is assumed that the fluid is incompressible and has no free-surface effect. Fluid is considered as a velocity potential variable at each node of the shell element where its motion is expressed in terms of nodal elastic displacement at the fluid-structure interface. Numerical simulation is done and vibration frequencies for different filling ratios are obtained and compared with existing experimental and theoretical results. The dynamic behavior for different shell geometries, filling ratios and boundary conditions with different radius to thickness ratios is summarized. This proposed hybrid finite element method can be used efficiently for analyzing the dynamic behavior of aerospace structures at less computational cost than other commercial FEM software.

In this study, aeroelastic analysis of a spherical shell subjected to the external supersonic airflow is carried out. The structural model is based on a combination of linear spherical shell theory and

the classic finite element method. In this hybrid method, the nodal displacements are found from the exact solution of shell governing equations rather than approximated by polynomial functions. Linearized first-order potential (piston) theory with the curvature correction term is coupled with the structural model to account for pressure loading. Linear mass, stiffness and damping matrices are found using the hybrid finite element formulation. Aeroelastic equations are derived and solved numerically. The results are validated using numerical and theoretical data available in the literature. The analysis is accomplished for spherical shells of different boundary conditions, geometries, flow parameters and radius to thickness ratios. Results show that the spherical shell loses its stability through coupled-mode flutter. This proposed hybrid finite element method can be used efficiently for design and analysis of spherical shells employed in high speed aircraft structures.

TABLE DES MATIÈRES

LISTE DES TABLEAUX

LISTE DES FIGURES

INTRODUCTION

Les problèmes liés aux vibrations des structures, de type coques, sont rencontrés dans différentes branches de l'industrie dont le génie aéronautique, le génie océanique et le génie civil. Les vibrations des coques sphériques minces sont d'une importance capitale dans l'industrie aérospatiale (conception des fusées et structure des lanceurs), dans lesquelles les structures doivent avoir une masse aussi légère que possible, une résistance aussi élevée que possible, et par conséquent montraient des amplitudes de vibration grandes.

La première tentative de formuler une théorie flexionnelle des coques, à partir des équations générales d'élasticité, a été entreprise par Aron en 1874 et a été suivie en 1888 par une méthode approximative formulée par Love et connue sous le nom de la première approximation de Love. Dans son analyse des coques minces, Love a développé la première théorie qui tient compte des effets de déformations dues à la flexion et des déformations membranaires. La formulation contient des études individuelles sur les coques sphériques comprenant des cas de modes de vibrations non extensionnelles étudiés par Lord Rayleigh et des modes de vibrations membranaires étudiées par Lamb. Depuis les travaux de Love, peu d'attention a été porté sur le problème de vibration des coques en tenant compte de la flexion. Vers les années cinquante, des géométries spécifiques ont été étudiées et ce n'est que vers les années soixante, que des études plus élaborées ont été entreprises pour différentes géométries de coques.

À partir de ce moment, plusieurs théories ont été avancées. Une nouvelle dérivation des équations des coques en coordonnées orthogonales a été élaborée. Certaines théories spéciales ont aussi été élaborées : Sanders a maintenu les hypothèses originales de Love mais a développé un système d'équations produisant zéro déformation lors d'un mouvement de corps rigide. Des théories, d'ordre supérieur, ont été présentées où l'hypothèse relative à l'épaisseur de la coque a été différentiée dans la formulation. Les effets des contraintes de cisaillement transversales ont été étudiés par plusieurs auteurs. Les effets des forces d'inerties ont été inclus.

Ces théories générales ont été largement utilisées pour l'analyse statique des coques minces de différentes géométries, particulièrement les coques sphériques. Les équations de Love ont été utilisées comme base, dans l'étude des tensions dans des coques sphériques soumises à des charges arbitraires. Différents auteurs ont établi les équations qui régissent le comportement des coques peu profondes.

Plusieurs méthodes ont été développées, particulièrement pour l'analyse dynamique des coques élastiques sphériques. Ces méthodes peuvent être résumées comme suit :

1) Méthode exacte :

L'idée générale est de réduire les équations de base en un système de deux équations différentielles avec deux inconnues. Par la suite, ces deux inconnues sont supposées être séparables en des composantes spatiales et temporelles. Le système peut être résolu en termes de fonctions de Bessel ou Legendre. Certains artifices ont été inventés pour réduire le nombre d' équations générales, en fonction du type de coques sphériques (profondes ou peu profondes), de la nature des vibrations (axisymétriques ou non axisymétriques) et des effets en considération (contraintes de cisaillement, inertie longitudinale, etc.). Dans l'étude des vibrations des coques peu profondes, on choisit généralement le déplacement transversal et la fonction contrainte, comme les deux inconnues. On utilise deux variables auxiliaires pour les déplacements axial et circonférentiel en considérant les effets des inerties longitudinales, transversales et rotationnelles, ainsi que l'effet de la déformation du cisaillement transversal sur les vibrations des coques sphériques peu profondes. Pour les vibrations arbitraires des coques sphériques profondes incluant les effets des contraintes de cisaillement transversales et les effets d' inerties, il faut introduire quatre fonctions auxiliaires, deux pour les déplacements axial et circonférentiel et deux autres pour les effets particuliers considérés.

2) Méthode variationelle

Dans cette méthode, les équations régissant le comportement des coques sont combinées en une seule équation variationelle. Les différentes techniques qui sont utilisées dans cette méthode, diffèrent dans la manière de construire les solutions approximatives. La technique la plus utilisée est celle de Rayleigh–Ritz où les solutions sont choisies en deux parties : les fonctions et les constantes arbitraires ; les premières doivent satisfaire les conditions aux limites et les dernières l'équation variationelle, donc, supposant une énergie potentielle minimale. Cette technique a été utilisée pour calculer la fréquence fondamentale dans une coque sphérique simplement supportée.

3) Méthode des éléments finis

C'est une méthode numérique dont la popularité est attribuée à sa flexibilité à traiter les milieux continus à géométrie complexe et des conditions aux limites complexes. Il y a une abondante littérature sur le sujet. Cette méthode peut être définie comme un moyen d'analyse des structures. Cette méthode permet de modéliser une structure par un système idéalisé plus simple que la structure d'origine. Dans chaque élément fini, le champ de contraintes ou de déplacements est décrit par des fonctions polynomiales. Les matrices de rigidité et de masse sont déterminées alors pour chaque élément. La structure complète est construite en assemblant un nombre fini d'éléments interconnectés par un nombre fini de nœuds. La technique d'assemblage conduit aux matrices masse et rigidité globales. Les conditions aux limites sont incorporées à ces matrices pour les réduire. Finalement les contraintes, les déplacements ou les déformations et les réactions aux différents nœuds sont calculés. S'il s'agit d'un problème de vibration, les fréquences naturelles et les formes modales sont aussi calculées. La méthode des éléments finis a été largement utilisée dans l'analyse vibratoire des coques sphériques.

Les trois méthodes évoquées ci-dessus ont chacune des avantages et des inconvénients. Un des critères pour le succès d'une méthode est sa capacité à prédire aussi bien les basses fréquences naturelles que les hautes fréquences naturelles et leurs modes avec une bonne exactitude. La méthode exacte peut être considérée la plus adéquate, mais cependant, demande des manipulations analytiques laborieuses pour réduire le système d'équations différentielles initial. En plus, la solution du système final fait appel aux fonctions de Legendre dont les tables sont rarement disponibles dans la littérature particulièrement lorsque le degré est un nombre complexe, ce qui est le cas pour les vibrations des coques sphériques.

La méthode variationelle de Rayleigh-Ritz et la méthode des éléments finis ont satisfait le critère du succès évoqué ci-dessus. Qui plus est, ces méthodes conduisent à un problème aux valeurs propres symétrique, facile à résoudre sur ordinateur. La méthode des éléments finis a un autre avantage supplémentaire, en sens, qu'elle est facile à formuler et que sa convergence est insensible aux conditions aux limites. Cependant, la méthode des éléments finis classique où le champ de déplacements est décrit en termes de polynômes, exige une certaine amélioration. En effet, les fonctions polynomiales ne peuvent pas satisfaire complètement le critère de convergence, à moins qu'un grand nombre d'éléments soit utilisé.

Le but de la présente étude est de contrecarrer ce désavantage. Une méthode des éléments finis hybride a été développée où le champ de déplacement est dérivé de la théorie des coques. Cette méthode a prouvé son efficacité à analyser le comportement dynamique de différentes structures car le critère de convergence est beaucoup plus rapide que les méthodes exactes. Les fréquences naturelles, aussi basses que hautes, ont été obtenues avec satisfaction.

Une méthode des éléments finis hybride est présentée dans cette thèse pour étudier la stabilité aéroélastique des coques sphériques à vide et soumises à un écoulement externe supersonique. La théorie linéaire des coques sphériques a été couplée avec la théorie du piston du premier ordre. L'effet de la correction de la courbure dans la théorie du piston a été pris en compte. L'analyse a été faite pour des coques avec différents géométries, différents rapports rayon-épaisseur et différentes conditions aux limites. La méthode des éléments finis hybride présentée dans cette thèse peut donner des résultats fiables avec un moindre effort de calcul comparé aux logiciels commerciaux car ces derniers imposent une certaine restriction lorsqu'une telle analyse est accomplie.

Finalement un logiciel basé sur une formulation modale d'éléments finis a été développé. Il est capable de faire l'analyse linéaire d'une coque sphérique à vide ou partiellement remplie de fluide ainsi que l'effet d'un écoulement d'air supersonique sur le flottement de la coque sphérique. Une telle formulation modale est destinée à être un outil de conception pratique pour les coques sphériques, afin de réduire le temps de calcul sans perdre la précision souhaitée dans la méthode des éléments finis.

CHAPITRE 1 REVUE BIBLIOGRAPHIQUE

1.1 Revue de la littérature

Les vibrations libres des coques à vide ont été étudiées par plusieurs chercheurs expérimentalement et analytiquement. Kalnins [1,2], dans une étude analytique, a utilisé deux variables auxiliaires pour les déplacements axial et circonférentiel tout en considérant les effets des inerties longitudinale, transversale et rotationnelle, ainsi que l'effet de la déformation due au cisaillement sur les vibrations des coques sphériques peu profondes.

Navaratna [4], Webster [5] Greene et al. [7] ont utilisé la méthode des éléments finis classique pour étudier les vibrations libres des coques sphériques minces. Cohen [3] en utilisant une méthode itérative similaire à la méthode de Stodola a déterminé les fréquences naturelles et les formes modales d'une coque sphérique. Kraus [6] a étudié le cas d'une coque sphérique encastrée en utilisant la théorie générale des coques sphériques, incluant les effets du cisaillement transversal et les effets d'inertie rotationnelle.

Tessler and Spiridigliozzi [8] ont donné les fréquences naturelles de deux types de coques sphériques encastrées. Le premier est une coque à 60° et l'autre hémisphérique. Différents rapports rayon-épaisseur s'étalant de 10 à 100, ont été considérés dans leur étude. Leur analyse s'est basée sur la théorie générale des coques sphériques. Narasimhan et Alwan [9] ont analysé les vibrations libres symétriques d'une calotte sphérique isotrope encastrée. Une analyse basée sur la théorie des coques épaisses a été donnée par Gautham et Ganesan [10] pour deux types de coque sphérique à 60°, l'une est simplement encastrée tandis que l'autre, est simplement supportée; la méthode semi-analytique a été utilisée pour réduire la dimension du problème. Les mêmes auteurs ont analysé dans un autre article le cas d'une coque sphérique encastrée hémisphérique [11].

Sai Ram et Sridhar babu [12] ont utilisé la méthode des éléments finis classique pour étudier les vibrations libres d'une calotte sphérique avec ou sans coupure. Buchanan et Rich [13] ont analysé deux cas de coques sphériques à 60°. Le premier est une coque simplement supportée, par contre, le deuxième est une coque encastrée. Ils ont utilisé la méthode des éléments finis classique.

Dans une récente étude Ventsel et al. [14] ont utilisé une formulation combinée de la méthode des éléments de frontières et de la méthode des éléments finis classique pour étudier les vibrations libres d'une coque sphérique hémisphérique. La coque sphérique est considérée isotrope et simplement supportée. Différents nombres d'ondes circonférentiels ont été pris en considération.

Les vibrations des coques sphériques contenant un fluide ont été par contre peu étudiées par les chercheurs expérimentalement ou analytiquement. Rayleigh [15] a résolu le problème des vibrations symétriques d'une coque sphérique rigide remplie de fluide. La solution du problème de vibration libre d'une membrane sphérique, contenant un fluide, peut être trouvée dans les travaux de Morse et Feshbach [16].

Le mouvement de la surface libre d'un fluide (ballottement) dans une coque sphérique non déformable a été analysé par peu de chercheurs, par exemple, Budiansky [17], Stofan et Armsted [18], Chu [19] et Karamanos et al [20]. Les oscillations des masses de fluide résultent du déplacement latéral ou de la rotation angulaire des coques sphériques.

D'autres chercheurs ont étudié des cas particuliers comme le cas d'une sphère remplie de fluide. Rand et Dimaggio [21] ont considéré les vibrations libres axisymétriques extensionnelles des sphères élastiques remplies de fluide, sans tenir compte de l'effet de torsion. Motivés par le fait que le crâne d'un être humain peut être représenté par une coque sphérique remplie de fluide, Engin et Liu [22] ont considéré les vibrations libres d'une sphère homogène contenant un fluide parfait et irrotationnel. Advani et Lee [23] ont analysé les vibrations d'une sphère remplie de fluide en utilisant une théorie des coques, d'ordre supérieur, incluant les effets du cisaillement transversal et de l'inertie rotationnelle. Guarino et Elger [24] ont analysé le spectre fréquentiel d'une sphère remplie de fluide avec ou sans une sphère solide insérée au centre du système afin d'explorer l'utilisation de la percussion auscultatoire, comme un instrument clinique de diagnostic. Les vibrations libres d'une sphère mince remplie d'un fluide compressible ont été étudiées par Bai et Wu [25]. Les vibrations libres générales non-axisymétriques d'une sphère élastique isotrope remplie d'un fluide compressible ont été analysées par Chen et Ding [26]. Young [27] a étudié les vibrations libres des sphères, composées d'un fluide compressible parfait, entouré par des couches sphériques de matériaux isotropes, homogènes, linéaires, élastiques.

Le cas des coques hémisphériques encastrées remplies de fluide a été étudié expérimentalement par Samoilov et Pavlov [28]. Kana et Nagy [29] ont entrepris une vaste analyse expérimentale des coques hémisphériques encastrées remplies d'eau.

Hwang [30] a analysé le cas du ballottement (sloshing) longitudinal d'un liquide dans un réservoir hémisphérique supporté par ses côtés. Chung et Rush [31] ont présenté une formulation rigoureuse et consistante des problèmes dynamiquement couplés ayant trait avec le mouvement d'une surface libre, d'une coque remplie de fluide. Un exemple numérique d'un réservoir hémisphérique rempli de fluide a été modélisé.

Komatsu [32,33] a utilisé une méthode hybride avec un coefficient de masse de fluide, ajouté au système d'équations. Il a validé son modèle avec des expériences sur des coques hémisphériques partiellement remplies de fluide avec deux conditions aux limites : une condition d'encastrement et l'autre de liberté. Plus récemment, Ventsel et al. [34] ont utilisé une méthode hybride combinant la méthode des éléments finis et la méthode des éléments frontières pour l'étude des vibrations libres d'une coque hémisphérique simplement supportée et remplie de fluide, avec différents nombres d'ondes circonférentielles.

L'aéroélasticité des coques et plaques a été étudiée par plusieurs chercheurs expérimentalement et analytiquement [36]. Dowel a dressé une étude exhaustive de l'aéroélasticité des plaques et des coques dans son livre [37]. Après l'introduction de la théorie du piston par Ashley et Zatarian [38] dans la modélisation aéroélastique, un nombre intéressant d'études expérimentales et théoriques ont été accomplies pour analyser le flottement supersonique des coques. Dans le cas général, toutes ces recherches sont concernées par le développement d'une relation analytique décrivant l'effet de la coque et des paramètres de l'écoulement sur la pression dynamique critique du flottement. Les modèles aéroélastiques, combinés avec la théorie linéaire ou non linéaire du piston, ont été couplés avec la théorie des coques, pour tenir compte de l'interaction fluide-structure. Les équations régissant l'interaction fluide-structure ont été traitées numériquement en utilisant la méthode de Galerkin.

Une analyse expérimentale exhaustive a été faite par Olson et Fung [39]. Ils ont étudié les effets des conditions aux limites et de l'état initial des contraintes dû à la pression interne et le chargement axial. Ils ont observé que les coques cylindriques pressurisées flottent à un niveau de pression inférieur à celui prédit par la théorie [40]. Plus tard, Evensen et Olson [41,42] ont

présenté une analyse non linéaire pour tenir compte du fait expérimental observé. Dowel [43] a analysé le comportement d'une coque cylindrique dans un écoulement supersonique pour différents paramètres de la coque et de l'écoulement. Une description complète de la modélisation du flottement des panneaux est donnée dans son livre. Une étude conduite par Carter et Strearman [44] a montré que la concordance entre la théorie et l'expérimental reportée dans la littérature existe seulement dans le cas d'un petit chargement statique appliqué sur la coque. Amabili et Pellicano [45] ont inclut les non-linéarités géométriques dans leur étude du flottement supersonique d'une coque cylindrique circulaire. Se basant sur une sélection adéquate des modes d'expansion pour discrétiser les équations aéroélastiques afin de faciliter la solution, ils ont réussi à capturer le comportement nonlinéaire de la coque correctement.

Certains auteurs se sont orienté vers l'étude numérique de ce problème. Les équations des déplacements virtuels ont été résolues en utilisant la méthode des éléments finis. Les équations aéroélastiques régissant le phénomène ont été formulées en appliquant la théorie classique des coques couplée avec la théorie du piston pour tenir compte des forces aérodynamiques. Par exemple, Bismarck-Nasr [46] a développé une méthode des éléments finis pour analyser le flottement supersonique d'une coque cylindrique sujette à une pression interne et un chargement axial. Ganapathi et al. [47] ont modélisé une coque cylindrique laminée anisotrope orthotropique placée dans un écoulement supersonique en utilisant la méthode des éléments finis et ont analysé l'effet des différentes géométries sur les limites de l'établissement du flottement.

L'aéroélasticité des coques coniques a été étudiée par peu de chercheurs. Le travail pionnier dans ce domaine est celui de Shulman [48]. Ueda et al [49] ont étudié théoriquement et expérimentalement le flottement supersonique d'une coque conique. Dixon et Hudson [50] ont analysé théoriquement le flottement et les vibrations d'une coque conique orthotropique.

Miserentino et Dixon [51] ont étudié expérimentalement les vibrations et le flottement d'une coque conique pressurisée. Bismarck-Nasr et Costa-Savio [52] ont analysé le flottement supersonique des coques coniques à l'aide de la méthode des éléments finis. Sunder et al. [53] ont appliqué avec succès la méthode des éléments finis pour analyser le flottement des coques coniques laminées. Dans une autre étude [54] ils ont trouvé l'angle optimum de la coque conique dans le flottement aéroélastique. Mason et Blotter [55] ont utilisé la méthode des éléments finis pour chercher les limites d'établissement du flottement pour une coque conique sujette à un

écoulement interne supersonique. Pidaparti et Yang Henry [56] ont mené une étude théorique afin de prédire l'établissement du flottement des coques coniques composites.

1.2 Plan de la thèse

Le contenu de ce mémoire est réparti sur une introduction, quatre chapitres et une conclusion qui répondent aux exigences d'une thèse, présentée sous forme d'articles. Chaque article comprend un résumé, une introduction, une formulation du problème, résultats et discussions et la liste des références. Après ces articles, on présente une conclusion qui résume l'ensemble des travaux accomplis durant la préparation de cette thèse.

Suite à une introduction sur le sujet abordé dans cette thèse, en l'occurrence les vibrations libres et l'interaction fluide-structure des coques sphériques, on présente dans le premier chapitre une revue bibliographique exhaustive sur les vibrations libres et les interactions fluide-structure des coques sphériques.

Le deuxième chapitre, qui correspond au 1er article, présente une formulation complète de la méthode des éléments finis hybride appliquée aux vibrations libres des coques sphériques vides.

Le troisième chapitre, qui correspond au 2^{e} article, traite des vibrations libres des coques sphériques partiellement remplies de fluide.

Dans le quatrième chapitre, qui correspond au 3^{e} article, on présente une analyse numérique du flottement des coques sphériques.

Une conclusion générale termine cette thèse et résume tous les résultats.

CHAPITRE 2 : ARTICLE 1- FREE VIBRATION OF SPHERICAL SHELLS USING A HYBRID FINITE ELEMENT METHOD

Department of Mechanical Engineering, Ecole Polytechnique de Montreal, C.P. 6079 Succursale Centre-ville, Montréal, Canada H3C 3A7

**mohamed.menaa@polymtl.ca* ***aouni.lakis@polymtl.ca*

Submitted, 3 May 2013 to the International Journal of Structural Stability and Dynamics

Abstract

In this study, free vibration analysis of spherical shell is carried out. The structural model is based on a combination of thin shell theory and the classical finite element method. Free vibration equations using the hybrid finite element formulation are derived and solved numerically. The results are validated using numerical and theoretical data available in the literature. The analysis is accomplished for spherical shells of different geometries, boundary conditions and radius to thickness ratios. This proposed hybrid finite element method can be used efficiently for design and analysis of spherical shells employed in high speed aircraft structures.

Keywords: spherical shell; hybrid finite element method; free vibration

1. Introduction

Shells of revolution, particularly spherical shells are one of the primary structural elements in high speed aircraft. Their applications include the propellant tank or gas-deployed skirt of space crafts. Free vibration of spherical shell has been investigated by numerous researchers experimentally and analytically.

Kalnins[1, 2], studying analytically free vibrations in shallow spherical shell, used two auxiliary variables for the axial and circumferential displacements while considering the effect of longitudinal, transverse and rotary inertia as well as transverse shear deformation on the non-asymmetric vibration of shallow spherical shells. Navaratna[4], Webster[5], Greene et al.[7] used the classical finite element method to study the free vibration of thin spherical shell. Cohen[3] using a

method of iteration like Stodola's method determined the natural frequencies and mode shapes of spherical shell. Kraus[6] investigated the case of clamped spherical shell using a general theory which included the effects of transverse shear stress and rotational inertia. Tessler and Spiridigliozzi[8] gave frequencies of 60° clamped spherical shell and hemispherical shell for radius to thickness ratios from 10 to 100 and their analysis was based upon shell theory. Narasimhan and Alwan[9] analyzed the axisymmetric free vibration of clamped isotropic spherical shell cap. Thick shell analysis was given by Gautham and Ganesan[10] for the analysis of a 60° clamped and simply supported spherical shells; the semi-analytical method was used to reduce the dimension of the problem. The same authors[11] investigated the analysis of a clamped isotropic hemispherical shell ($\phi_0 = 90^\circ$). Sai Ram and Sridhar Babu[12] used the classical finite elements method to study the free vibration of composite spherical shell cap with or without a cutout. Buchanan and Rich[13] investigated the case of 60° clamped and simply supported spherical shells using classical finite elements method. Recently, Ventsel et al.[14] used a combined formulation of the boundary elements method and finite elements method to study the free vibration of an isotropic simply supported hemispherical shell with different circumferential mode numbers.

The objective of the present study is to develop a general hybrid finite element package for predicting the dynamic behavior of isotropic spherical shells with boundary conditions which can be varied as desired. The solution scheme is based on the hybrid finite element method. This method uses displacements functions derived from the shell theory instead of polynomials in classical finite element method. The element is a spherical frustum instead of the usual triangular or rectangular shell element. This developed method demonstrated precise and fast convergence with few elements. On the other hand, the present theory, because of its usage of shell classical theory for the displacement functions can easily be adapted to take the hydrodynamic effects into account. Finally, again because of the use of shell classical theory, we can obtain the high as well as the low frequencies with high accuracy.

2. Finite element formulation

In this study the structure is modeled using hybrid finite element method which is a combination of spherical shell theory and classical finite element method. In this hybrid finite element method, the displacement functions are found from exact solution of spherical shell theory rather approximated by polynomial functions done in classical finite element method. In

the spherical coordinate system *(R,θ,ϕ)* shown in Fig. 1, five out of the six equations of equilibrium for spherical shells under external load are written as follows :

$$\begin{aligned}
&\frac{\partial N_\phi}{\partial \phi}+\frac{1}{\sin\phi}\frac{\partial N_{\phi\theta}}{\partial \theta}+\left(N_\phi-N_\theta\right)\cot\phi+Q_\phi=0\\
&\frac{\partial N_{\phi\theta}}{\partial \phi}+\frac{1}{\sin\phi}\frac{\partial N_\theta}{\partial \theta}+2N_{\phi\theta}\cot\phi+Q_\theta=0\\
&\frac{\partial Q_\phi}{\partial \phi}+\frac{1}{\sin\phi}\frac{\partial Q_\theta}{\partial \theta}+Q_\phi\cot\phi-(N_\phi+N_\theta)=0\\
&\frac{\partial M_\phi}{\partial \phi}+\frac{1}{\sin\phi}\frac{\partial M_{\phi\theta}}{\partial \theta}+\left(M_\phi-M_\theta\right)\cot\phi-RQ_\phi=0\\
&\frac{\partial M_{\phi\theta}}{\partial \phi}+\frac{1}{\sin\phi}\frac{\partial M_\theta}{\partial \theta}+2M_{\phi\theta}\cot\phi-RQ_\theta=0
\end{aligned} \tag{1}$$

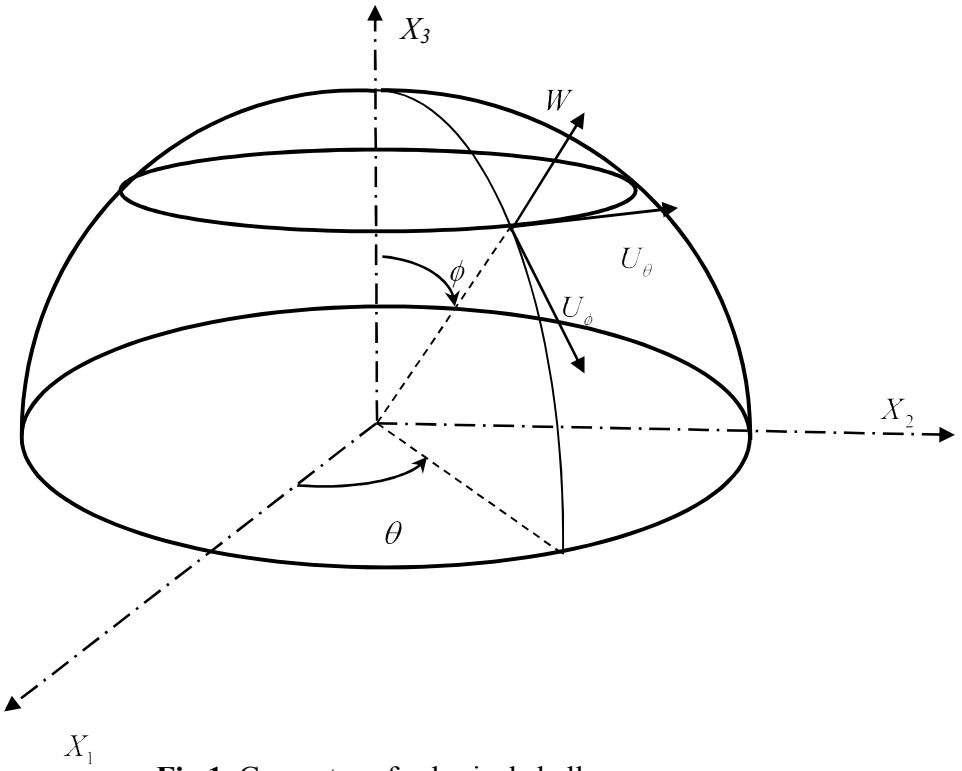

Fig.1. Geometry of spherical shell

where N_ϕ, N_θ, $N_{\phi\theta}$ are membrane stress resultants; M_ϕ, M_θ, $M_{\phi\theta}$ the bending stress resultants and Q_ϕ, Q_θ the shear forces (Fig. 2). The sixth equation, which is an identity equation for spherical shells, is not presented here.

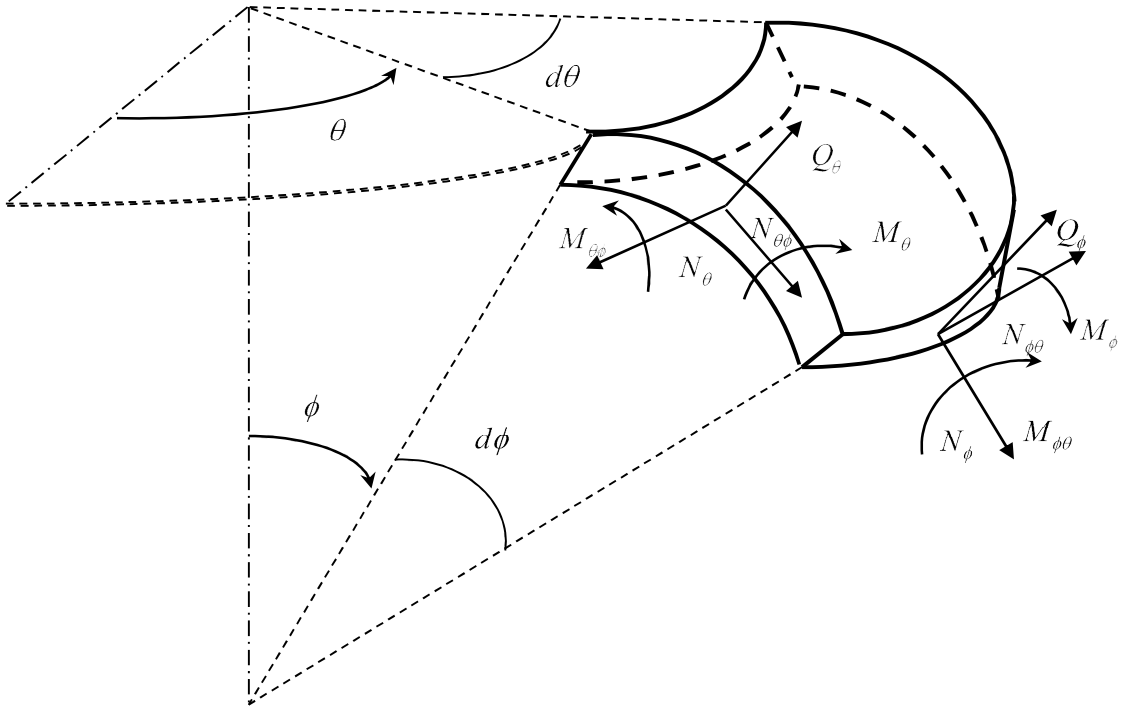

Fig.2. Stress resultants and stress couples

Strain and displacements for three displacements in axial U_ϕ, radial W and circumferential U_θ are related as follows:

$$\{\varepsilon\}=\begin{Bmatrix}\varepsilon_\phi\\ \varepsilon_\theta\\ 2\varepsilon_{\phi\theta}\\ \kappa_\phi\\ \kappa_\theta\\ 2\kappa_{\phi\theta}\end{Bmatrix}=\begin{Bmatrix}\frac{1}{R}\left(\frac{\partial U_\phi}{\partial\phi}+W\right)\\ \frac{1}{R}\left(\frac{1}{\sin\phi}\frac{\partial U_\theta}{\partial\theta}+U_\phi\cot\phi+W\right)\\ \frac{1}{R}\left(\frac{\partial U_\theta}{\partial\phi}+\frac{1}{\sin\phi}\frac{\partial U_\phi}{\partial\theta}-U_\theta\cot\phi\right)\\ \frac{1}{R^2}\left(\frac{\partial U_\phi}{\partial\phi}-\frac{\partial^2 W}{\partial\phi^2}\right)\\ \frac{1}{R^2}\left(\frac{1}{\sin\phi}\frac{\partial U_\theta}{\partial\theta}+U_\phi\cot\phi-\frac{1}{\sin^2\phi}\frac{\partial^2 W}{\partial\theta^2}-\cot\phi\frac{\partial W}{\partial\phi}\right)\\ \frac{1}{R^2}\left(\frac{\partial U_\theta}{\partial\phi}+\frac{1}{\sin\phi}\frac{\partial U_\phi}{\partial\theta}-U_\theta\cot\phi+2\frac{1}{\sin\phi}\cot\phi\frac{\partial W}{\partial\theta}-2\frac{1}{\sin\phi}\frac{\partial^2 W}{\partial\phi\partial\theta}\right)\end{Bmatrix} \tag{2}$$

Displacements, U, W and V in the global Cartesian coordinate system are related to displacements, $U_{\phi i}$, W_i and $U_{\theta i}$ indicated in Fig 3. by:

$$\begin{Bmatrix}U\\ W\\ V\end{Bmatrix}=\begin{bmatrix}\sin\phi_i & -\cos\phi_i & 0\\ \cos\phi_i & \sin\phi_i & 0\\ 0 & 0 & 1\end{bmatrix}\begin{Bmatrix}U_{\phi i}\\ W_i\\ U_{\theta i}\end{Bmatrix} \tag{3}$$

The stress vector $\{\sigma\}$ is expressed as a function of strain $\{\varepsilon\}$ by

$$\{\sigma\}=[P]\{\varepsilon\} \tag{4}$$

where $[P]$ is the elasticity matrix for an anisotropic shell given by:

$$[P]=\begin{bmatrix}P_{11} & P_{12} & 0 & P_{14} & P_{15} & 0\\ P_{21} & P_{22} & 0 & P_{24} & P_{25} & 0\\ 0 & 0 & P_{33} & 0 & 0 & 0\\ P_{41} & P_{42} & 0 & P_{44} & P_{45} & 0\\ P_{51} & P_{52} & 0 & P_{54} & P_{55} & 0\\ 0 & 0 & P_{36} & 0 & 0 & P_{66}\end{bmatrix} \tag{5}$$

Upon substitution of equations (2), (4) and (5) into equations (1), a system of equilibrium equations can be obtained as a function of displacements:

$$\begin{aligned} L_1\left(U_\phi, W, U_\theta, P_{ij}\right) &= 0 \\ L_2\left(U_\phi, W, U_\theta, P_{ij}\right) &= 0 \\ L_3\left(U_\phi, W, U_\theta, P_{ij}\right) &= 0 \end{aligned} \tag{6}$$

These three linear partial differentials operators L_1, L_2 and L_3 are given in the Appendix, and P_{ij} are elements of the elasticity matrix, which, for an isotropic thin shell with thickness *h* is given by:

$$[P] = \begin{bmatrix} D & \nu D & 0 & 0 & 0 & 0 \\ \nu D & D & 0 & 0 & 0 & 0 \\ 0 & 0 & \dfrac{(1-\nu)D}{2} & 0 & 0 & 0 \\ 0 & 0 & 0 & K & \nu K & 0 \\ 0 & 0 & 0 & \nu K & K & 0 \\ 0 & 0 & 0 & 0 & 0 & \dfrac{(1-\nu)K}{2} \end{bmatrix} \tag{7}$$

where $D = \dfrac{Et}{1-\nu^2}$ is the membrane stiffness and $K = \dfrac{Et^3}{12\left(1-\nu^2\right)}$ is the bending stiffness.

The element is a circumferential spherical frustum shown in Fig. 3. It has two nodal circles with four degrees of freedom; axial, radial, circumferential and rotation at each node. This element type makes it possible to use thin shell equations easily to find the exact solution of displacement functions rather than an approximation with polynomial functions as done in classical finite element method. For motions associated with the *n*th circumferential wave number we may write:

$$\begin{Bmatrix} U_\phi(\phi,\theta) \\ W(\phi,\theta) \\ U_\theta(\phi,\theta) \end{Bmatrix} = \begin{bmatrix} \cos n\theta & 0 & 0 \\ 0 & \cos n\theta & 0 \\ 0 & 0 & \sin n\theta \end{bmatrix} \begin{Bmatrix} u_{\phi n}(\phi) \\ w_n(\phi) \\ u_{\theta n}(\phi) \end{Bmatrix} = [T] \begin{Bmatrix} u_{\phi n}(\phi) \\ w_n(\phi) \\ u_{\theta n}(\phi) \end{Bmatrix} \tag{8}$$

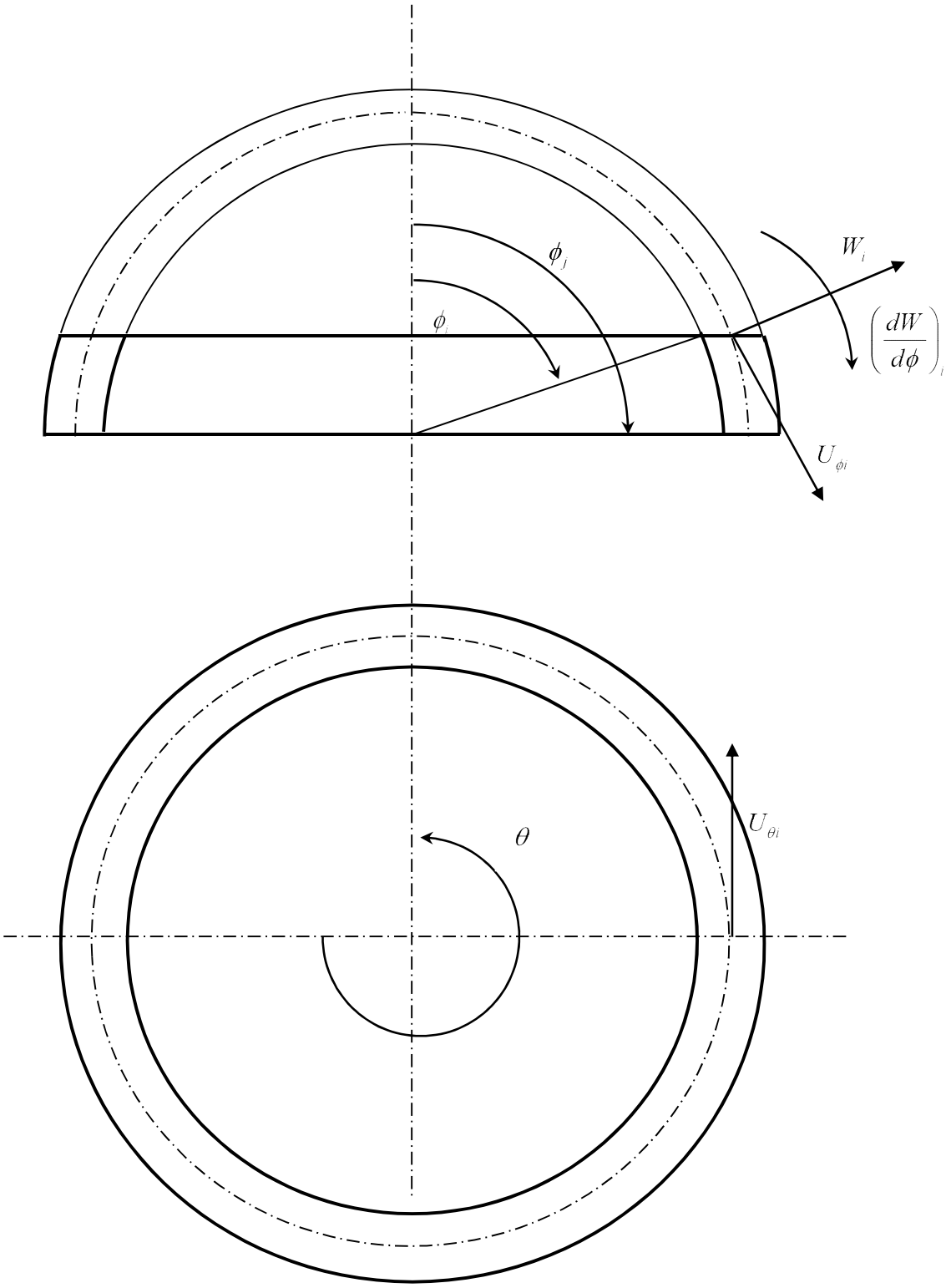

Fig. 3. Spherical frustum element

The transversal displacement $w_n(\phi)$ can be expressed as:

$$w_n(\phi) = \sum_{i=1}^{3} w_i^n \tag{9}$$

where

$$w_i^n = A_i P_{\mu_i}^n(\cos\phi) + B_i Q_{\mu_i}^n(\cos\phi) \tag{10}$$

and where $P_{\mu_i}^n(\cos\phi)$ and $Q_{\mu_i}^n(\cos\phi)$ are the associated Legendre functions of the first and second kinds respectively of order n and degree μ_i.

The expression of the axial displacement $u_{\phi n}(\phi)$ is:

$$u_{\phi n}(\phi) = \sum_{i=1}^{3} E_i \frac{dw_i^n}{d\phi} - \frac{n^2}{2\sin\phi}\psi(\phi) \tag{11}$$

where the coefficient E_i is given by:

$$E_i = \frac{\lambda_i + k(1+\nu) - (1-\nu)}{(1+k)(\lambda_i - 1 + \nu)} \tag{12}$$

The auxiliary function ψ is given by the expression:

$$\psi(\phi) = A_4 P_1^n(\cos\phi) + B_4 Q_1^n(\cos\phi) \tag{13}$$

Finally the circumferential displacement $u_{\theta n}(\phi)$ can be expressed as:

$$u_{\theta n}(\phi) = -n\sum_{i=1}^{3} \frac{1}{\sin\phi} E_i w_i^n + \frac{n}{2}\frac{d\psi}{d\phi} \tag{14}$$

The degree μ_i is obtained from the expression

$$\mu_i = \left(\frac{1}{4} + \lambda_i\right)^{1/2} - \frac{1}{2} \tag{15}$$

where λ_i is one the roots of the cubic equation:

$$\lambda^3 - h_1\lambda^2 + h_2\lambda - h_3 = 0 \tag{16}$$

where

$$\begin{aligned} h_1 &= 4 \\ h_2 &= 4 + (1+k)(1-\nu^2) \\ h_3 &= 2(1+k)(1-\nu^2) \end{aligned} \tag{17}$$

with $k = 12\dfrac{R^2}{h^2}$

The above equation has three roots with one root real and two others are complex conjugate roots.

The Legendre functions $P^n_{\mu_1}$, $P^{n-1}_{\mu_1}, Q^n_{\mu_1}$ and $Q^{n-1}_{\mu_1}$ are real functions whereas $P^n_{\mu_i}$, $P^{n-1}_{\mu_i}, Q^n_{\mu_i}$ and $Q^{n-1}_{\mu_i}$ (i = 2,3) are complex functions so we can write:

$$\begin{aligned} P^n_{\mu_2} &= \mathrm{Re}(P^n_{\mu_2}) + i\,\mathrm{Im}(P^n_{\mu_2}) \\ P^n_{\mu_3} &= \mathrm{Re}(P^n_{\mu_2}) - i\,\mathrm{Im}(P^n_{\mu_2}) \\ Q^n_{\mu_2} &= \mathrm{Re}(Q^n_{\mu_2}) + i\,\mathrm{Im}(Q^n_{\mu_2}) \\ Q^n_{\mu_3} &= \mathrm{Re}(Q^n_{\mu_2}) - i\,\mathrm{Im}(Q^n_{\mu_2}) \\ P^{n-1}_{\mu_2} &= \mathrm{Re}(P^{n-1}_{\mu_2}) + i\,\mathrm{Im}(P^{n-1}_{\mu_2}) \\ P^{n-1}_{\mu_3} &= \mathrm{Re}(P^{n-1}_{\mu_2}) - i\,\mathrm{Im}(P^{n-1}_{\mu_2}) \\ Q^{n-1}_{\mu_2} &= \mathrm{Re}(Q^{n-1}_{\mu_2}) + i\,\mathrm{Im}(Q^{n-1}_{\mu_2}) \\ Q^{n-1}_{\mu_3} &= \mathrm{Re}(P^{n-1}_{\mu_2}) - i\,\mathrm{Im}(Q^{n-1}_{\mu_2}) \end{aligned} \tag{18}$$

Setting

$$\begin{aligned} (n-\mu_1-1)\left(n+\mu_1\right) &= c_1 \\ (n-\mu_2-1)\left(n+\mu_2\right) &= c_2 + ic_3 \\ (n-\mu_3-1)\left(n+\mu_3\right) &= c_2 - ic_3 \end{aligned} \tag{19}$$

$$
\begin{aligned}
E_1 &= e_1 \\
E_2 &= e_2 - ie_3 \\
E_3 &= e_2 + ie_3
\end{aligned} \tag{20}
$$

Substituting equations (18), (19) and (20) in equations (9), (11) and (14) we have:

$$
\begin{aligned}
u_{n\phi}(\phi) = {} & \left(-ne_1 \cot\phi P_{\mu_1}^n + e_1 c_1 P_{\mu_1}^{n-1}\right) A_1 \\
& + \left[-ne_2 \cot\phi \,\mathrm{Re}(P_{\mu_2}^n) - ne_3 \cot\phi \,\mathrm{Im}(P_{\mu_2}^n) + (e_2c_2 + e_3c_3)\,\mathrm{Re}(P_{\mu_2}^{n-1}) + (e_3c_2 - e_2c_3)\,\mathrm{Im}(P_{\mu_2}^{n-1})\right](A_2 + A_3) \\
& + \left[\ ne_3 \cot\phi \,\mathrm{Re}(P_{\mu_2}^n) - ne_2 \cot\phi \,\mathrm{Im}(P_{\mu_2}^n) - (e_3c_2 - e_2c_3)\,\mathrm{Re}(P_{\mu_2}^{n-1}) + (e_2c_2 + e_3c_3)\,\mathrm{Im}(P_{\mu_2}^{n-1})\right] i(A_2 - A_3) \\
& + \left[-\frac{n^2}{2\sin\phi} P_1^n\right] A_4 \\
& + \left(-ne_1 \cot\phi Q_{\mu_1}^n + e_1 c_1 Q_{\mu_1}^{n-1}\right) B_1 \\
& + \left[-ne_2 \cot\phi \,\mathrm{Re}(Q_{\mu_2}^n) - ne_3 \cot\phi \,\mathrm{Im}(Q_{\mu_2}^n) + (e_2c_2 + e_3c_3)\,\mathrm{Re}(Q_{\mu_2}^{n-1}) + (e_3c_2 - e_2c_3)\,\mathrm{Im}(Q_{\mu_2}^{n-1})\right](B_2 + B_3) \\
& + \left[\ ne_3 \cot\phi \,\mathrm{Re}(Q_{\mu_2}^n) - ne_2 \cot\phi \,\mathrm{Im}(Q_{\mu_2}^n) - (e_3c_2 - e_2c_3)\,\mathrm{Re}(Q_{\mu_2}^{n-1}) + (e_2c_2 + e_3c_3)\,\mathrm{Im}(Q_{\mu_2}^{n-1})\right] i(B_2 - B_3) \\
& + \left[-\frac{n^2}{2\sin\phi} Q_1^n\right] B_4
\end{aligned}
$$

$$
w_n(\phi) = P_{\mu_1}^n A_1 + \mathrm{Re}(P_{\mu_2}^n)(A_2 + A_3) + \mathrm{Im}(P_{\mu_2}^n) i(A_2 - A_3) + Q_{\mu_1}^n B_1 + \mathrm{Re}(Q_{\mu_2}^n)(B_2 + B_3) + \mathrm{Im}(Q_{\mu_2}^n) i(B_2 - B_3)
$$

$$
\begin{aligned}
u_{n\theta}(\phi) = {} & -ne_1 P_{\mu_1}^n \frac{1}{\sin\phi} A_1 \\
& - \left[ne_2 \frac{1}{\sin\phi}\mathrm{Re}(P_{\mu_2}^n) + ne_3 \frac{1}{\sin\phi}\mathrm{Im}(P_{\mu_2}^n)\right](A_2 + A_3) + \left[ne_3 \frac{1}{\sin\phi}\mathrm{Re}(P_{\mu_2}^n) - ne_2 \frac{1}{\sin\phi}\mathrm{Im}(P_{\mu_2}^n)\right] i(A_2 - A_3) \\
& + \left[-\frac{n^2}{2}\cot\phi P_1^n + \frac{n}{2}(n-2)(n+1) P_1^{n-1}\right] A_4 \\
& - ne_1 Q_{\mu_1}^n \frac{1}{\sin\phi} B_1 \\
& - \left[ne_2 \frac{1}{\sin\phi}\mathrm{Re}(Q_{\mu_2}^n) + ne_3 \frac{1}{\sin\phi}\mathrm{Im}(Q_{\mu_2}^n)\right](B_2 + B_3) + \left[ne_3 \frac{1}{\sin\phi}\mathrm{Re}(Q_{\mu_2}^n) - ne_2 \frac{1}{\sin\phi}\mathrm{Im}(Q_{\mu_2}^n)\right] i(B_2 - B_3) \\
& + \left[-\frac{n^2}{2}\cot\phi Q_1^n + \frac{n}{2}(n-2)(n+1) Q_1^{n-1}\right] B_4
\end{aligned} \tag{21}
$$

In deriving the above relation we used the recursive relations:

$$\frac{dP_{\mu_i}^n}{d\phi} = -n\cot\phi P_{\mu_i}^n + (n-\mu_i-1)(n+\mu_i)P_{\mu_i}^{n-1}$$
$$\frac{dQ_{\mu_i}^n}{d\phi} = -n\cot\phi Q_{\mu_i}^n + (n-\mu_i-1)(n+\mu_i)Q_{\mu_i}^{n-1} \tag{22}$$

Using matrix formulation, the displacement functions can be expressed as follows:

$$\begin{Bmatrix} U_\phi(\phi,\theta) \\ W(\phi,\theta) \\ U_\theta(\phi,\theta) \end{Bmatrix} = [T] \begin{Bmatrix} u_{\phi n}(\phi) \\ w_n(\phi) \\ u_{\theta n}(\phi) \end{Bmatrix} = [T][R]\{C\} \tag{23}$$

The vector $\{C\}$ is given by the expression:

$$\{C\}^T = \begin{Bmatrix} A_1 & A_2+A_3 & i(A_2-A_3) & A_4 & B_1 & B_2+B_3 & i(B_2-B_3) & B_4 \end{Bmatrix} \tag{24}$$

The elements of matrix $[R]$ are given in the Appendix.

In the finite element method, the vector C is eliminated in favor of displacements at elements nodes. At each finite element node, the three displacements (axial, transversal and circumferential) and the rotation are applied. The displacement of node *i* are defined by the vector:

$$\{\delta_i\} = \begin{Bmatrix} u_{\phi n}^i & w_n^i & \left(\frac{dw_n}{dx}\right)^i & u_{\theta n}^i \end{Bmatrix}^T \tag{25}$$

The element in Fig. 3 with two nodal lines (*i* and *j*) and eight degrees of freedom will have the following nodal displacement vector:

$$\begin{Bmatrix} \delta_i \\ \delta_j \end{Bmatrix} = \begin{Bmatrix} u_{\phi n}^i & w_n^i & \left(\frac{dw_n}{d\phi}\right)^i & u_{\theta n}^i & u_{\phi n}^j & w_n^j & \left(\frac{dw_n}{d\phi}\right)^j & u_{\theta n}^j \end{Bmatrix}^T = [A]\{C\} \tag{26}$$

with

$$\frac{dw_n}{d\phi}=\left(-n\cot\phi P_{\mu_1}^{n}+c_1P_{\mu_1}^{n-1}\right)A_1+\left[-n\cot\phi\,\mathrm{Re}(P_{\mu_2}^{n})+c_2\,\mathrm{Re}(P_{\mu_2}^{n-1})-c_3\,\mathrm{Im}(P_{\mu_2}^{n-1})\right](A_2+A_3)$$
$$+\left[-n\cot\phi\,\mathrm{Im}(P_{\mu_2}^{n})+c_3\,\mathrm{Re}(P_{\mu_2}^{n-1})+c_2\,\mathrm{Im}(P_{\mu_2}^{n-1})\right]i(A_2-A_3)+\left(-n\cot\phi Q_{\mu_1}^{n}+c_1Q_{\mu_1}^{n-1}\right)B_1$$
$$+\left[-n\cot\phi\,\mathrm{Re}(Q_{\mu_2}^{n})+c_2\,\mathrm{Re}(Q_{\mu_2}^{n-1})-c_3\,\mathrm{Im}(Q_{\mu_2}^{n-1})\right](B_2+B_3)$$
$$+\left[-n\cot\phi\,\mathrm{Im}(Q_{\mu_2}^{n})+c_3\,\mathrm{Re}(Q_{\mu_2}^{n-1})+c_2\,\mathrm{Im}(Q_{\mu_2}^{n-1})\right]i(B_2-B_3) \tag{27}$$

The terms of matrix $[A]$ are obtained from the values of matrix $[R]$ and $\frac{dw_n}{dx}$ are given in the appendix. Now, pre-multiplying by $[A]^{-1}$ equation (26) one obtains the matrix of the constant C_i as a function of the degree of freedom:

$$\{C\}=[A]^{-1}\begin{Bmatrix}\delta_i\\ \delta_j\end{Bmatrix} \tag{28}$$

Finally, one substitutes the vector $\{C\}$ into equation and obtains the displacement functions as follows:

$$\begin{Bmatrix}U_\phi(\phi,\theta)\\ W(\phi,\theta)\\ U_\theta(\phi,\theta)\end{Bmatrix}=[T][R][A]^{-1}\begin{Bmatrix}\delta_i\\ \delta_j\end{Bmatrix}=[N]\begin{Bmatrix}\delta_i\\ \delta_j\end{Bmatrix} \tag{29}$$

The strain vector $\{\varepsilon\}$ can be determined from the displacement functions U_ϕ, U_θ, W and the deformation–displacement as:

$$\{\varepsilon\}=\begin{bmatrix}[T] & [0]\\ [0] & [T]\end{bmatrix}[Q]\{C\}=\begin{bmatrix}[T] & [0]\\ [0] & [T]\end{bmatrix}[Q][A]^{-1}\begin{Bmatrix}\delta_i\\ \delta_j\end{Bmatrix}=[B]\begin{Bmatrix}\delta_i\\ \delta_j\end{Bmatrix} \tag{30}$$

where matrix $[Q]$ is given in the appendix.

This relation can be used to find the stress vector, equation (4), in terms of the nodal degrees of freedom vector:

$$\{\sigma\} = [P][B]\begin{Bmatrix}\delta_i \\ \delta_j\end{Bmatrix} \tag{31}$$

Based on the finite element formulation, the local stiffness and mass matrices are:

$$\begin{aligned}[k]_{loc} &= \iint_A [B]^T [P][B]\, dA \\ [m]_{loc} &= \rho\, h \iint_A [N]^T [N]\, dA\end{aligned} \tag{32}$$

where ρ is the density and h is the thickness of shell.

The surface element of the shell wall is $dA = R^2 \sin\phi d\phi d\theta$. After integrating over θ, the preceding equations become

$$\begin{aligned}[k]_{loc} &= \left[A^{-1}\right]^T \left(\pi R^2 \int_{\phi_i}^{\phi_j} [Q]^T [P][Q] \sin\phi d\phi\right)\left[A^{-1}\right] = \left[A^{-1}\right]^T [G]\left[A^{-1}\right] \\ [m]_{loc} &= \rho h\left[A^{-1}\right]^T \left(\pi R^2 \int_{\phi_i}^{\phi_j} [R]^T [R] \sin\phi d\phi\right)\left[A^{-1}\right] = \rho h\left[A^{-1}\right]^T [S]\left[A^{-1}\right]\end{aligned} \tag{33}$$

In the global system the element stiffness and mass matrices are

$$\begin{aligned}[k] &= [LG]^T \left[A^{-1}\right]^T [G]\left[A^{-1}\right][LG] \\ [m] &= \rho h [LG]^T \left[A^{-1}\right]^T [S]\left[A^{-1}\right][LG]\end{aligned} \tag{34}$$

where

$$[LG]=\begin{bmatrix} \sin\phi_i & -\cos\phi_i & 0 & 0 & 0 & 0 & 0 & 0 \\ \cos\phi_i & \sin\phi_i & 0 & 0 & 0 & 0 & 0 & 0 \\ 0 & 0 & 1 & 0 & 0 & 0 & 0 & 0 \\ 0 & 0 & 0 & 1 & 0 & 0 & 0 & 0 \\ 0 & 0 & 0 & 0 & \sin\phi_j & -\cos\phi_j & 0 & 0 \\ 0 & 0 & 0 & 0 & \cos\phi_j & \sin\phi_j & 0 & 0 \\ 0 & 0 & 0 & 0 & 0 & 0 & 1 & 0 \\ 0 & 0 & 0 & 0 & 0 & 0 & 0 & 1 \end{bmatrix} \tag{35}$$

From these equations, one can assemble the mass and stiffness matrix for each element to obtain the mass and stiffness matrices for the whole shell: $[M]$ and $[K]$. Each elementary matrix is 8x8, therefore the final dimensions of $[M]$ and $[K]$ will be 4*(N+1) where N is the number of elements of the shell.

3. Numerical results

In order to test the efficiency and the accuracy of our model, we used the theory developed in this paper to calculate the natural frequencies and modes of uniform thin elastic spherical shell, which were both non-shallow(ϕ_0 <30) and shallow, of various dimensions and under different boundary conditions. These cases have already been investigated by other authors using others methods. For purposes of comparisons among the natural frequencies obtained, it is eminently practical at this stage to introduce the non-dimensional natural frequency:

$$\Omega = \omega R\left(\frac{\rho}{E}\right)^{\frac{1}{2}} \tag{36}$$

where:

ω is the natural angular frequency,

R is the radius of the reference surface,

ρ is the density,

E is the modulus of elasticity.

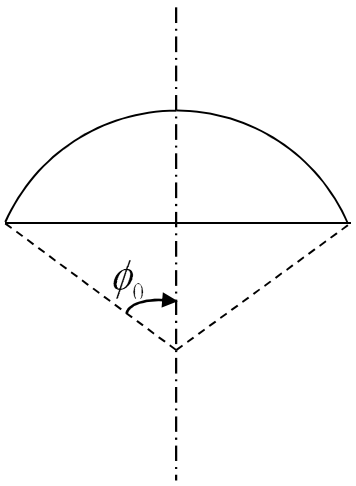

Fig.4. Definition of angle ϕ_0

3.1 Case 1: clamped spherical shell with ϕ_0 =10°

Narassihan and Alwar[9] investigated the case of an axisymmetric clamped spherical shell. The analysis is based on the application of the Chebyshev-Galerkin spectral method for the evaluation of free vibration frequencies and mode shapes. Sai Ram and Sreedhar Babu[12] analyzed the same case with the classical finite element method using 80 elements. Each element is an eight nodded degenerated isoparametric shell element with nine degrees of freedom at each node. With our model and using 6 finite elements, the natural were computed, the results are shown in Table 1.

Table 1: Normalized natural frequencies for 10° clamped spherical shell with $\frac{R}{h} = 200$

Mode	Present	Sai Ram and Sreedhar babu[12]	Narassihan and Alwar [9]
1	1.4861	1.4577	1.4588
2	2.2498	2.2931	2.2999
3	4.4779	4.5773	4.5461

3.2 Case 2: clamped spherical shell with ϕ_0 =30°

This case was investigated analytically by Kalnins[1] using classical theory and transverse vibration theory. With our theory, we used 8 finite elements to study the spherical shell with the results shown in Table 2. The frequencies we obtained with our model are very comparable to Kalinin's values. The maxim displacement values were:

$$\frac{W_{\max}}{(U_\phi)_{\max}} = 3.61 \qquad \frac{W_{\max}}{(U_\theta)_{\max}} = 1.54$$

It was observed that at lower natural frequency, motion of the spherical shell is mainly dominated by its radial component.

Table 2: Normalized natural frequencies for 30° clamped spherical shell with $\frac{R}{h} = 20$

Mode	Present theory	Kalnins[1]
1	1.169	1.168
2	2.224	2.589
3	3.303	3.230
4	4.200	4.288
5	4.923	4.683

3.3 Case 3: spherical shell ϕ_0 =60° under the three boundary conditions: clamped, simply supported and free

The free axisymmetric vibration of the spherical shell in this case was studied by Kalnins[2], Cohen[3], Navaratna[4], Webster[5], Greene et al.[7], Tessler and Spiridigliozzi[8], Gautham and Ganesan[10] and Buchanan and Rich[13]. In the present investigation, the shell was investigated with 10 elements; the results are given respectively for clamped, simply supported and free shells in Tables 3, 4 and 5.

The natural modes corresponding to the lowest shell natural frequencies under the two boundary conditions are illustrated in figures 5 and 6. They reveal that at the lowest natural frequency, spherical shell motion is radial.

It is easy to see that all displacements U_ϕ, W and U_θ are all zero at the top ($\phi = 0$) of the spherical shell.

Table 3: Normalized natural frequencies for 60° clamped spherical shell with $\frac{R}{h} = 20$

Mode	Kalnins[2]	Navaratna[4]	Webster[5]	Tessler and Spiridigliozzi[8]	Gautham and Ganesan[10]	Buchanan and Rich[13]	Present theory
1	1.006	1.008	1.007	1.000	1.001	1.001	1.031
2	1.391	1.395	1.391	1.368	1.373	1.370	1.496
3	-	1.702	1.700	1.673	1.678	1.675	1.760
4	-	2.126	2.095	-	-	2.094	2.089
5	2.375	2.387	2.386	2.260	-	2.256	2.276
6	3.486	3.506	3.851	3.213	-	3.209	3.311
7	3.991	3.996	4.062	3.965	-	3.964	3.775
8	-	4.159	4.151	-	-	4.060	4.073
9	4.947	5.001	5.962	4.442	-	4.427	4.826
10	-	6.037	6.208	5.773	-	5.740	5.777

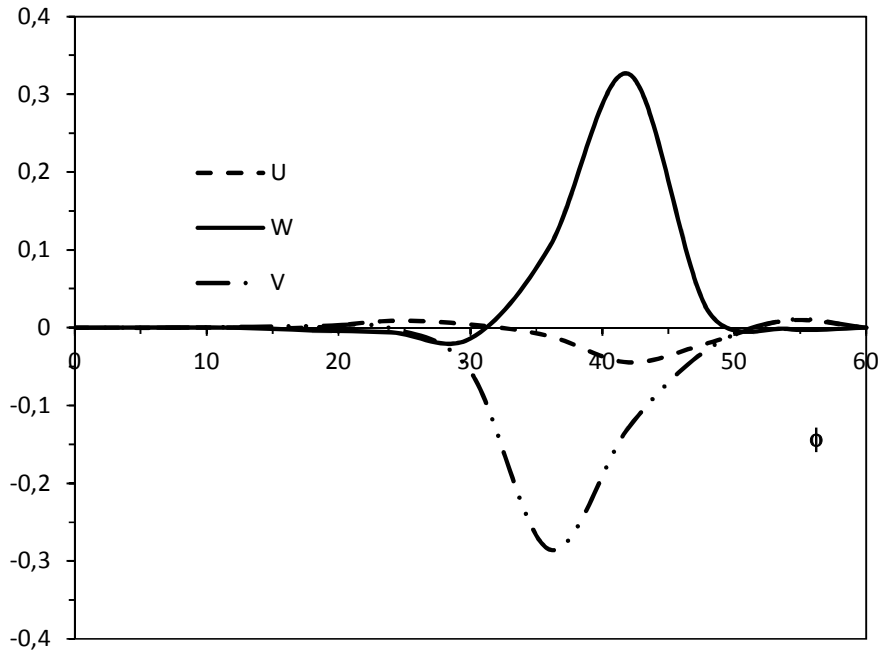

Fig.5. Displacements versus ϕ coordinate for clamped spherical shell ϕ_0 =60

Table 4: Normalized natural frequencies for 60° simply supported spherical shell R/h=20

Mode	Kalnins [2]	Navaratna [4]	Greene et al[7]	Cohen[3]	Gautham and Ganesan[10]	Buchanan and Rich[13]	Present Theory
1	0.962	0.963	0.974	0.959	-	0.956	0.981
2	1.334	1.338	1.338	1.325	1.315	1.308	1.412
3	-	1.653	1.652	1.646	1.639	1.612	1.646
4	2.128	2.131	2.162	-	-	2.044	2.038
5	-	2.141	-	-	-	2.059	2.115
6	3.176	3.185	-	-	-	2.965	2.934
7	3.988	3.933	-	-	-	3.837	3.871
8	-	4.159	-	-	-	4.000	4.017
9	4.575	4.601	-	-	-	4.148	4.138
10	-	6.031	-	-	-	5.608	5.773

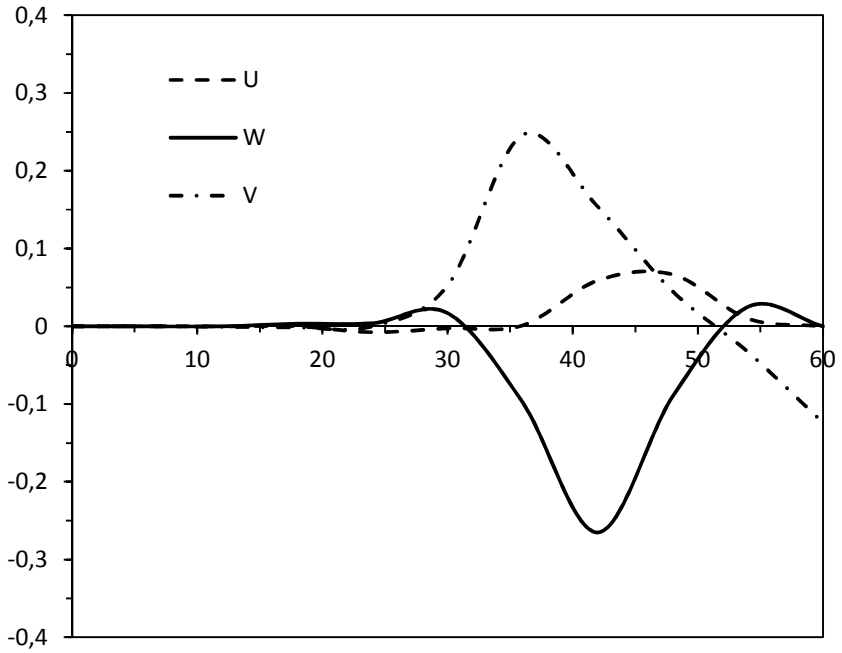

Fig.6. Displacements versus ϕ coordinate for simply supported spherical shell ϕ_0 =60

Table 5: Normalized natural frequencies for 60° free spherical shell with $\frac{R}{h} = 20$

Mode	Kalnins[2]	Navaratna[4]	Webster[5]	Present theory
1	0.931	0.932	0.931	0.938
2	1.088	1.094	1.089	1.062
3	1.533	1.544	1.535	1.426
4	2.348	2.363	2.360	2.425
5	2.544	2.548	2.551	2.725
6	-	2.982	2.985	2.944
7	3.497	3.519	4.023	4.264
8	-	4.971	4.950	4.973
9	4.951	4.980	5.548	5.793
10	5.230	5.543	6.224	6.605

3.4 Case 4: Spherical shell with ϕ_0 =90°

Kraus[6] investigated the case of simply supported spherical shell using a general theory which included the effects of transverse shear stress and rotational inertia. For cases both with and without these effects, he determined the natural frequencies for the shell motion that was independent of θ for circumferential mode number $n = 0$. Tessler and Spiridigliozzi[8], Gautham and Ganesan[11] analyzed the case of clamped hemispherical shell. Ventsel et al.[14] studied the case of simply supported spherical shell using the boundary elements method for various circumferential mode numbers $(n = 0,\ n = 1, n = 2)$. With our model and using 12 finite elements, the natural frequencies were computed for clamped and simply supported shells. The results are shown respectively in table 6 and table 7. The maximum displacements values are:

$$\left(U_\phi\right)_{\max} = 0.3381 \qquad W_{\max} = 0.2317 \qquad \left(U_\theta\right)_{\max} = 0.0854$$

The result is that at the lowest natural frequency, the motion of spherical shell is predominately by the axial displacement.

Table 6: Normalized natural frequencies for 90° clamped spherical shell with $\frac{R}{h} = 10$

Mode	Tessler and Spiridigliozzi[8]	Gautham and Ganesan [11]	Present theory
1	0.8481	0.8439	0.8327
2	1.2328	1.2317	1.1919
3	1.5902	1.5808	1.5041
4	1.9435	1.9267	1.9161

Table 7: Normalized natural frequencies for 90° simply supported spherical shell

Mode	Kraus [6] $\frac{R}{h}=10$	Kraus [6] $\frac{R}{h}=50$	Ventsel et al.[4] $\frac{R}{h}=200$	Present theory $\frac{R}{h}=50$
1	0.8060	0.7548	0.7441	0.7579
2	1.2054	0.9432	0.9281	0.9034
3	1.6179	1.0152	0.9693	0.9499
4	1.9051	1.1082	-	1.1089
5	2.7205	1.2523	-	1.2759
6	2.9301	1.4576	-	1.4723
7	4.0274	1.6558	-	1.6237
8	5.5142	1.7636	-	1.7634

4. Conclusion

The purpose of the investigation described in this paper is to determine the natural frequencies and shape modes of free vibrations of spherical shell. The modal analysis is based on hybrid approach combining the classical finite element method and the classical shell theory. This theoretical approach is much more precise than usual finite element methods because the displacement functions are derived from exact solutions of equilibrium equations for spherical shells. The mass and stiffness matrices are determined by numerical integration. The results obtained for spherical shells with different angles and different boundary conditions are compared with results available in the literature. Very good agreement was found. This approach resulted in a very precise element that leads to fast convergence and less numerical difficulties from the computational point of view. Because of its use of classical shell theory for the displacement functions, the presented method may easily be adapted to take fluid-structure effects into account. A paper under preparation on the effect fluid on vibrations of shells confirms this approach. For the same reason, we can obtain the high as well as low frequencies with very good accuracy.

Appendix

$$L_1(U_\phi,U_\theta,W)=\left(\frac{P_{11}}{R}+\frac{P_{41}}{R^2}\right)\left[\frac{\partial}{\partial\phi}\left(\frac{\partial U_\phi}{\partial\phi}+W\right)+\left(\frac{\partial U_\phi}{\partial\phi}+W\right)\cot(\phi)\right]$$
$$+\left(\frac{P_{12}}{R}+\frac{P_{42}}{R^2}\right)\left[\frac{\partial}{\partial\phi}\left(\frac{1}{\sin(\phi)}\frac{\partial U_\theta}{\partial\theta}+U_\phi\cot(\phi)+W\right)+\left(\frac{1}{\sin(\phi)}\frac{\partial U_\theta}{\partial\theta}+U_\phi\cot(\phi)+W\right)\cot(\phi)\right]$$
$$+\frac{1}{R}\left(\frac{P_{14}}{R}+\frac{P_{44}}{R^2}\right)\left[\frac{\partial}{\partial\phi}\left(\frac{\partial U_\phi}{\partial\phi}-\frac{\partial^2 W}{\partial\phi^2}\right)+\left(\frac{\partial U_\phi}{\partial\phi}-\frac{\partial^2 W}{\partial\phi^2}\right)\cot(\phi)\right]$$
$$+\frac{1}{R}\left(\frac{P_{15}}{R}+\frac{P_{45}}{R^2}\right)\left[\frac{\partial}{\partial\phi}\left(\frac{1}{\sin(\phi)}\frac{\partial U_\theta}{\partial\theta}+U_\phi\cot(\phi)-\frac{1}{\sin^2(\phi)}\frac{\partial^2 W}{\partial\theta^2}-\frac{\partial W}{\partial\phi}\cot(\phi)\right)+\left(\frac{1}{\sin(\phi)}\frac{\partial U_\theta}{\partial\theta}+U_\phi\cot(\phi)-\frac{1}{\sin^2(\phi)}\frac{\partial^2 W}{\partial\theta^2}-\frac{\partial W}{\partial\phi}\cot(\phi)\right)\cot(\phi)\right]$$
$$-\left(\frac{P_{21}}{R}+\frac{P_{51}}{R^2}\right)\left(\frac{\partial U_\phi}{\partial\phi}+W\right)\cot(\phi)$$
$$-\left(\frac{P_{22}}{R}+\frac{P_{52}}{R^2}\right)\left(\frac{1}{\sin(\phi)}\frac{\partial U_\theta}{\partial\theta}+U_\phi\cot(\phi)+W\right)\cot(\phi)$$
$$-\frac{1}{R}\left(\frac{P_{24}}{R}+\frac{P_{54}}{R^2}\right)\left(\frac{\partial U_\phi}{\partial\phi}-\frac{\partial^2 W}{\partial\phi^2}\right)\cot(\phi)$$
$$-\frac{1}{R}\left(\frac{P_{25}}{R}+\frac{P_{55}}{R^2}\right)\left(\frac{1}{\sin(\phi)}\frac{\partial U_\theta}{\partial\theta}+U_\phi\cot(\phi)-\frac{1}{\sin^2(\phi)}\frac{\partial^2 W}{\partial\theta^2}-\frac{\partial W}{\partial\phi}\cot(\phi)\right)\cot(\phi)$$
$$+\left(\frac{P_{33}}{R}+\frac{P_{63}}{R^2}\right)\frac{1}{\sin(\phi)}\frac{\partial}{\partial\theta}\left(\frac{\partial U_\theta}{\partial\phi}+\frac{1}{\sin(\phi)}\frac{\partial U_\varphi}{\partial\theta}-U_\theta\cot(\phi)\right)$$
$$+\frac{1}{R}\left(\frac{P_{36}}{R}+\frac{P_{66}}{R^2}\right)\frac{1}{\sin(\phi)}\frac{\partial}{\partial\theta}\left(\frac{\partial U_\theta}{\partial\phi}+\frac{1}{\sin(\phi)}\frac{\partial U_\varphi}{\partial\theta}-U_\theta\cot(\phi)+2\frac{\cot(\phi)}{\sin(\phi)}\frac{\partial W}{\partial\theta}-\frac{2}{\sin(\phi)}\frac{\partial^2 W}{\partial\phi\,\partial\theta}\right)$$

$$L_2(U_\phi,U_\theta,W)=\left(\frac{P_{21}}{R}+\frac{P_{51}}{R^2}\right)\frac{1}{\sin(\phi)}\frac{\partial}{\partial\theta}\left(\frac{\partial U_\phi}{\partial\phi}+W\right)$$
$$+\left(\frac{P_{22}}{R}+\frac{P_{52}}{R^2}\right)\frac{1}{\sin(\phi)}\frac{\partial}{\partial\theta}\left(\frac{1}{\sin(\phi)}\frac{\partial U_\theta}{\partial\theta}+U_\phi\cot(\phi)+W\right)$$
$$+\frac{1}{R}\left(\frac{P_{24}}{R}+\frac{P_{54}}{R^2}\right)\frac{1}{\sin(\phi)}\frac{\partial}{\partial\theta}\left(\frac{\partial U_\phi}{\partial\phi}-\frac{\partial^2 W}{\partial\phi^2}\right)$$
$$+\frac{1}{R}\left(\frac{P_{25}}{R}+\frac{P_{55}}{R^2}\right)\frac{1}{\sin(\phi)}\frac{\partial}{\partial\theta}\left(\frac{1}{\sin(\phi)}\frac{\partial U_\theta}{\partial\theta}+U_\phi\cot(\phi)-\frac{1}{\sin^2(\phi)}\frac{\partial^2 W}{\partial\theta^2}-\frac{\partial W}{\partial\phi}\cot(\phi)\right)$$
$$+\left(\frac{P_{33}}{R}+\frac{P_{63}}{R^2}\right)\left[\frac{\partial}{\partial\phi}\left(\frac{\partial U_\theta}{\partial\phi}+\frac{1}{\sin(\phi)}\frac{\partial U_\varphi}{\partial\theta}-U_\theta\cot(\phi)\right)+2\left(\frac{\partial U_\theta}{\partial\phi}+\frac{1}{\sin(\phi)}\frac{\partial U_\varphi}{\partial\theta}-U_\theta\cot(\phi)\right)\cot(\phi)\right]$$
$$+\frac{1}{R}\left(\frac{P_{36}}{R}+\frac{P_{66}}{R^2}\right)\left[\frac{\partial}{\partial\phi}\left(\frac{\partial U_\theta}{\partial\phi}+\frac{1}{\sin(\phi)}\frac{\partial U_\varphi}{\partial\theta}-U_\theta\cot(\phi)+2\frac{\cot(\phi)}{\sin(\phi)}\frac{\partial W}{\partial\theta}-\frac{2}{\sin(\phi)}\frac{\partial^2 W}{\partial\phi\,\partial\theta}\right)+2\left(\frac{\partial U_\theta}{\partial\phi}+\frac{1}{\sin(\phi)}\frac{\partial U_\varphi}{\partial\theta}-U_\theta\cot(\phi)+2\frac{\cot(\phi)}{\sin(\phi)}\frac{\partial W}{\partial\theta}-\frac{2}{\sin(\phi)}\frac{\partial^2 W}{\partial\phi\,\partial\theta}\right)\cot t(\phi)\right]$$

$$
\begin{aligned}
&L_3(U_\phi, U_\theta, W) = -\left(\frac{P_{11}}{R} + \frac{P_{21}}{R}\right)\left(\frac{\partial U_\phi}{\partial \phi} + W\right) \\
&-\left(\frac{P_{12}}{R} + \frac{P_{22}}{R}\right)\left(\frac{1}{\sin(\phi)}\frac{\partial U_\theta}{\partial \theta} + U_\phi \cot(\phi) + W\right) \\
&-\left(\frac{P_{14}}{R^2} + \frac{P_{24}}{R^2}\right)\left(\frac{\partial U_\phi}{\partial \phi} - \frac{\partial^2 W}{\partial \phi^2}\right) \\
&-\left(\frac{P_{15}}{R^2} + \frac{P_{25}}{R^2}\right)\left(\frac{1}{\sin(\phi)}\frac{\partial U_\theta}{\partial \theta} + U_\phi \cot(\phi) - \frac{1}{\sin^2(\phi)}\frac{\partial^2 W}{\partial \theta^2} - \frac{\partial W}{\partial \phi}\cot(\phi)\right) \\
&+\frac{P_{41} - P_{51}}{R^2}\left(\cot(\phi)\frac{\partial}{\partial \phi}\left(\frac{\partial U_\phi}{\partial \phi} + W\right) - \left(\frac{\partial U_\phi}{\partial \phi} + W\right)\right) \\
&+\frac{1}{R^2 \sin(\phi)}\left[P_{41}\frac{\partial}{\partial \phi}\left(\sin(\phi)\frac{\partial}{\partial \phi}\left(\frac{\partial U_\phi}{\partial \phi} + W\right)\right) + P_{51}\frac{\partial}{\partial \theta}\left(\frac{\partial U_\phi}{\partial \phi} + W\right)\right] \\
&+\frac{P_{42} - P_{52}}{R^2}\left(\cot(\phi)\frac{\partial}{\partial \phi}\left(\frac{1}{\sin(\phi)}\frac{\partial U_\theta}{\partial \theta} + U_\phi \cot(\phi) + W\right) - \left(\frac{1}{\sin(\phi)}\frac{\partial U_\theta}{\partial \theta} + U_\phi \cot(\phi) + W\right)\right) \\
&+\frac{1}{R^2 \sin(\phi)}\left[P_{42}\frac{\partial}{\partial \phi}\left(\sin(\phi)\frac{\partial}{\partial \phi}\left(\frac{1}{\sin(\phi)}\frac{\partial U_\theta}{\partial \theta} + U_\phi \cot(\phi) + W\right)\right) + P_{52}\frac{\partial}{\partial \theta}\left(\frac{1}{\sin(\phi)}\frac{\partial U_\theta}{\partial \theta} + U_\phi \cot(\phi) + W\right)\right] \\
&+\frac{P_{44} - P_{54}}{R^3}\left(\cot(\phi)\frac{\partial}{\partial \phi}\left(\frac{\partial U_\phi}{\partial \phi} - \frac{\partial^2 W}{\partial \phi^2}\right) - \left(\frac{\partial U_\phi}{\partial \phi} - \frac{\partial^2 W}{\partial \phi^2}\right)\right) \\
&+\frac{1}{R^3 \sin(\phi)}\left[P_{44}\frac{\partial}{\partial \phi}\left(\sin(\phi)\frac{\partial}{\partial \phi}\left(\frac{\partial U_\phi}{\partial \phi} - \frac{\partial^2 W}{\partial \phi^2}\right)\right) + P_{54}\frac{\partial}{\partial \theta}\left(\frac{\partial U_\phi}{\partial \phi} - \frac{\partial^2 W}{\partial \phi^2}\right)\right] \\
&+\frac{P_{45} - P_{55}}{R^3}\left(\cot(\phi)\frac{\partial}{\partial \phi}\left(\frac{1}{\sin(\phi)}\frac{\partial U_\theta}{\partial \theta} + U_\phi \cot(\phi) - \frac{1}{\sin^2(\phi)}\frac{\partial^2 W}{\partial \theta^2} - \frac{\partial W}{\partial \phi}\cot(\phi)\right) - \left(\frac{1}{\sin(\phi)}\frac{\partial U_\theta}{\partial \theta} + U_\phi \cot(\phi) - \frac{1}{\sin^2(\phi)}\frac{\partial^2 W}{\partial \theta^2} - \frac{\partial W}{\partial \phi}\cot(\phi)\right)\right) \\
&+\frac{1}{R^3 \sin(\phi)}\left[P_{45}\frac{\partial}{\partial \phi}\left(\sin(\phi)\frac{\partial}{\partial \phi}\left(\frac{1}{\sin(\phi)}\frac{\partial U_\theta}{\partial \theta} + U_\phi \cot(\phi) - \frac{1}{\sin^2(\phi)}\frac{\partial^2 W}{\partial \theta^2} - \frac{\partial W}{\partial \phi}\cot(\phi)\right)\right) + P_{55}\frac{\partial}{\partial \theta}\left(\frac{1}{\sin(\phi)}\frac{\partial U_\theta}{\partial \theta} + U_\phi \cot(\phi) - \frac{1}{\sin^2(\phi)}\frac{\partial^2 W}{\partial \theta^2} - \frac{\partial W}{\partial \phi}\cot(\phi)\right)\right] \\
&+\frac{P_{63}}{R^2 \sin(\phi)}\left[\frac{\partial^2}{\partial \phi \partial \theta}\left(\frac{\partial U_\theta}{\partial \phi} + \frac{1}{\sin(\phi)}\frac{\partial U_\varphi}{\partial \theta} - U_\theta \cot(\phi)\right) + 3\cot(\phi)\left(\frac{\partial}{\partial \theta}\frac{\partial U_\theta}{\partial \phi} + \frac{1}{\sin(\phi)}\frac{\partial U_\varphi}{\partial \theta} - U_\theta \cot(\phi)\right)\right] \\
&+\frac{P_{66}}{R^3 \sin(\phi)}\left[\frac{\partial^2}{\partial \phi \partial \theta}\left(\frac{\partial U_\theta}{\partial \phi} + \frac{1}{\sin(\phi)}\frac{\partial U_\varphi}{\partial \theta} - U_\theta \cot(\phi) + 2\frac{\cot(\phi)}{\sin(\phi)}\frac{\partial W}{\partial \theta} - \frac{2}{\sin(\phi)}\frac{\partial^2 W}{\partial \phi \partial \theta}\right) + 3\cot(\phi)\left(\frac{\partial U_\theta}{\partial \phi} + \frac{1}{\sin(\phi)}\frac{\partial U_\varphi}{\partial \theta} - U_\theta \cot(\phi) + 2\frac{\cot(\phi)}{\sin(\phi)}\frac{\partial W}{\partial \theta} - \frac{2}{\sin(\phi)}\frac{\partial^2 W}{\partial \phi \partial \theta}\right)\right]
\end{aligned}
$$

$$R(1,1) = \left(-e_1 n \cot\phi P^n_{\mu_1} + e_1 c_1 P^{n-1}_{\mu_1}\right)$$

$$R(1,2) = -ne_2 \cot\phi \,\mathrm{Re}(P^n_{\mu_2}) - ne_3 \cot\phi \,\mathrm{Im}(P^n_{\mu_2}) + (e_2c_2 + e_3c_3)\,\mathrm{Re}(P^{n-1}_{\mu_2}) + (e_3c_2 - e_2c_3)\,\mathrm{Im}(P^{n-1}_{\mu_2})$$

$$R(1,3) = ne_3 \cot\phi \,\mathrm{Re}(P^n_{\mu_2}) - ne_2 \cot\phi \,\mathrm{Im}(P^n_{\mu_2}) - (e_3c_2 - e_2c_3)\,\mathrm{Re}(P^{n-1}_{\mu_2}) + (e_2c_2 + e_3c_3)\,\mathrm{Im}(P^{n-1}_{\mu_2})$$

$$R(1,4) = -\frac{n^2}{2\sin\phi} P^n_1$$

$$R(1,5) = \left(-e_1 n \cot\phi Q^n_{\mu_1} + e_1 c_1 Q^{n-1}_{\mu_1}\right)$$

$$R(1,6) = -ne_2 \cot\phi \,\mathrm{Re}(Q^n_{\mu_2}) - ne_3 \cot\phi \,\mathrm{Im}(Q^n_{\mu_2}) + (e_2c_2 + e_3c_3)\,\mathrm{Re}(Q^{n-1}_{\mu_2}) + (e_3c_2 - e_2c_3)\,\mathrm{Im}(Q^{n-1}_{\mu_2})$$

$$R(1,7) = ne_3 \cot\phi \,\mathrm{Re}(Q^n_{\mu_2}) - ne_2 \cot\phi \,\mathrm{Im}(Q^n_{\mu_2}) - (e_3c_2 - e_2c_3)\,\mathrm{Re}(Q^{n-1}_{\mu_2}) + (e_2c_2 + e_3c_3)\,\mathrm{Im}(Q^{n-1}_{\mu_2})$$

$$R(1,8) = -\frac{n^2}{2\sin\phi} Q^n_1$$

$$R(2,1) = P^n_{\mu_1}$$

$$R(2,2) = \mathrm{Re}(P^n_{\mu_2})$$

$$R\left(2,3\right) = \mathrm{Im}(P^n_{\mu_2})$$

$$R\left(2,4\right) = 0$$

$$R(2,5) = Q^n_{\mu_1}$$

$$R(2,6) = \mathrm{Re}(Q^n_{\mu_2})$$

$$R\left(2,7\right) = \mathrm{Im}(Q^n_{\mu_2})$$

$$R\left(2,8\right) = 0$$

$$R\left(3,1\right) = -ne_1 \frac{1}{\sin\phi} P^n_{\mu_1}$$

$$R(3,2) = -ne_2 \frac{1}{\sin\phi}\mathrm{Re}(P^n_{\mu_2}) - ne_3 \frac{1}{\sin\phi}\mathrm{Im}(P^n_{\mu_2})$$

$$R(3,3) = ne_3 \frac{1}{\sin\phi}\mathrm{Re}(P^n_{\mu_2}) - ne_2 \frac{1}{\sin\phi}\mathrm{Im}(P^n_{\mu_2})$$

$$R(3,4) = -\frac{n^2}{2}\cot\phi P^n_1 + \frac{n}{2}(n-2)(n+1)P^{n-1}_1$$

$$R(3,5) = -ne_1 \frac{1}{\sin\phi} Q^n_{\mu_1}$$

$$R(3,6) = -ne_2 \frac{1}{\sin\phi}\mathrm{Re}(Q^n_{\mu_2}) - ne_3 \frac{1}{\sin\phi}\mathrm{Im}(Q^n_{\mu_2})$$

$$R(3,7) = ne_3 \frac{1}{\sin\phi}\mathrm{Re}(Q^n_{\mu_2}) - ne_2 \frac{1}{\sin\phi}\mathrm{Im}(Q^n_{\mu_2})$$

$$R(3,8) = -\frac{n^2}{2}\cot\phi Q^n_1 + \frac{n}{2}(n-2)(n+1)Q^{n-1}_1$$

$$A(1,j) = R(1,j),\quad A(2,j) = R(2,j),\quad A(3,j) = \frac{dw_n}{d\phi}(j),\quad A(4,j) = R(3,j) \text{ with } \phi = \phi_i$$

$$A(5,j) = R(1,j),\ A(6,j) = R(2,j)\ ;\ A(7,j) = \frac{dw_n}{d\phi}(j),\ A(8,j) = R(3,j) \text{ with } \phi = \phi_j$$

j=1,…, 8

$$Q(1,1)=\frac{1}{R}\left[e_1c_1+ne_1(\frac{1}{\sin^2\phi}+n\cot^2\phi)+1\right]P_{\mu_1}^n-\frac{e_1}{r}c_1\cot\phi P_{\mu_1}^{n-1}$$

$$Q(1,2)=\frac{1}{R}\left[\left(e_2c_2+e_3c_3\right)+ne_2(\frac{1}{\sin^2\phi}+n\cot^2\phi)+1\right]\mathrm{Re}(P_{\mu_2}^n)$$
$$+\frac{1}{R}\left[\left(e_3c_2-e_2c_3\right)+ne_3(\frac{1}{\sin^2\phi}+n\cot^2\phi)\right]\mathrm{Im}(P_{\mu_2}^n)$$
$$-\frac{1}{R}\left(e_2c_2+e_3c_3\right)\cot\phi\,\mathrm{Re}(P_{\mu_2}^{n-1})-\frac{1}{R}\left(e_3c_2-e_2c_3\right)\cot\phi\,\mathrm{Im}(P_{\mu_2}^{n-1})$$

$$Q(1,3)=-\frac{1}{R}\left[\left(e_3c_2-e_2c_3\right)+ne_3(\frac{1}{\sin^2\phi}+n\cot^2\phi)\right]\mathrm{Re}(P_{\mu_2}^n)$$
$$+\frac{1}{R}\left[\left(e_2c_2+e_3c_3\right)+ne_2(\frac{1}{\sin^2\phi}+n\cot^2\phi)+1\right]\mathrm{Im}(P_{\mu_2}^n)$$
$$+\frac{1}{R}\left(e_3c_2-e_2c_3\right)\cot\phi\,\mathrm{Re}(P_{\mu_2}^{n-1})-\frac{1}{R}\left(e_2c_2+e_3c_3\right)\cot\phi\,\mathrm{Im}(P_{\mu_2}^{n-1})$$

$$Q(1,4)=\frac{n^2}{2R}(n+1)\frac{1}{\sin\phi}\cot\phi P_1^n-\frac{n^2}{2R}(n-2)(n+1)\frac{1}{\sin\phi}P_1^{n-1}$$

$$Q(1,5)=\frac{1}{R}\left[e_1c_1+ne_1(\frac{1}{\sin^2\phi}+n\cot^2\phi)+1\right]Q_{\mu_1}^n-\frac{e_1}{r}c_1\cot\phi Q_{\mu_1}^{n-1}$$

$$Q(1,6)=\frac{1}{R}\left[\left(e_2c_2+e_3c_3\right)+ne_2(\frac{1}{\sin^2\phi}+n\cot^2\phi)+1\right]\mathrm{Re}(Q_{\mu_2}^n)$$
$$+\frac{1}{R}\left[\left(e_3c_2-e_2c_3\right)+ne_3(\frac{1}{\sin^2\phi}+n\cot^2\phi)\right]\mathrm{Im}(Q_{\mu_2}^n)$$
$$-\frac{1}{R}\left(e_2c_2+e_3c_3\right)\cot\phi\,\mathrm{Re}(Q_{\mu_2}^{n-1})-\frac{1}{R}\left(e_3c_2-e_2c_3\right)\cot\phi\,\mathrm{Im}(Q_{\mu_2}^{n-1})$$

$$Q(1,7)=-\frac{1}{R}\left[\left(e_3c_2-e_2c_3\right)+ne_3(\frac{1}{\sin^2\phi}+n\cot^2\phi)\right]\mathrm{Re}(Q_{\mu_2}^n)$$
$$+\frac{1}{R}\left[\left(e_2c_2+e_3c_3\right)+ne_2(\frac{1}{\sin^2\phi}+n\cot^2\phi)+1\right]\mathrm{Im}(Q_{\mu_2}^n)$$
$$+\frac{1}{R}\left(e_3c_2-e_2c_3\right)\cot\phi\,\mathrm{Re}(Q_{\mu_2}^{n-1})-\frac{1}{R}\left(e_2c_2+e_3c_3\right)\cot\phi\,\mathrm{Im}(Q_{\mu_2}^{n-1})$$

$$Q(1,8)=\frac{n^2}{2R}(n+1)\frac{1}{\sin\phi}\cot\phi Q_1^n-\frac{n^2}{2R}(n-2)(n+1)\frac{1}{\sin\phi}Q_1^{n-1}$$

$$Q(2,1)=\frac{1}{R}\left[1-ne_1(n\frac{1}{\sin^2\phi}+\cot^2\phi)\right]P_{\mu_1}^n+\frac{e_1}{r}c_1\cot\phi P_{\mu_1}^{n-1}$$

$$Q(2,2)=\frac{1}{R}\left[1-ne_2(n\frac{1}{\sin^2\phi}+\cot^2\phi)\right]\mathrm{Re}(P_{\mu_2}^n)-\frac{ne_3}{R}(n\frac{1}{\sin^2\phi}+\cot^2\phi)\,\mathrm{Im}(P_{\mu_2}^n)$$
$$+\frac{1}{R}(e_2c_2+e_3c_3)\cot\phi\,\mathrm{Re}(P_{\mu_2}^{n-1})+\frac{1}{R}(e_3c_2-e_2c_3)\cot\phi\,\mathrm{Im}(P_{\mu_2}^{n-1})$$

$$Q(2,3)=\frac{ne_3}{R}(n\frac{1}{\sin^2\phi}+\cot^2\phi)\,\mathrm{Re}(P_{\mu_2}^n)+\frac{1}{R}\left[1-ne_2(n\frac{1}{\sin^2\phi}+\cot^2\phi)\right]\mathrm{Im}(P_{\mu_2}^n)$$
$$-\frac{1}{R}(e_3c_2-e_2c_3)\cot\phi\,\mathrm{Re}(P_{\mu_2}^{n-1})+\frac{1}{R}(e_2c_2+e_3c_3)\cot\phi\,\mathrm{Im}(P_{\mu_2}^{n-1})$$

$$Q(2,4)=-\frac{n^2}{2R}(n+1)\frac{1}{\sin\phi}\cot\phi P_1^n+\frac{n^2}{2R}(n-2)(n+1)\frac{1}{\sin\phi}P_1^{n-1}$$

$$Q(2,5)=\frac{1}{R}\left[1-ne_1(\frac{1}{\sin^2\phi}+n\cot^2\phi)\right]Q_{\mu_1}^n+\frac{e_1}{r}c_1\cot\phi Q_{\mu_1}^{n-1}$$

$$Q(2,6)=\frac{1}{R}\left[1-ne_2(n\frac{1}{\sin^2\phi}+\cot^2\phi)\right]\mathrm{Re}(Q_{\mu_2}^n)-\frac{ne_3}{R}(n\frac{1}{\sin^2\phi}+\cot^2\phi)\,\mathrm{Im}(Q_{\mu_2}^n)$$
$$+\frac{1}{R}(e_2c_2+e_3c_3)\cot\phi\,\mathrm{Re}(Q_{\mu_2}^{n-1})+\frac{1}{R}(e_3c_2-e_2c_3)\cot\phi\,\mathrm{Im}(Q_{\mu_2}^{n-1})$$

$$Q(2,7)=\frac{ne_3}{R}(n\frac{1}{\sin^2\phi}+\cot^2\phi)\,\mathrm{Re}(Q_{\mu_2}^n)+\frac{1}{R}\left[1-ne_2(n\frac{1}{\sin^2\phi}+\cot^2\phi)\right]\mathrm{Im}(Q_{\mu_2}^n)$$
$$-\frac{1}{R}(e_3c_2-e_2c_3)\cot\phi\,\mathrm{Re}(Q_{\mu_2}^{n-1})+\frac{1}{R}(e_2c_2+e_3c_3)\cot\phi\,\mathrm{Im}(Q_{\mu_2}^{n-1})$$

$$Q(2,8)=-\frac{n^2}{2R}(n+1)\frac{1}{\sin\phi}\cot\phi Q_1^n+\frac{n^2}{2R}(n-2)(n+1)\frac{1}{\sin\phi}Q_1^{n-1}$$

$$Q(3,1)=\frac{2n}{R}e_1(n+1)\frac{1}{\sin\phi}\cot\phi P^n_{\mu_1}-\frac{2n}{R}e_1c_1\frac{1}{\sin\phi}P^{n-1}_{\mu_1}$$

$$Q(3,2)=\frac{2n}{R}e_2(n+1)\frac{1}{\sin\phi}\cot\phi\,\mathrm{Re}(P^n_{\mu_2})+\frac{2n}{R}e_3(n+1)\frac{1}{\sin\phi}\cot\phi\,\mathrm{Im}(P^n_{\mu_2})$$
$$-\frac{2n}{R}(e_2c_2+e_3c_3)\frac{1}{\sin\phi}\mathrm{Re}(P^{n-1}_{\mu_2})-\frac{2n}{R}(e_3c_2-e_2c_3)\frac{1}{\sin\phi}\mathrm{Im}(P^{n-1}_{\mu_2})$$

$$Q(3,3)=-\frac{2n}{R}e_3(n+1)\frac{1}{\sin\phi}\cot\phi\,\mathrm{Re}(P^n_{\mu_2})+\frac{2n}{R}e_2(n+1)\frac{1}{\sin\phi}\cot\phi\,\mathrm{Im}(P^n_{\mu_2})$$
$$+\frac{2n}{R}(e_3c_2-e_2c_3)\frac{1}{\sin\phi}\mathrm{Re}(P^{n-1}_{\mu_2})-\frac{2n}{R}(e_2c_2+e_3c_3)\frac{1}{\sin\phi}\mathrm{Im}(P^{n-1}_{\mu_2})$$

$$Q(3,4)=\frac{n}{2R}(n+1)\left[(n-2)+n\left(\frac{1}{\sin^2\phi}+\cot^2\phi\right)\right]P^n_1-\frac{n}{R}(n-2)(n+1)\cot\phi P^{n-1}_1$$

$$Q(3,5)=\frac{2n}{R}e_1(n+1)\frac{1}{\sin\phi}\cot\phi Q^n_{\mu_1}-\frac{2n}{R}c_1\frac{1}{\sin\phi}Q^{n-1}_{\mu_1}$$

$$Q(3,6)=\frac{2n}{R}e_2(n+1)\frac{1}{\sin\phi}\cot\phi\,\mathrm{Re}(Q^n_{\mu_2})+\frac{2n}{R}e_3(n+1)\frac{1}{\sin\phi}\cot\phi\,\mathrm{Im}(Q^n_{\mu_2})$$
$$-\frac{2n}{R}(e_2c_2+e_3c_3)\frac{1}{\sin\phi}\mathrm{Re}(Q^{n-1}_{\mu_2})-\frac{2n}{R}(e_3c_2-e_2c_3)\frac{1}{\sin\phi}\mathrm{Im}(Q^{n-1}_{\mu_2})$$

$$Q(3,7)=-\frac{2n}{R}e_3(n+1)\frac{1}{\sin\phi}\cot\phi\,\mathrm{Re}(Q^n_{\mu_2})+\frac{2n}{R}e_2(n+1)\frac{1}{\sin\phi}\cot\phi\,\mathrm{Im}(Q^n_{\mu_2})$$
$$+\frac{2n}{R}(e_3c_2-e_2c_3)\frac{1}{\sin\phi}\mathrm{Re}(Q^{n-1}_{\mu_2})-\frac{2n}{R}(e_2c_2+e_3c_3)\frac{1}{\sin\phi}\mathrm{Im}(Q^{n-1}_{\mu_2})$$

$$Q(3,8)=\frac{n}{2R}(n+1)\left[(n-2)+n\left(\frac{1}{\sin^2\phi}+\cot^2\phi\right)\right]Q^n_1-\frac{n}{R}(n-2)(n+1)\cot\phi Q^{n-1}_1$$

$$Q(4,1)=\frac{1}{R^2}\left[\left(e_1-1\right)c_1+n\left(e_1-1\right)\left(\frac{1}{\sin^2\phi}+n\cot^2\phi\right)\right]P_{\mu_1}^n-\frac{e_1-1}{R^2}c_1\cot\phi P_{\mu_1}^{n-1}$$

$$\begin{aligned}Q(4,2)=&\frac{1}{R^2}\left[\left(e_2-1\right)c_2+e_3c_3+n\left(e_2-1\right)\left(\frac{1}{\sin^2\phi}+n\cot^2\phi\right)\right]\mathrm{Re}\left(P_{\mu_2}^n\right)\\&+\frac{1}{R^2}\left[e_3c_2-\left(e_2-1\right)c_3+ne_3\left(\frac{1}{\sin^2\phi}+n\cot^2\phi\right)\right]\mathrm{Im}\left(P_{\mu_2}^n\right)\\&-\frac{1}{R^2}\left[\left(e_2-1\right)c_2+e_3c_3\right]\cot\phi\,\mathrm{Re}\left(P_{\mu_2}^{n-1}\right)-\frac{1}{R^2}\left[e_3c_2-\left(e_2-1\right)c_3\right]\cot\phi\,\mathrm{Im}\left(P_{\mu_2}^{n-1}\right)\end{aligned}$$

$$\begin{aligned}Q(4,3)=&-\frac{1}{R^2}\left[e_3c_2-\left(e_2-1\right)c_3+ne_3\left(\frac{1}{\sin^2\phi}+n\cot^2\phi\right)\right]\mathrm{Re}\left(P_{\mu_2}^n\right)\\&+\frac{1}{R^2}\left[\left(e_2-1\right)c_2+e_3c_3+n\left(e_2-1\right)\left(\frac{1}{\sin^2\phi}+n\cot^2\phi\right)\right]\mathrm{Im}\left(P_{\mu_2}^n\right)\\&+\frac{1}{R^2}\left[e_3c_2-\left(e_2-1\right)c_3\right]\cot\phi\,\mathrm{Re}\left(P_{\mu_2}^{n-1}\right)-\frac{1}{R^2}\left[\left(e_2-1\right)c_2+e_3c_3\right]\cot\phi\,\mathrm{Im}\left(P_{\mu_2}^{n-1}\right)\end{aligned}$$

$$Q(4,4)=\frac{n^2}{2R^2}\left(n+1\right)\frac{1}{\sin\phi}\cot\phi P_1^n-\frac{n^2}{2R^2}(n-2)(n+1)\frac{1}{\sin\phi}P_1^{n-1}$$

$$Q(4,5)=\frac{1}{R^2}\left[\left(e_1-1\right)c_1+n\left(e_1-1\right)\left(\frac{1}{\sin^2\phi}+n\cot^2\phi\right)\right]Q_{\mu_1}^n-\frac{e_1-1}{R^2}c_1\cot\phi Q_{\mu_1}^{n-1}$$

$$\begin{aligned}Q(4,6)=&\frac{1}{R^2}\left[\left(e_2-1\right)c_2+e_3c_3+n\left(e_2-1\right)\left(\frac{1}{\sin^2\phi}+n\cot^2\phi\right)\right]\mathrm{Re}\left(Q_{\mu_2}^n\right)\\&+\frac{1}{R^2}\left[e_3c_2-\left(e_2-1\right)c_3+ne_3\left(\frac{1}{\sin^2\phi}+n\cot^2\phi\right)\right]\mathrm{Im}\left(Q_{\mu_2}^n\right)\\&-\frac{1}{R^2}\left[\left(e_2-1\right)c_2+e_3c_3\right]\cot\phi\,\mathrm{Re}\left(Q_{\mu_2}^{n-1}\right)-\frac{1}{R^2}\left[e_3c_2-\left(e_2-1\right)c_3\right]\cot\phi\,\mathrm{Im}\left(Q_{\mu_2}^{n-1}\right)\end{aligned}$$

$$\begin{aligned}Q(4,7)=&-\frac{1}{R^2}\left[e_3c_2-\left(e_2-1\right)c_3+ne_3\left(\frac{1}{\sin^2\phi}+n\cot^2\phi\right)\right]\mathrm{Re}\left(Q_{\mu_2}^n\right)\\&+\frac{1}{R^2}\left[\left(e_2-1\right)c_2+e_3c_3+n\left(e_2-1\right)\left(\frac{1}{\sin^2\phi}+n\cot^2\phi\right)\right]\mathrm{Im}\left(Q_{\mu_2}^n\right)\\&+\frac{1}{R^2}\left[e_3c_2-\left(e_2-1\right)c_3\right]\cot\phi\,\mathrm{Re}\left(Q_{\mu_2}^{n-1}\right)-\frac{1}{R^2}\left[\left(e_2-1\right)c_2+e_3c_3\right]\cot\phi\,\mathrm{Im}\left(Q_{\mu_2}^{n-1}\right)\end{aligned}$$

$$Q(4,8)=\frac{n^2}{2R^2}\left(n+1\right)\frac{1}{\sin\phi}\cot\phi Q_1^n-\frac{n^2}{2R^2}(n-2)(n+1)\frac{1}{\sin\phi}Q_1^{n-1}$$

$$Q(5,1)=\frac{n}{R^2}(1-e_1)\left(\cot^2\phi+n\frac{1}{\sin^2\phi}\right)P_{\mu_1}^n+\frac{(e_1-1)}{R^2}c_1\cot\phi P_{\mu_1}^{n-1}$$

$$Q(5,2)=\frac{n}{R^2}(1-e_2)\left(\cot^2\phi+n\frac{1}{\sin^2\phi}\right)\mathrm{Re}\left(P_{\mu_2}^n\right)-\frac{ne_3}{R^2}\left(\cot^2\phi+n\frac{1}{\sin^2\phi}\right)\mathrm{Im}\left(P_{\mu_2}^n\right)$$
$$+\frac{1}{R^2}\left[(e_2-1)c_2+e_3c_3\right]\cot\phi\,\mathrm{Re}\left(P_{\mu_2}^{n-1}\right)+\frac{1}{R^2}\left[e_3c_2-(e_2-1)c_3\right]\cot\phi\,\mathrm{Im}\left(P_{\mu_2}^{n-1}\right)$$

$$Q(5,3)=\frac{ne_3}{R^2}\left(\cot^2\phi+n\frac{1}{\sin^2\phi}\right)\mathrm{Re}\left(P_{\mu_2}^n\right)+\frac{n}{R^2}(1-e_2)\left(\cot^2\phi+n\frac{1}{\sin^2\phi}\right)\mathrm{Im}\left(P_{\mu_2}^n\right)$$
$$-\frac{1}{R^2}\left[e_3c_2-(e_2-1)c_3\right]\cot\phi\,\mathrm{Re}\left(P_{\mu_2}^{n-1}\right)+\frac{1}{R^2}\left[(e_2-1)c_2+e_3c_3\right]\cot\phi\,\mathrm{Im}\left(P_{\mu_2}^{n-1}\right)$$

$$Q(5,4)=-\frac{n}{2R^2}(n+1)\frac{1}{\sin\phi}\cot\phi P_1^n+\frac{n}{2R^2}(n-2)(n+1)\frac{1}{\sin\phi}P_1^{n-1}$$

$$Q(5,5)=\frac{n}{R^2}(1-e_1)\left(\cot^2\phi+n\frac{1}{\sin^2\phi}\right)Q_{\mu_1}^n+\frac{(e_1-1)}{R^2}c_1\cot\phi Q_{\mu_1}^{n-1}$$

$$Q(5,6)=\frac{n}{R^2}(1-e_2)\left(\cot^2\phi+n\frac{1}{\sin^2\phi}\right)\mathrm{Re}\left(Q_{\mu_2}^n\right)-\frac{ne_3}{R^2}\left(\cot^2\phi+n\frac{1}{\sin^2\phi}\right)\mathrm{Im}\left(Q_{\mu_2}^n\right)$$
$$+\frac{1}{R^2}\left[(e_2-1)c_2+e_3c_3\right]\cot\phi\,\mathrm{Re}\left(Q_{\mu_2}^{n-1}\right)+\frac{1}{R^2}\left[e_3c_2-(e_2-1)c_3\right]\cot\phi\,\mathrm{Im}\left(Q_{\mu_2}^{n-1}\right)$$

$$Q(5,7)=\frac{ne_3}{R^2}\left(\cot^2\phi+n\frac{1}{\sin^2\phi}\right)\mathrm{Re}\left(Q_{\mu_2}^n\right)+\frac{n}{R^2}(1-e_2)\left(\cot^2\phi+n\frac{1}{\sin^2\phi}\right)\mathrm{Im}\left(Q_{\mu_2}^n\right)$$
$$-\frac{1}{R^2}\left[e_3c_2-(e_2-1)c_3\right]\cot\phi\,\mathrm{Re}\left(Q_{\mu_2}^{n-1}\right)+\frac{1}{R^2}\left[(e_2-1)c_2+e_3c_3\right]\cot\phi\,\mathrm{Im}\left(Q_{\mu_2}^{n-1}\right)$$

$$Q(5,8)=-\frac{n}{2R^2}(n+1)\frac{1}{\sin\phi}\cot\phi Q_1^n+\frac{n}{2R^2}(n-2)(n+1)\frac{1}{\sin\phi}Q_1^{n-1}$$

$$Q(6,1)=\frac{2n}{R^2}(n+1)(e_1-1)\frac{1}{\sin\phi}\cot\phi P^n_{\mu_1}+\frac{2n}{R^2}(1-e_1)c_1\frac{1}{\sin\phi}P^{n-1}_{\mu_1}$$

$$Q(6,2)=\frac{2n(n+1)}{R^2}(e_2-1)\frac{1}{\sin\phi}\cot\phi\,\mathrm{Re}\left(P^n_{\mu_2}\right)+\frac{2n(n+1)}{R^2}e_3\frac{1}{\sin\phi}\cot\phi\,\mathrm{Im}\left(P^n_{\mu_2}\right)$$
$$-\frac{2n}{R^2}\left[(e_2-1)c_2+e_3c_3\right]\frac{1}{\sin\phi}\mathrm{Re}\left(P^{n-1}_{\mu_2}\right)-\frac{2n}{R^2}\left[e_3c_2-(e_2-1)c_3\right]\frac{1}{\sin\phi}\mathrm{Im}\left(P^{n-1}_{\mu_2}\right)$$

$$Q(6,3)=-\frac{2n(n+1)}{R^2}e_3\frac{1}{\sin\phi}\cot\phi\,\mathrm{Re}\left(P^n_{\mu_2}\right)+\frac{2n(n+1)}{R^2}(e_2-1)\frac{1}{\sin\phi}\cot\phi\,\mathrm{Im}\left(P^n_{\mu_2}\right)$$
$$+\frac{2n}{R^2}\left[e_3c_2-(e_2-1)c_3\right]\frac{1}{\sin\phi}\mathrm{Re}\left(P^{n-1}_{\mu_2}\right)-\frac{2n}{R^2}\left[(e_2-1)c_2+e_3c_3\right]\frac{1}{\sin\phi}\mathrm{Im}\left(P^{n-1}_{\mu_2}\right)$$

$$Q(6,4)=\frac{n}{2R^2}(n+1)\left[(n-2)+n\left(\frac{1}{\sin^2\phi}+\cot^2\phi\right)\right]P^n_1-\frac{n}{R^2}(n-2)(n+1)\cot\phi P^{n-1}_1$$

$$Q(6,5)=\frac{2n}{R^2}(n+1)(e_1-1)\frac{1}{\sin\phi}\cot\phi Q^n_{\mu_1}+\frac{2n}{R^2}(1-e_1)c_1\frac{1}{\sin\phi}Q^{n-1}_{\mu_1}$$

$$Q(6,6)=\frac{2n(n+1)}{R^2}(e_2-1)\frac{1}{\sin\phi}\cot\phi\,\mathrm{Re}\left(Q^n_{\mu_2}\right)+\frac{2n(n+1)}{R^2}e_3\frac{1}{\sin\phi}\cot\phi\,\mathrm{Im}\left(Q^n_{\mu_2}\right)$$
$$-\frac{2n}{R^2}\left[(e_2-1)c_2+e_3c_3\right]\frac{1}{\sin\phi}\mathrm{Re}\left(Q^{n-1}_{\mu_2}\right)-\frac{2n}{R^2}\left[e_3c_2-(e_2-1)c_3\right]\frac{1}{\sin\phi}\mathrm{Im}\left(Q^{n-1}_{\mu_2}\right)$$

$$Q(6,7)=-\frac{2n(n+1)}{R^2}e_3\frac{1}{\sin\phi}\cot\phi\,\mathrm{Re}\left(Q^n_{\mu_2}\right)+\frac{2n(n+1)}{R^2}(e_2-1)\frac{1}{\sin\phi}\cot\phi\,\mathrm{Im}\left(Q^n_{\mu_2}\right)$$
$$+\frac{2n}{R^2}\left[e_3c_2-(e_2-1)c_3\right]\frac{1}{\sin\phi}\mathrm{Re}\left(Q^{n-1}_{\mu_2}\right)-\frac{2n}{R^2}\left[(e_2-1)c_2+e_3c_3\right]\frac{1}{\sin\phi}\mathrm{Im}\left(Q^{n-1}_{\mu_2}\right)$$

$$Q(6,8)=\frac{n}{2R^2}(n+1)\left[(n-2)+n\left(\frac{1}{\sin^2\phi}+\cot^2\phi\right)\right]Q^n_1-\frac{n}{R^2}(n-2)(n+1)\cot\phi Q^{n-1}_1$$

In deriving the above relation we used the recursive relations:

$$\frac{d^2P^n_\mu}{d\phi^2}=\left[(n-\mu-1)(n+\mu)+n\left(\frac{1}{\sin^2\phi}+n\cot^2\phi\right)\right]P^n_\mu-\cot\phi(n-\mu-1)(n+\mu)P^{n-1}_\mu$$

$$\frac{d^2Q^n_\mu}{d\phi^2}=\left[(n-\mu-1)(n+\mu)+n\left(\frac{1}{\sin^2\phi}+n\cot^2\phi\right)\right]Q^n_\mu-\cot\phi(n-\mu-1)(n+\mu)Q^{n-1}_\mu$$

References

[1] A. Kalnins, Free non-symmetric vibrations of shallow spherical shells, *J. Acoust. Soc. Am.,* **33** (1961) 1102-1107.

[2] A. Kalnins, Effect of bending on vibration of spherical shell, *J. Acoust. Soc. Am.,* **36** (1964) 74-81.

[3] G.A. Cohen, Computer analysis of asymmetric free vibrations of ring stiffened orthotropic shells of revolution, *AIAA J.,* **3** (1965) 2305-2312.

[4] D. R. Navaratna, Natural Vibration of Deep Spherical Shells, *AIAA J.*, **4** (1966) 2056-2058.

[5] J.J. Webster, Free vibrations of shells of revolution using ring finite elements, *Int. J. Mech. Sci.* **9** (1967) 559-570.

[6] H. Kraus, *Thin elastic shells* (John Wiley and Sons, New York, 1967).

[7] B.E. Greene, R.E. Jones, R.W. Mc Lay and D.R.Strome, Dynamic analysis of shells using doubly curved finite elements, Proceedings of The Second Conference on Matrix methods in Structural Mechanics, TR-68-150(1968) 185-212

[8] A.Tessler, L. Spirichigliozzi, Resolving membrane and shear locking phenomena in curved deformable axisymmetric shell element, *Int. J. for Num. Meth. Eng.*, **26**(1988) 1071-1080.

[9] M.C. Narasimhan, R.S. Alwar, Free vibration analysis of laminated orthotropic spherical shell, *J. Sound Vibr.,* **54**(1992) 515-529.

[10] B. P. Gautham, N. Ganesan, Free vibration analysis of thick spherical shells, *Comp. Struct. J.*, **45**(1992) 307-313.

[11] B. P. Gautham, N. Ganesan, Free vibration characteristics of isotropic and laminated orthotropic shell caps, *J. Sound Vibr.,* **204**(1997) 17-40.

[12] K.S. Sai Ram, T. Sreedhar Babu, Free vibration of composite spherical shell cap with and without a cutout, *Comp. Struct. J.,* **80**(2002) 1749-1756.

[13] G.R. Buchanan, B.S. Rich, Effect of boundary conditions on free vibrations of thick isotropic spherical shells, *J. Vib. Control,* 18(2002) 389-403.

[14] E.S. Ventsel, V. Naumenko, E. Strelnikova and E. Yeseleva, Free vibrations of shells of revolution filled with fluid, *J. Eng. Anal. Boundary Elem.,* **34**(2010) 856-862

CHAPITRE 3 : ARTICLE 2 – DYNAMICAL ANALYSIS OF SPHERICAL SHELL PARTIALLY FILLED WITH FLUID

Mohamed Menaa, Aouni A. Lakis.

Department of Mechanical Engineering, Ecole Polytechnique de Montreal, C.P. 6079 Succursale Centre-ville, Montréal, Canada H3C 3A7

Submitted, 22 may 2013 to Computers and Fluids Journal

Abstract

In the present study, a hybrid finite element method is applied to investigate the free vibration of spherical shell partially filled with fluid. The structural model is based on a combination of thin shell theory and the classical finite element method. It is assumed that the fluid is incompressible and has no free-surface effect. Fluid is considered as a velocity potential variable at each node of the shell element where its motion is expressed in terms of nodal elastic displacement at the fluid-structure interface. Numerical simulation is done and vibration frequencies for different filling ratios are obtained and compared with existing experimental and theoretical results. The dynamic behavior for different shell geometries, filling ratios and boundary conditions with different radius to thickness ratios is summarized. This proposed hybrid finite element method can be used efficiently for analyzing the dynamic behavior of aerospace structures at less computational cost than other commercial FEM software.

1. Introduction

Shells of revolution, particularly spherical shells are one of the primary structural elements in high speed aircraft. Their applications include the propellant tank or gas-deployed skirt of space crafts. Space shuttles need a large thrust within a short time interval; thus a large propellant tank is required. Dynamic behavior in the lightweight, thin-walled tank is an important aspect in its design. These liquid propelled space launch vehicles experience a significant longitudinal disturbance during thrust build up and also due to the effect of launch mechanism. Dynamic analysis of such a problem in the presence of fluid-structure interaction is one of the challenging subjects in aerospace engineering. Great care must be taken during the design of spacecraft vehicles to prevent dynamic instability.

Free vibration of spherical shell containing a fluid has been investigated by few researchers experimentally and analytically. Rayleigh [1] solved the problem of axisymmetric vibrations of a fluid in a rigid spherical shell. The solution for vibrations of the fluid-filled spherical membrane appears in the work of Morse and Feshbach [2].

The fluid movement on the surface of fluid (sloshing) in non-deformable spherical shell has been investigated by a few researchers such as Budiansky [3], Stofan and Armsted [4], Chu [5], Karamanos et al. [6]. The oscillations of the fluid masses result from the lateral displacement or angular rotation of the spherical shell. Others researchers have studied particular cases like the case of a sphere filled with fluid. Rand and Dimaggio [7] considered the free vibrations for axisymmetric, extensional and non-torsional of fluid-filled elastic spherical shells. Motivated by the fact that human head can be represented as a spherical shell filled by fluid, Engin and Liu [8] considered the free vibration of a thin homogenous spherical shell containing an inviscid irrotational fluid. Advani and Lee [9] investigated the vibration of the fluid-filled shell using higher-order shell theory including transverse shear and rotational inertia. Guarino and Elger [11] have looked at the frequency spectra of a fluid-filled sphere, both with and without a central solid sphere, in order to explore the use of auscultatory percussion as a clinical diagnostic tool. Free vibration of a thin spherical shell filled with a compressible fluid is investigated by Bai and Wu [12].The general non-axisymmetric free vibration of a spherically isotropic elastic spherical shell filled with a compressible fluid medium has been investigated by Chen and Ding [13]. Young [14] studied the free vibration of spheres composed of inviscid compressible liquid cores surrounded by spherical layers of linear elastic, homogeneous and isotropic materials.

The case of hemispherical shells filled with fluid was studied experimentally by Samoilov and Pavlov [15]. Hwang [16] investigated the case of the longitudinal sloshing of liquid in a flexible hemispherical tank supported along the edge. Chung and Rush [17] presented a rigorous and consistent formulation of dynamically coupled problems dealing with motion of a surface-fluid-shell system. A numerical example of a hemispherical bulkhead filled with fluid is modeled.

Komatsu [18] [19] used a hybrid method with a fluid mass coefficient added to his system of equations. He also validated his model with experiments on hemispherical shells partially filled with fluid under two boundary conditions: a clamped boundary condition and a free boundary

condition. Recently, Ventsel et al. [20] used a combined formulation of the boundary elements method and finite elements method to study the free vibration of an isotropic simply supported hemispherical shell with different circumferential mode numbers.

For a spherical shell that is partially liquid-filled, if one wishes to consider the hydroelastic vibration developed as a consequence of interaction between hydrodynamic pressure of liquid and elastic deformation of the shell, this is a complex problem. Numerical method such as the finite element method (FEM) are therefore used since they are powerful tools that can adequately describe the dynamic behavior of such system which contains complex structures, boundary conditions, materials and loadings. Some powerful commercial FEM software exists, such as ANSYS, ABAQUS and NASTRAN. When using these tools to model such a complex FSI problem, a large numbers of elements are required in order to get good convergence. The hybrid approach presented in this study provides very fast and precise convergence with less numerical cost compared to these commercial software packages.

In this work a combined formulation of shell theory and a hybrid finite element method (FEM) is applied to model the shell structure. Nodal displacements are found from exact solution of shell theory. This hybrid FEM has been applied to produce efficient and robust models during analysis of both cylindrical and conical shells. A spherical shell which has been filled partially with incompressible and inviscid is modeled in this study. The fluid is characterized as a velocity potential variable at each node of the shell finite element mesh; then fluid and structures are coupled through the linearized Bernoulli's equation and impermeable boundary condition at the fluid-structure interface. Dynamic analysis of the structure under various geometries, boundary conditions and filling ratios is analyze.

2. Formulation

2.1 Structural modeling

In this study the structure is modeled using hybrid finite element method which is a combination of spherical shell theory and classical finite element method. In this hybrid finite element method, the displacement functions are found from exact solution of spherical shell theory rather approximated by polynomial functions done in classical finite element method. In the spherical coordinate system (R,θ,ϕ) shown in Fig. 1, five out of the six equations of

equilibrium for spherical shells under external load are written as follows :

$$
\begin{aligned}
&\frac{\partial N_\phi}{\partial \phi}+\frac{1}{\sin\phi}\frac{\partial N_{\phi\theta}}{\partial \theta}+\left(N_\phi-N_\theta\right)\cot\phi+Q_\phi=0\\
&\frac{\partial N_{\phi\theta}}{\partial \phi}+\frac{1}{\sin\phi}\frac{\partial N_\theta}{\partial \theta}+2N_{\phi\theta}\cot\phi+Q_\theta=0\\
&\frac{\partial Q_\phi}{\partial \phi}+\frac{1}{\sin\phi}\frac{\partial Q_\theta}{\partial \theta}+Q_\phi\cot\phi-(N_\phi+N_\theta)=0\\
&\frac{\partial M_\phi}{\partial \phi}+\frac{1}{\sin\phi}\frac{\partial M_{\phi\theta}}{\partial \theta}+\left(M_\phi-M_\theta\right)\cot\phi-RQ_\phi=0\\
&\frac{\partial M_{\phi\theta}}{\partial \phi}+\frac{1}{\sin\phi}\frac{\partial M_\theta}{\partial \theta}+2M_{\phi\theta}\cot\phi-RQ_\theta=0
\end{aligned}
\tag{1}
$$

where N_ϕ, N_θ, $N_{\phi\theta}$ are membrane stress resultants; M_ϕ, M_θ, $M_{\phi\theta}$ the bending stress resultants and Q_ϕ, Q_θ the shear forces (Fig. 2). The sixth equation, which is an identity equation for spherical shells, is not presented here.

Strain and displacements for three displacements in axial U_ϕ, radial W and circumferential U_θ are related as follows:

$$
\{\varepsilon\}=\begin{Bmatrix}\varepsilon_\phi\\ \varepsilon_\theta\\ 2\varepsilon_{\phi\theta}\\ \kappa_\phi\\ \kappa_\theta\\ 2\kappa_{\phi\theta}\end{Bmatrix}=\begin{Bmatrix}\frac{1}{R}\left(\frac{\partial U_\phi}{\partial \phi}+W\right)\\ \frac{1}{R}\left(\frac{1}{\sin\phi}\frac{\partial U_\theta}{\partial \theta}+U_\phi\cot\phi+W\right)\\ \frac{1}{R}\left(\frac{\partial U_\theta}{\partial \phi}+\frac{1}{\sin\phi}\frac{\partial U_\phi}{\partial \theta}-U_\theta\cot\phi\right)\\ \frac{1}{R^2}\left(\frac{\partial U_\phi}{\partial \phi}-\frac{\partial^2 W}{\partial \phi^2}\right)\\ \frac{1}{R^2}\left(\frac{1}{\sin\phi}\frac{\partial U_\theta}{\partial \theta}+U_\phi\cot\phi-\frac{1}{\sin^2\phi}\frac{\partial^2 W}{\partial \theta^2}-\cot\phi\frac{\partial W}{\partial \phi}\right)\\ \frac{1}{R^2}\left(\frac{\partial U_\theta}{\partial \phi}+\frac{1}{\sin\phi}\frac{\partial U_\phi}{\partial \theta}-U_\theta\cot\phi+2\frac{1}{\sin\phi}\cot\phi\frac{\partial W}{\partial \theta}-2\frac{1}{\sin\phi}\frac{\partial^2 W}{\partial \phi\partial \theta}\right)\end{Bmatrix}
\tag{2}
$$

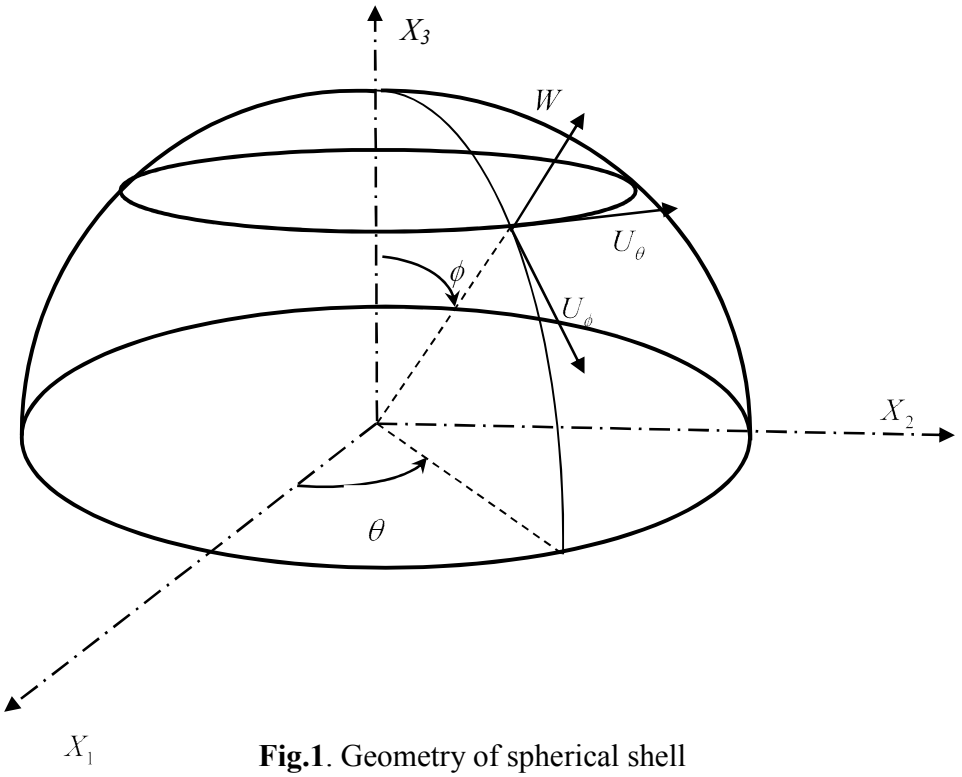

Fig.1. Geometry of spherical shell

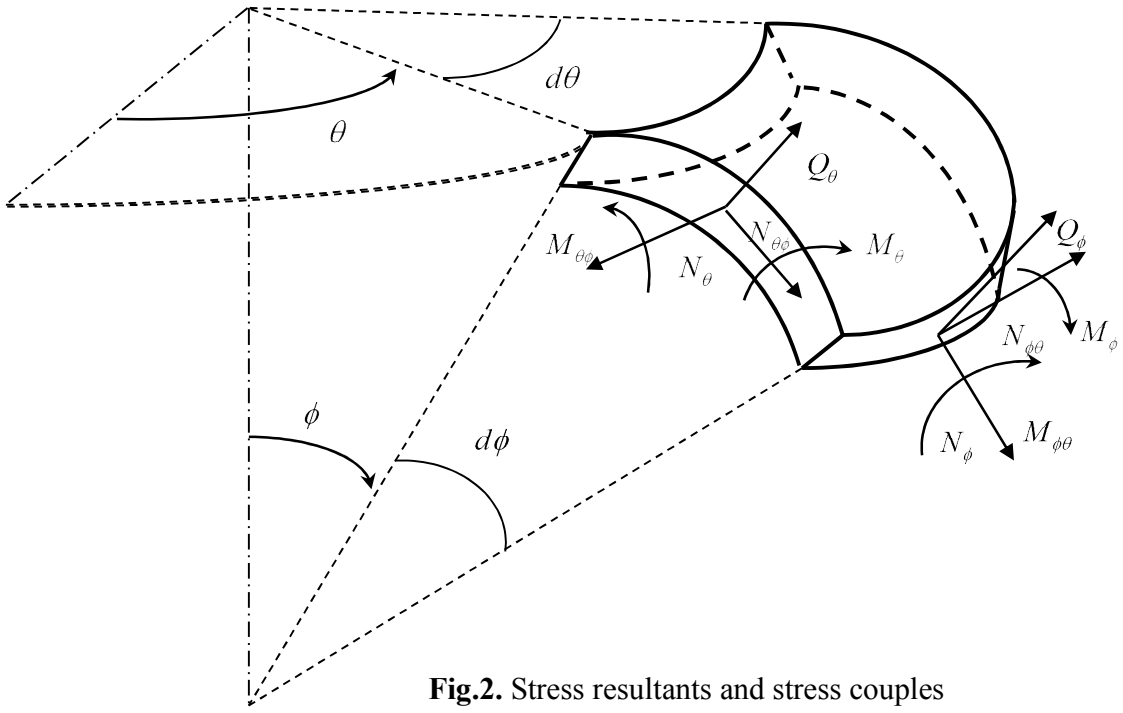

Fig.2. Stress resultants and stress couples

Displacements U, W and V in the global Cartesian coordinate system are related to displacements $U_{\phi i}$, W_i and $U_{\theta i}$ indicated in Fig 3. by:

$$\begin{Bmatrix} U \\ W \\ V \end{Bmatrix} = \begin{bmatrix} \sin\phi_i & -\cos\phi_i & 0 \\ \cos\phi_i & \sin\phi_i & 0 \\ 0 & 0 & 1 \end{bmatrix} \begin{Bmatrix} U_{\phi i} \\ W_i \\ U_{\theta i} \end{Bmatrix} \tag{3}$$

The stress vector $\{\sigma\}$ is expressed as function of strain $\{\varepsilon\}$ by

$$\{\sigma\} = [P]\{\varepsilon\} \tag{4}$$

where $[P]$ is the elasticity matrix for an anisotropic shell given by:

$$[P] = \begin{bmatrix} P_{11} & P_{12} & 0 & P_{14} & P_{15} & 0 \\ P_{21} & P_{22} & 0 & P_{24} & P_{25} & 0 \\ 0 & 0 & P_{33} & 0 & 0 & 0 \\ P_{41} & P_{42} & 0 & P_{44} & P_{45} & 0 \\ P_{51} & P_{52} & 0 & P_{54} & P_{55} & 0 \\ 0 & 0 & P_{36} & 0 & 0 & P_{66} \end{bmatrix} \tag{5}$$

Upon substitution of equations (2), (4) and (5) into equations (1), a system of equilibrium equations can be obtained as a function of displacements:

$$\begin{aligned} L_1\left(U_\phi, W, U_\theta, P_{ij}\right) &= 0 \\ L_2\left(U_\phi, W, U_\theta, P_{ij}\right) &= 0 \\ L_3\left(U_\phi, W, U_\theta, P_{ij}\right) &= 0 \end{aligned} \tag{6}$$

These three linear partial differentials operators L_1, L_2 and L_3 are given in [21], and P_{ij} are elements of the elasticity matrix, which, for an isotropic thin shell with thickness *h* is given by:

$$[P]=\begin{bmatrix} D & \nu D & 0 & 0 & 0 & 0 \\ \nu D & D & 0 & 0 & 0 & 0 \\ 0 & 0 & \dfrac{(1-\nu)D}{2} & 0 & 0 & 0 \\ 0 & 0 & 0 & K & \nu K & 0 \\ 0 & 0 & 0 & \nu K & K & 0 \\ 0 & 0 & 0 & 0 & 0 & \dfrac{(1-\nu)K}{2} \end{bmatrix} \tag{7}$$

where $D=\dfrac{Et}{1-\nu^2}$ is the membrane stiffness and $K=\dfrac{Et^3}{12(1-\nu^2)}$ is the bending stiffness.

The element is a circumferential spherical frustum shown in Fig. 3. It has two nodal circles with four degrees of freedom; axial, radial, circumferential and rotation at each node. This element type makes it possible to use thin shell equations easily to find the exact solution of displacement functions rather than an approximation with polynomial functions as done in classical finite element method

For motions associated with the *n*th circumferential wave number we may write:

$$\begin{Bmatrix} U_\phi(\phi,\theta) \\ W(\phi,\theta) \\ U_\theta(\phi,\theta) \end{Bmatrix}=\begin{bmatrix} \cos n\theta & 0 & 0 \\ 0 & \cos n\theta & 0 \\ 0 & 0 & \sin n\theta \end{bmatrix}\begin{Bmatrix} u_{\phi n}(\phi) \\ w_n(\phi) \\ u_{\theta n}(\phi) \end{Bmatrix}=[T]\begin{Bmatrix} u_{\phi n}(\phi) \\ w_n(\phi) \\ u_{\theta n}(\phi) \end{Bmatrix} \tag{8}$$

Using matrix formulation, the displacement functions can be expressed as follows:

$$\begin{Bmatrix} U_\phi(\phi,\theta) \\ W(\phi,\theta) \\ U_\theta(\phi,\theta) \end{Bmatrix}=[T]\begin{Bmatrix} u_{\phi n}(\phi) \\ w_n(\phi) \\ u_{\theta n}(\phi) \end{Bmatrix}=[T][R]\{C\} \tag{9}$$

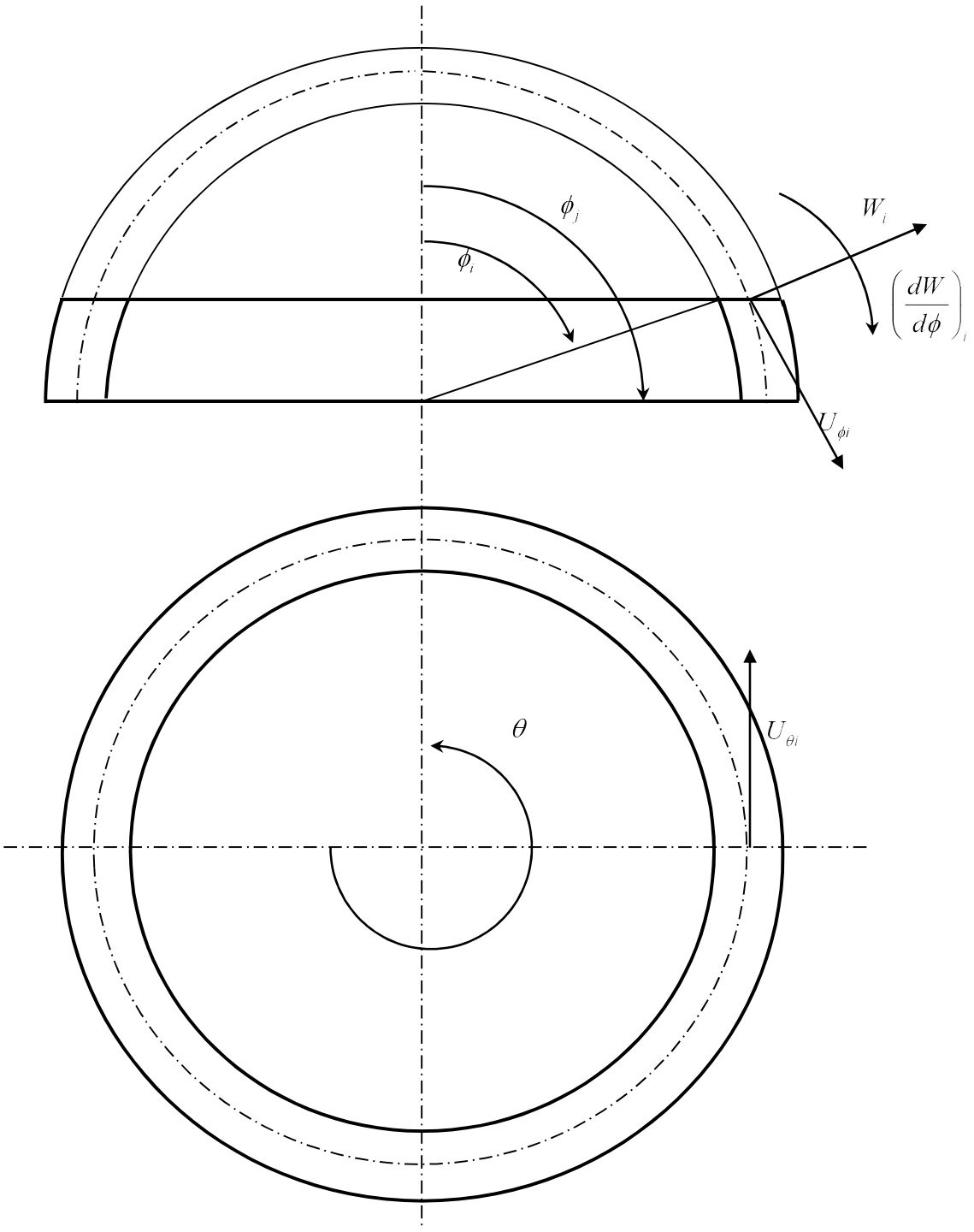

Fig. 3. Spherical frustum element

The vector $\{C\}$ is given by the expression:

$$\{C\}^T = \{A_1 \quad A_2 + A_3 \quad i(A_2 - A_3) \quad A_4 \quad B_1 \quad B_2 + B_3 \quad i(B_2 - B_3) \quad B_4\} \tag{10}$$

The elements of matrix $[R]$ and details of theory are given in the [21].

In the finite element method, the vector C is eliminated in favor of displacements at elements nodes. At each finite element node, the three displacements (axial, transversal and circumferential) and the rotation are applied. The displacement of node *i* are defined by the vector:

$$\{\delta_i\} = \left\{ u^i_{\phi n} \quad w^i_n \quad \left(\frac{dw_n}{dx}\right)^i \quad u^i_{\theta n} \right\}^T \tag{11}$$

The element in Fig. 3 with two nodal lines (*i* and *j*) and eight degrees of freedom will have the following nodal displacement vector:

$$\begin{Bmatrix} \delta_i \\ \delta_j \end{Bmatrix} = \left\{ u^i_{\phi n} \quad w^i_n \quad \left(\frac{dw_n}{d\phi}\right)^i \quad u^i_{\theta n} \quad u^j_{\phi n} \quad w^j_n \quad \left(\frac{dw_n}{d\phi}\right)^j \quad u^j_{\theta n} \right\}^T = [A]\{C\} \tag{12}$$

The terms of matrix $[A]$, obtained from the values of matrix $[R]$ and $\frac{dw_n}{dx}$, are given in [21]. Now, pre-multiplying by $[A]^{-1}$ equation (12) one obtains the matrix of the constant C_i as a function of the degree of freedom:

$$\{C\} = [A]^{-1} \begin{Bmatrix} \delta_i \\ \delta_j \end{Bmatrix} \tag{13}$$

Finally, one substitutes the vector $\{C\}$ into equation (13) and obtains the displacement functions as follows:

$$\begin{Bmatrix} U_\phi(\phi,\theta) \\ W(\phi,\theta) \\ U_\theta(\phi,\theta) \end{Bmatrix} = [T][R][A]^{-1} \begin{Bmatrix} \delta_i \\ \delta_j \end{Bmatrix} = [N] \begin{Bmatrix} \delta_i \\ \delta_j \end{Bmatrix} \tag{14}$$

The strain vector $\{\varepsilon\}$ can be determined from the displacement functions U_ϕ, U_θ,W and the deformation –displacement as:

$$\{\varepsilon\} = \begin{bmatrix} [T] & [0] \\ [0] & [T] \end{bmatrix} [Q]\{C\} = \begin{bmatrix} [T] & [0] \\ [0] & [T] \end{bmatrix} [Q][A]^{-1} \begin{Bmatrix} \delta_i \\ \delta_j \end{Bmatrix} = [B] \begin{Bmatrix} \delta_i \\ \delta_j \end{Bmatrix} \tag{15}$$

where matrix $[Q]$ is given [21].

This relation can be used to find the stress vector, equation (4), in terms of the nodal degrees of freedom vector:

$$\{\sigma\} = [P][B] \begin{Bmatrix} \delta_i \\ \delta_j \end{Bmatrix} \tag{16}$$

Based on the finite element formulation, the local stiffness and mass matrices are:

$$\begin{aligned} [k]_{loc} &= \iint_A [B]^T [P][B] dA \\ [m]_{loc} &= \rho\, h \iint_A [N]^T [N] dA \end{aligned} \tag{17}$$

where ρ is the density and h is the thickness of shell.

The surface element of the shell wall is $dA = R^2 \sin\phi d\phi d\theta$. After integrating over θ, the preceding equations become

$$[k]_{loc} = \left[A^{-1}\right]^T \left(\pi R^2 \int_{\phi_i}^{\phi_j} [Q]^T [P][Q] \sin\phi d\phi \right) \left[A^{-1}\right] = \left[A^{-1}\right]^T [G] \left[A^{-1}\right]$$

$$[m]_{loc} = \rho h\left[A^{-1}\right]^T \left(\pi R^2 \int_{\phi_i}^{\phi_j} [R]^T [R] \sin\phi d\phi\right)\left[A^{-1}\right] = \rho h\left[A^{-1}\right]^T [S]\left[A^{-1}\right] \tag{18}$$

In the global system the element stiffness and mass matrices are

$$\begin{aligned}[k] &= [LG]^T \left[A^{-1}\right]^T [G]\left[A^{-1}\right][LG] \\ [m] &= \rho h[LG]^T \left[A^{-1}\right]^T [S]\left[A^{-1}\right][LG]\end{aligned} \tag{19}$$

where

$$[LG] = \begin{bmatrix} \sin\phi_i & -\cos\phi_i & 0 & 0 & 0 & 0 & 0 & 0 \\ \cos\phi_i & \sin\phi_i & 0 & 0 & 0 & 0 & 0 & 0 \\ 0 & 0 & 1 & 0 & 0 & 0 & 0 & 0 \\ 0 & 0 & 0 & 1 & 0 & 0 & 0 & 0 \\ 0 & 0 & 0 & 0 & \sin\phi_j & -\cos\phi_j & 0 & 0 \\ 0 & 0 & 0 & 0 & \cos\phi_j & \sin\phi_j & 0 & 0 \\ 0 & 0 & 0 & 0 & 0 & 0 & 1 & 0 \\ 0 & 0 & 0 & 0 & 0 & 0 & 0 & 1 \end{bmatrix} \tag{20}$$

From these equations, one can assemble the mass and stiffness matrix for each element to obtain the mass and stiffness matrices for the whole shell: $[M]$ and $[K]$. Each elementary matrix is 8x8, therefore the final dimensions of $[M]$ and $[K]$ will be 4*(N+1) where N is the number of elements of the shell.

2.2 Fluid modeling

The Laplace equation satisfied by velocity potential for inviscid, incompressible and irrotational fluid in the spherical system is written as:

$$\nabla^2\varphi = \frac{1}{r^2}\frac{\partial}{\partial r}\left(r^2\frac{\partial\varphi}{\partial r}\right) + \frac{1}{r^2\sin\phi}\frac{\partial}{\partial\phi}\left(\sin\phi\frac{\partial\varphi}{\partial\phi}\right) + \frac{1}{r^2\sin^2\phi}\frac{\partial^2\varphi}{\partial\theta^2} = 0 \tag{21}$$

where the velocity components are:

$$V_\phi = U_f + \frac{1}{r}\frac{\partial \varphi}{\partial \phi} \qquad V_r = \frac{\partial \varphi}{\partial r} \qquad V_\theta = \frac{1}{r\sin\phi}\frac{\partial \varphi}{\partial \theta} \tag{22}$$

Using the Bernouilli equation, hydrodynamic pressure in terms of velocity potential φ and fluid density ρ_f is found as:

$$P_f = -\rho_f\left(\frac{\partial \varphi}{\partial t} + \frac{U_f}{r}\frac{\partial \varphi}{\partial \phi}\right)_{r=R} \tag{23}$$

The impermeability condition, which ensures contact between the shell surface and the peripheral fluid, is written as:

$$V_r\big|_{r=R} = \left.\frac{\partial \varphi}{\partial r}\right|_{r=R} = \left.\left(\frac{\partial W}{\partial t} + \frac{U_f}{r}\frac{\partial W}{\partial \phi}\right)\right|_{r=R} \tag{24}$$

with

$$W = \sum_{j=1}^{3}\left(A_j P_{\mu_j}^n\left(\cos\phi\right) + B_j Q_{\mu_j}^n\left(\cos\phi\right)\right)\cos n\theta e^{i\omega t} \tag{25}$$

Method of separation of variables for the velocity potential solution can be done as follows:

$$\varphi\left(\phi, r, \theta\right) = \sum_{j=1}^{3} R_j(r) S_j(\phi, \theta, t)$$

Placing this relation into the impermeability condition (24), we can find the function $S_j(\phi,\theta,t)$ in term of radial displacement:

$$S_j(\phi,\theta,t) = \frac{1}{R_j^{\cdot}(R)}\left.\left(\frac{\partial W}{\partial t} + \frac{U_f}{r}\frac{\partial W}{\partial \phi}\right)\right|_{r=R} \tag{26}$$

Hence the equation becomes

$$\varphi\left(\phi, r, \theta\right) = \sum_{j=1}^{3}\frac{R_j(r)}{R_j^{\cdot}(R)}\left.\left(\frac{\partial W}{\partial t} + \frac{U_f}{r}\frac{\partial W}{\partial \phi}\right)\right|_{r=R} \tag{27}$$

With substitution of the above equation into Laplace equation (21), the following second order equation in terms of $R_j(r)$ is obtained

$$R_j''(r)+\frac{2}{r}R_j'(r)-\frac{\mu_j\left(\mu_j+1\right)}{r^2}R_j(r)=0 \tag{28}$$

Solution of the above differential equation yields the following:

$$R_j(r)=A_j r^{\mu_j}+\frac{B_j}{r^{\mu_j}} \tag{29}$$

For internal flow $B_j=0$

Finally, the hydrodynamic pressure in terms of radial displacement is written:

$$P_f=-\rho_f\sum_{j=1}^{3}\frac{R}{\mu_j}\left[\ddot{W}_j+2\frac{U_f}{R}\dot{W}_j'+\frac{U_f^2}{R^2}W_j''\right] \tag{30}$$

We put:

$$\begin{aligned}\frac{R}{\mu_1}&=f_1\\ \frac{R}{\mu_2}&=f_2-if_3\\ \frac{R}{\mu_3}&=f_2+if_3\end{aligned} \tag{31}$$

And the pressure loading in terms of nodal degrees of freedom is written as:

$$\{P\}=\begin{Bmatrix}0\\P_f\\0\end{Bmatrix}=-\rho_f\left[T\right]\left[R_1^f\right]\left[A^{-1}\right]\begin{Bmatrix}\ddot{\delta}_i\\\ddot{\delta}_j\end{Bmatrix}-2\rho_f\frac{U_f}{R}\left[T\right]\left[R_2^f\right]\left[A^{-1}\right]\begin{Bmatrix}\dot{\delta}_i\\\dot{\delta}_j\end{Bmatrix}-2\rho_f\frac{U_f^2}{R^2}\left[T\right]\left[R_3^f\right]\left[A^{-1}\right]\begin{Bmatrix}\delta_i\\\delta_j\end{Bmatrix} \tag{32}$$

The matrix $\left[R_1^f\right]$ is given by:

$$\left[R_1^f\right]=\begin{bmatrix} 0 & 0 & 0 & 0 & 0 & 0 & 0 & 0 \\ P_{\mu_1}^n & \mathrm{Re}(P_{\mu_2}^n) & \mathrm{Im}(P_{\mu_2}^n) & 0 & Q_{\mu_1}^n & \mathrm{Re}(Q_{\mu_2}^n) & \mathrm{Im}(Q_{\mu_2}^n) & 0 \\ 0 & 0 & 0 & 0 & 0 & 0 & 0 & 0 \end{bmatrix}[F] \tag{33}$$

where $[F]$ is expressed as:

$$[F]=\begin{bmatrix} f_1 & 0 & 0 & 0 & 0 & 0 & 0 & 0 \\ 0 & f_2 & -f_3 & 0 & 0 & 0 & 0 & 0 \\ 0 & f_3 & f_2 & 0 & 0 & 0 & 0 & 0 \\ 0 & 0 & 0 & 0 & 0 & 0 & 0 & 0 \\ 0 & 0 & 0 & 0 & f_1 & 0 & 0 & 0 \\ 0 & 0 & 0 & 0 & 0 & f_2 & -f_3 & 0 \\ 0 & 0 & 0 & 0 & 0 & f_3 & f_2 & 0 \\ 0 & 0 & 0 & 0 & 0 & 0 & 0 & 0 \end{bmatrix}0 \tag{34}$$

The matrix $\left[R_2^f\right]$ is given by:

$$\begin{aligned}\left[R_2^f\right]=-n\cot\phi&\begin{bmatrix} 0 & 0 & 0 & 0 & 0 & 0 & 0 & 0 \\ P_{\mu_1}^n & \mathrm{Re}(P_{\mu_2}^n) & \mathrm{Im}(P_{\mu_2}^n) & 0 & Q_{\mu_1}^n & \mathrm{Re}(Q_{\mu_2}^n) & \mathrm{Im}(Q_{\mu_2}^n) & 0 \\ 0 & 0 & 0 & 0 & 0 & 0 & 0 & 0 \end{bmatrix}[F] \\ +&\begin{bmatrix} 0 & 0 & 0 & 0 & 0 & 0 & 0 & 0 \\ P_{\mu_1}^{n-1} & \mathrm{Re}(P_{\mu_2}^{n-1}) & \mathrm{Im}(P_{\mu_2}^{n-1}) & 0 & Q_{\mu_1}^{n-1} & \mathrm{Re}(Q_{\mu_2}^{n-1}) & \mathrm{Im}(Q_{\mu_2}^{n-1}) & 0 \\ 0 & 0 & 0 & 0 & 0 & 0 & 0 & 0 \end{bmatrix}[F][C]\end{aligned} \tag{35}$$

where matrix $[C]$ is given by:

$$[C]=\begin{bmatrix} c_1 & 0 & 0 & 0 & 0 & 0 & 0 & 0 \\ 0 & c_2 & c_3 & 0 & 0 & 0 & 0 & 0 \\ 0 & -c_3 & c_2 & 0 & 0 & 0 & 0 & 0 \\ 0 & 0 & 0 & 0 & 0 & 0 & 0 & 0 \\ 0 & 0 & 0 & 0 & c_1 & 0 & 0 & 0 \\ 0 & 0 & 0 & 0 & 0 & c_2 & c_3 & 0 \\ 0 & 0 & 0 & 0 & 0 & -c_3 & c_2 & 0 \\ 0 & 0 & 0 & 0 & 0 & 0 & 0 & 0 \end{bmatrix} \tag{36}$$

The matrix $\left[R_3^f\right]$ is given by:

$$\left[R_3^f\right] = n\left(\frac{1}{\sin^2\phi} + n\cot^2\phi\right)\begin{bmatrix} 0 & 0 & 0 & 0 & 0 & 0 & 0 & 0 \\ P_{\mu_1}^n & \mathrm{Re}(P_{\mu_2}^n) & \mathrm{Im}(P_{\mu_2}^n) & 0 & Q_{\mu_1}^n & \mathrm{Re}(Q_{\mu_2}^n) & \mathrm{Im}(Q_{\mu_2}^n) & 0 \\ 0 & 0 & 0 & 0 & 0 & 0 & 0 & 0 \end{bmatrix}[F]$$
$$+\begin{bmatrix} 0 & 0 & 0 & 0 & 0 & 0 & 0 & 0 \\ P_{\mu_1}^n & \mathrm{Re}(P_{\mu_2}^n) & \mathrm{Im}(P_{\mu_2}^n) & 0 & Q_{\mu_1}^n & \mathrm{Re}(Q_{\mu_2}^n) & \mathrm{Im}(Q_{\mu_2}^n) & 0 \\ 0 & 0 & 0 & 0 & 0 & 0 & 0 & 0 \end{bmatrix}[F][C] \tag{37}$$
$$-\cot\phi\begin{bmatrix} 0 & 0 & 0 & 0 & 0 & 0 & 0 & 0 \\ P_{\mu_1}^{n-1} & \mathrm{Re}(P_{\mu_2}^{n-1}) & \mathrm{Im}(P_{\mu_2}^{n-1}) & 0 & Q_{\mu_1}^{n-1} & \mathrm{Re}(Q_{\mu_2}^{n-1}) & \mathrm{Im}(Q_{\mu_2}^{n-1}) & 0 \\ 0 & 0 & 0 & 0 & 0 & 0 & 0 & 0 \end{bmatrix}[F][C]$$

The general force vector due the fluid pressure loading is given by:

$$\left\{F_p\right\} = \iint_A [N]^T \{P\}\, dA \tag{38}$$

After substituting for pressure field vector and matrix $[N]$ in the above equation, the local matrix $\left[m_f\right]$ can be found from the following:

$$\left[m_f\right]_{loc} = -\rho_f\left[A^{-1}\right]^T\left(\pi R^2\int_{\phi_i}^{\phi_j}[R]^T\left[R_1^f\right]\sin\phi d\phi\right)\left[A^{-1}\right] = -\rho_f\left[A^{-1}\right]^T\left[S_f\right]\left[A^{-1}\right] \tag{39}$$

The local damping matrix is given by:

$$\left[c_f\right]_{loc} = -2\rho_f\frac{U_f}{R}\left[A^{-1}\right]^T\left(\pi R^2\int_{\phi_i}^{\phi_j}[R]^T\left[R_2^f\right]\sin\phi d\phi\right)\left[A^{-1}\right] = -2\rho_f\frac{U_f}{R}\left[A^{-1}\right]^T\left[D_f\right]\left[A^{-1}\right] \tag{40}$$

Finally the local stiffness matrix is given by:

$$\left[k_f\right]_{loc} = -\rho_f\frac{U_f^2}{R^2}\left[A^{-1}\right]^T\left(\pi R^2\int_{\phi_i}^{\phi_j}[R]^T\left[R_3^f\right]\sin\phi d\phi\right)\left[A^{-1}\right] = -\rho_f\frac{U_f^2}{R^2}\left[A^{-1}\right]^T\left[G_f\right]\left[A^{-1}\right] \tag{41}$$

In the global system the element stiffness and mass matrices are

$$\begin{aligned}\left[m_f\right] &= -\rho_f \left[LG\right]^T \left[A^{-1}\right]^T \left[S_f\right]\left[A^{-1}\right]\left[LG\right] \\ \left[c_f\right] &= -2\rho_f \frac{U_f}{R}\left[LG\right]^T \left[A^{-1}\right]^T \left[D_f\right]\left[A^{-1}\right]\left[LG\right] \\ \left[k_f\right] &= -\rho_f \frac{U_f^2}{R^2}\left[LG\right]^T \left[A^{-1}\right]^T \left[G_f\right]\left[A^{-1}\right]\left[LG\right]\end{aligned} \tag{42}$$

From these equations, one can assemble the mass and stiffness matrix for each element to obtain the mass and stiffness matrices for the whole shell: $\left[M_f\right]$ and $\left[K_f\right]$.

The governing equation which accounts for fluid-shell interaction in the presence of axial internal pressure is derived as:

$$\left[\left[M_s\right]-\left[M_f\right]\right]\begin{Bmatrix}\ddot{\delta}_i \\ \ddot{\delta}_j\end{Bmatrix}-\left[C_f\right]\begin{Bmatrix}\dot{\delta}_i \\ \dot{\delta}_j\end{Bmatrix}+\left[\left[K_s\right]-\left[K_f\right]\right]\begin{Bmatrix}\delta_i \\ \delta_j\end{Bmatrix}=0 \tag{43}$$

where subscripts *s* and *f* refer to shells in vacuum and fluid respectively.

The global fluid matrices mentioned in the above equation may be obtained, respectively by superimposing the damping and stiffness matrices for each individual fluid finite element. After applying the boundary conditions the global matrices are reduced to squares matrices of order $4(N+1)$-J, where N is the number of finite elements in the shell and J is the number of constraints applied. Finally, the eigenvalue problem is solved by means of the equation reduction technique. Equation may be rewritten as follows:

$$\begin{bmatrix}[0] & [M] \\ [M] & -\left[C_f\right]\end{bmatrix}\begin{Bmatrix}\{\ddot{\delta}\} \\ \{\dot{\delta}\}\end{Bmatrix}+\begin{bmatrix}-[M] & [0] \\ [0] & [K]\end{bmatrix}\begin{Bmatrix}\{\dot{\delta}\} \\ \{\delta\}\end{Bmatrix}=\{0\} \tag{44}$$

where

$$\left[K\right]=\left[K_s\right]-\left[K_f\right]$$

$$\left[M\right]=\left[M_s\right]-\left[M_f\right]$$

$\{\delta\}$ is the global displacement vector. $[C_f]$ and $[K_f]$ represent the Coriolis and centrifugal forces induced by the flowing fluid. The eigenvalue problem is given by:

$$[[DD] - \Lambda[I]] = [0] \tag{45}$$

where

$$[DD] = \begin{bmatrix} [0] & [I] \\ [K]^{-1}[M_s] & -[K]^{-1}[C_f] \end{bmatrix}$$

$\Lambda = \frac{1}{\omega^2}$ and $[I]$ is the identity matrix.

An in house computer code was developed as part of this work to establish the structural matrices of each element based on equations developed using the theoretical approach. The calculations for each finite element are performed in two stages: the first dealing with solid shell and the second with the effect of the flowing fluid.

3. Results and discussion

In this section numerical results are presented and compared with existing experimental, analytical and numerical data.

3.1. Validation and comparison

The main advantages of this proposed hybrid is its fast and precise convergence; 12 elements were required for the convergence of the frequency for a clamped spherical shell.

For the cases investigated in the present paper, the predicted dimensionless frequencies are expressed by the following relation:

$$\Omega = \omega R\left(\frac{\rho}{E}\right)^{\frac{1}{2}} \tag{46}$$

where:

ω is the natural angular frequency,

R is the radius of the reference surface,

ρ is the density,

E is the modulus of elasticity.

Results for different filling ratios and modes numbers compared to experimental, theoretical and numerical analyses are presented.

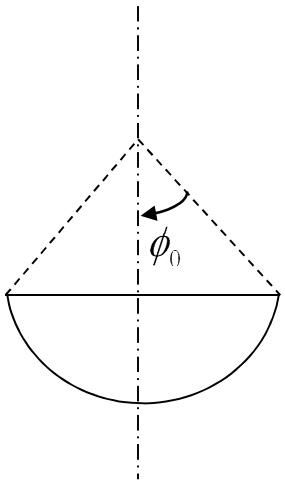

Fig.4. Definition of angle ϕ_0

3.2. Case of a spherical shell with ϕ_0 *=60°*

The case considered here is a simply supported spherical shell with ϕ_0 =60° with the following characteristics and studied by Komatsu [18]: the material density ρ = 2270 kg/m^3, the Poisson coefficient ν=0.3, Young modulus of elasticity: E=70 GPa, the radius to thickness ratio R/h=24.

The figure 5 shows that when the shell is partially filled, the dimensionless frequency initially drops sharply, and then as the shell becomes fuller, the frequency drops less quickly. Free-surface

effects of the liquid surface and sloshing of the fluid are not taken into account in this study. This assumption relies on the fact that the sloshing frequencies have a period of vibration that is much longer than the period of vibration of the spherical shell. As can be seen, there is perfect agreement between both methods.

The comparatively good accuracy of our method can be explained by that fact that the formulation used is a combination of the finite element method and classical shell theory where the displacement functions are derived from exact solutions of shell equations. On the other hand, integrations of all matrices (solid and fluid) are calculated numerically over the solid–fluid element. This numerical model can easily be used to study partially filled spherical shells by imposing a null density of fluid for the circumferential finite elements which are not submerged.

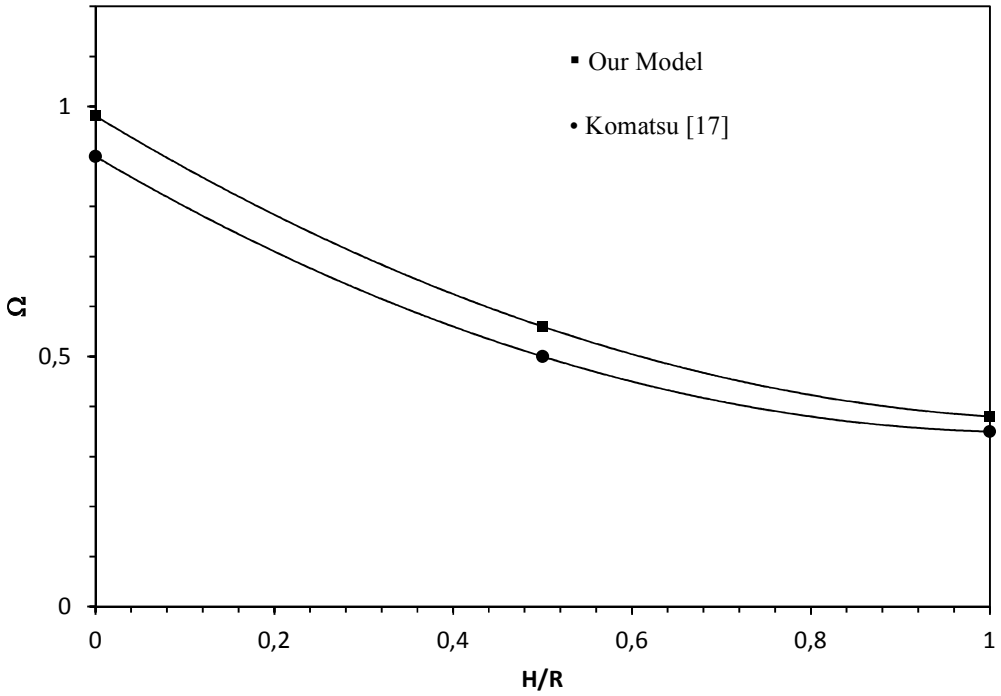

Fig. 5. Dimensionless frequency as function H/R where H is the height of the fluid and R is the shell radius in simply supported spherical shell of with ϕ_0 =60°

The secondstudy we carried out is on the effect of radius to thickness ratio R/h on the natural frequencies in both the case where the shell is empty or full. Figure 6 shows as the mass of shell

is greater when the shell is thick, the effect of fluid is less important in a thick shell than for a thin shell. The same figure shows that ratio of natural frequencies of an empty shell and full shell is of order 10 for R/h=1000. But this ratio was 3 for R/h=243.

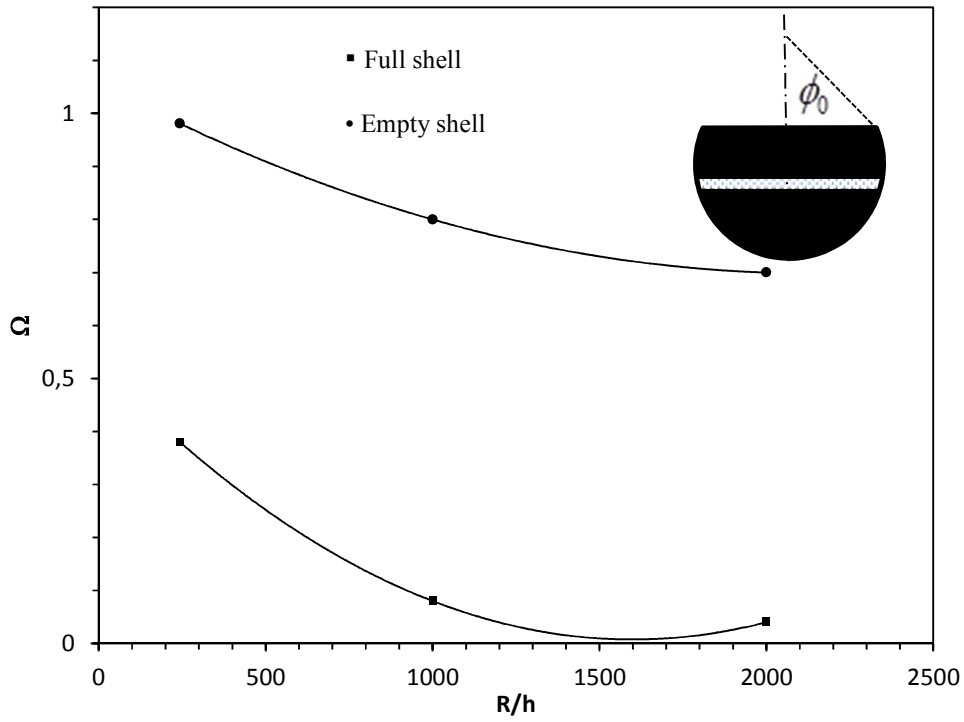

Fig. 6. Dimensionless frequency as function of radius to thickness ratio R/h in simply supported spherical shell of with ϕ_0 =60°

3.3. Case of a hemispherical shell

This case was investigated by many authors**.** The problem of a hemispherical shell completely filled with water was investigated by Ventsel et Al [20]**.** The solution of the problem of hydroelastic vibrations has been obtained using the methods of the boundary element (BEM) and the finite element (FEM). These data are obtained by applying the simply supported condition which is an adequate condition for liquid storage tanks. The hemispherical shell is considered empty or filled with fluid and having the following parameters: the shell radius R=5.08m, the

thickness h=0.0254m, the modulus of elasticity E=70GPa, Poisson ratio ν=0.3, the material density ρ= 2270 kg/m^3, the fluid density ρ_f= 1000 kg/m^3. Very good agreement can be seen (Table 1). The ratio of empty shell frequency and completely filled shell frequency is 4.5 for the first axial mode.

Table 1. Dimensionless frequencies for a simply supported hemispherical shell

	Ventsel et al[20]		Present theory	
(n, m)	H/R =0	H/R=1	H/R=0	H/R=1
2,1	0.8987	0.2004	0.9057	0.2134
2,2	0.9611	0.2579	0.9658	0.2604
2,3	0.9838	0.3020	0.9901	0.3102

The case of a hemispherical shell completely filled with water clamped along equator was investigated experimentally by Samoilov and Pavlov. The characteristics of the shell were as follows: shell radius R=0.133m, thickness h=0.0007m, modulus of elasticity E=4.016GPa, Poisson ratio ν=0.4, material density ρ= 1180kg/m^3. Table 2 shows the dimensionless frequencies obtained by these authors and compared to the frequencies obtained by our model.

Table 2. Dimensionless frequencies for a clamped hemispherical shell completely filled with fluid (ϕ_0 =90°)

m	Samoilov and Pavlov[15]	Present Theory
1	0.0978	0.1038
2	0.1382	0.1451
3	0.1676	0.1789

Data resulting from experiments conducted by Kana and Nagy [10] on a clamped hemispherical shell filled with water are shown in Table 3. The shell has a density of 2.59 10^{-4} lb-s^2/in^4 and has a radius 5 in and a thickness of 0.03 in. The elastic modulus is 10^7 lb/in^2 and the Poisson coefficient is 0.3.

Table 3. Dimensionless frequencies for a clamped hemispherical shell completely filled with fluid

m	Kana and Nagy[10]	Present Theory
1	0.1199	0.1239
2	0.1919	0.2036
3	0.2398	0.2436

The fourth example is the case of a clamped hemispherical shell that was studied experimentally by Hwang [16]. The shell is made of aluminum with density of 2.59 10^{-4} lb-s^2/in^4 and has a radius 200 in and a thickness of 0.1 in. The elastic modulus is 10^7 lb/in^2 and the Poisson coefficient is 0.3. The fluid inside the shell is liquid oxygen with a density of 1.06 10^{-4} lb-s^2/in^4. This example of a hemispherical bulkhead filled with liquid oxygen was modeled by Chung and Rush [17] and investigated numerically. The same study was conducted by Komatsu and Matsuhima [19] experimentally. The results are presented in Table 4.

Table 4. Dimensionless frequencies for a clamped hemispherical shell completely filled with liquid oxygen

Present model	Hwang[14]	Chung and Rush [15]	Komatsu [17]
0.066	0.0689	0.0625	0.065

4. Conclusion

The problem of free vibration of a partially liquid-filled spherical shell under different shell geometries, filling ratios and boundary conditions with different radius to thickness ratios is investigated. An efficient hybrid finite element method is presented to analyze the dynamic behaviour of liquid- filled spherical shell. Shell theory of spherical shell is coupled Laplace equation of an inviscid fluid to account for hydrodynamic pressure of an internal fluid. This theoretical approach is much more precise than usual finite element methods because the displacement functions are derived from exact solutions of shell equilibrium equations for spherical shells. The mass and stiffness matrices are determined by numerical integration. The velocity potential and Bernoulli's equation are adopted to express the fluid pressure acting on the structure which yields three forces (inertial, centrifugal and Coriolis) in the case of flowing fluid.
The results obtained for spherical shells with various geometric configurations and different boundary conditions are compared with results available in the literature. Very good agreement was found. This approach resulted in a very precise element that leads to fast convergence and less numerical difficulties from the computational point of view.
The proposed hybrid finite element method provides the capability to analyze cases involving application of different complex boundaries and loading patterns for spherical shells.

References

[1] Rayleigh L., On the vibrations of a gas contained within a rigid spherical envelope, Proceedings of London Math Society 4 (1872) 93-103.

[2] Morse, P.M., Feshbach, H, *Methods of Theoretical Physics Part II*, McGraw-Hill, New York (1953)

[3] Budiansky, B Sloshing of liquids in circular canals and spherical tanks, Journal of Aerospace Sciences 27(1960) 161-173

[4] Stofan, A.J., Armstead A.L, Analytical and experimental investigation of forces and frequencies resulting from liquid sloshing in a spherical tank, NASA TN D-128 (1962).

[5] Chu W. H., Fuel sloshing in a spherical tank filled to an arbitrarily depth, AIAA Journal 2 (1964) 1972-1979.

[6] Karamanos S.P., Patkas L.A., Papaprokopiou D., Numerical analysis of externally induced sloshing in spherical liquid containers, Computational Methods in Applied Sciences 21(2011) 489-512

[7] Rand R., Dimaggio F., Vibrations of fluid–filled spherical and spheroidal shells, Journal of the Acoustical Society of America 42(1967) 1278-1286.

[8] Engin A.E., Liu Y.K., Axisymmetric response of a fluid filled spherical shell in free vibrations. Journal of Biomechanics 3 (1970) 11-22

[9] Advani S.H., Lee Y.C., Free vibrations of fluid filled spherical shells, Journal of Sound and Vibration, 12 (1970) 453-462.

[10] Kana D.D., Nagy A., An experimental Study of axisymmetric modes in various propellant tanks containing liquid N72-14782 (1971)

[11] Guarino J. C., Elger D.F., Modal Analysis of fluid filled elastic shell containing an elastic sphere, Journal of Sound and Vibration, 156(1992) 461-479.

[12] Bai M.R., Wu K., Free vibration of thin spherical shell containing a compressible fluid , Journal of the Acoustical Society of America 95(1994) 3300-3310.

[13] Chen W.Q., Ding H.J., Natural frequencies of a fluid filled anisotropic spherical shell, Journal of the Acoustical Society of America 105(1999) 174-182.

[14] Young P.G., A parametric study on the axisymmetric modes of vibrations of multi layered spherical shells with liquid cores of relevance to head impact modelling , Journal of Sound and Vibration, 256 (2002) 665-680

[15] Samoilov Y.A., Pavolv B.S., The vibrations of a hemispherical shell filled with liquid Journal Izvestiya Vuzov Avias Tekh 3(1964) 79-86

[16] Hwang C., Longitudinal sloshing of a liquid in flexible hemispherical tank, Journal of Applied Mechanics 32(1965) 665-670.

[17] Chung T.J., Rush R.H., Dynamically coupled motion of surface fluid shell system, Journal of Applied Mechanics 43(1976) 507-508.

[18] Komatsu K., Vibration analysis of spherical shells partially filled with a liquid using an added mass coefficient, Transactions of the Japan Society for Aeronautical and Space Sciences 22(1979) 70-79

[19] Komatsu K., Matsuhima M., Some experiments on the vibrations of hemispherical shells partially filled with a liquid, Journal of Sound and Vibration 64(1979) 35-44

[20] Ventsel E.S, Naumenko V., Strelnikova E., Yeseleva E., Free vibrations of shells of revolution filled with fluid, Journal of Engineering Analysis with Boundary Elements 34(2010) 856-862.

[21] Menaa M, Lakis A.A., Hybrid finite element method applied to the analysis of free vibration of a spherical shell. EPM-RT-2013-02.

CHAPITRE 4 ARTICLE 3 -NUMERICAL INVESTIGATION OF THE FLUTTER OF A SPHERICAL SHELL

Mohamed Menaa, Aouni A. Lakis.

Department of Mechanical Engineering, Ecole Polytechnique de Montreal, C.P. 6079 Succursale Centre-ville, Montréal, Canada H3C 3A7

Accepted, 13 July 2013 by Journal of Vibration and Acoustics

Abstract

In this study, aeroelastic analysis of a spherical shell subjected to external supersonic airflow is carried out. The structural model is based on a combination of linear spherical shell theory and the classic finite element method. In this hybrid method, the nodal displacements are found from the exact solution of shell governing equations rather than approximated by polynomial functions. Linearized first-order potential (piston) theory with the curvature correction term is coupled with the structural model to account for pressure loading. Linear mass, stiffness and damping matrices are found using the hybrid finite element formulation. Aeroelastic equations are derived and solved numerically. The results are validated using numerical and theoretical data available in literature. The analysis is accomplished for spherical shells of different boundary conditions, geometries, flow parameters and radius to thickness ratios. Results show that the spherical shell loses its stability through coupled-mode flutter. This proposed hybrid finite element method can be used efficiently for design and analysis of spherical shells employed in high speed aircraft structures.

1. Introduction

Shells of revolution, particularly spherical shells are one of the primary structural elements in high speed aircraft. Their applications include the propellant tank or gas-deployed skirt of spacecraft. Due to the aerodynamic shape combined with thin wall thicknesses, spherical shells are more disposed to dynamic instability or flutter induced by high- Mach number gas flow. It is therefore important to understand the effect of different flow parameters and loadings on their aeroelastic response.

Aeroelastic analysis of shells and plates has been studied by numerous researchers experimentally and analytically [1]. Dowell gives an exhaustive study of the aeroelasticity of shells and plates in his book [2]. After introducing the application of piston theory in the aeroelastic modeling presented by Ashley and Zatarian [3], a number of interesting experimental and theoretical studies were carried out to investigate supersonic flutter of cylindrical shells. In general, all of this research was concerned with the development of an analytical relation to describe the effect of shell and flow parameters on the critical flutter dynamic pressure. Aeroelastic models in combination with linear or nonlinear piston theory were coupled to the theory of shells to account for fluid-structure interaction. The resulting governing equations were treated numerically using the Galerkin method. A comprehensive experimental test was done by Olson and Fung [4]. They studied the effects of shell boundary conditions and initial stress state due to internal pressure and axial load. It is observed that pressurized cylindrical shell fluttered at a lower level of freestream static pressure than predicted by theory [5]. Later, Evensen and Olson [6, 7] presented a nonlinear analysis to take account of this observed effect. Dowell [8] also analyzed the behaviour of a cylindrical shell in supersonic flow for different flow and shell parameters. A complete description of panel flutter modeling is given in his book [2]. A study by Carter and Strearman [9] showed that agreement between the theory and experiments reported in the literature exists in cases that involve a small amount of static preload acting on the shell. Amabili and Pellicano [10] included geometric nonlinearities in their study of supersonic flutter of a circular cylindrical shell. Based on the selection of expansion modes to discretize the aeroelastic equations to facilitate their solution, they succeeded in capturing the nonlinear behaviour of the shell correctly.

There are also some researchers who focused their efforts on the numerical study of this problem. For the equations of virtual displacements were solved using the finite elements method. Aeroelastic governing equations were formulated by applying classical shell theory coupled with the piston theory for evaluation of aerodynamic forces. For example, Bismarck-Nasr [11] developed a FEM applied to supersonic flutter of circular shell subjected to internal pressure and axial loading. Ganapathi et al. [12] modeled an orthotropic and laminated anisotropic cylindrical shell in supersonic flow using FEM and analyzed the effect of different shell geometries on the flutter boundaries.

Aeroelasticity of conical shells has also been investigated by few researchers. The leading work in this field was conducted by Shulman [13]. Ueda, Kobayashi and Kihira [14] investigated theoretically and experimentally the supersonic flutter of a conical shell. Dixon and Hudson [15] studied the flutter and vibration of an orthotropic conical shell theoretically. Miserentino and Dixon [16] investigated experimentally the vibration and flutter of a pressurized truncated conical shell. Bismarck-Nasr and Costa-Savio [17] studied the supersonic flutter of conical shells with finite element method. Sunder et al. [18] applied successfully the finite element analysis to calculate the flutter of a laminated conical shell. In another study they found the optimum cone angle in aeroelastic flutter [19]. Mason and Blotter [20] used a finite element technique to find the flutter boundary for a conical shell (a typical rocket nozzle element) subjected to an internal supersonic gas flow. Pidaparti and Yang Henry [21] have done a theoretical study to predict the onset of flutter instability for composites conical shells.

An analytical approach to the supersonic flutter of spherical shell becomes very complicated if one wishes to include different parameters. Therefore, numerical methods such as the finite element method (FEM) impose their efficiency for cases involving changes to all factors affecting flutter boundaries. The aim of the present study is to develop a hybrid finite element method in order to predict the aeroelastic behaviour of isotropic spherical shells with different parameters. The finite element is a spherical frustum instead of the usual rectangular shell element. Linear thin shell theory is coupled with linear piston theory. The linear mass, damping and stiffness matrices are obtained. The aeroelastic equation of motion is driven out to a standard eigenvalue problem. The flutter boundary is found by analyzing the real and imaginary parts of the eigenvalues as freestream pressure is varied.

2. Formulation

2.1 Structural modeling

In this study the structure is modeled using hybrid finite element method which is a combination of spherical shell theory and classical finite element method. In this hybrid finite element method, the displacement functions are found from exact solution of spherical shell theory rather approximated by polynomial functions as is done in classical finite element method.

In the spherical coordinate system (R,θ,ϕ) shown in Fig. 1, five out of the six equations of equilibrium for spherical shells under external load are written as follows :

$$\begin{aligned}
&\frac{\partial N_\phi}{\partial \phi}+\frac{1}{\sin\phi}\frac{\partial N_{\phi\theta}}{\partial \theta}+\left(N_\phi-N_\theta\right)\cot\phi+Q_\phi=0\\
&\frac{\partial N_{\phi\theta}}{\partial \phi}+\frac{1}{\sin\phi}\frac{\partial N_\theta}{\partial \theta}+2N_{\phi\theta}\cot\phi+Q_\theta=0\\
&\frac{\partial Q_\phi}{\partial \phi}+\frac{1}{\sin\phi}\frac{\partial Q_\theta}{\partial \theta}+Q_\phi\cot\phi-(N_\phi+N_\theta)=0\\
&\frac{\partial M_\phi}{\partial \phi}+\frac{1}{\sin\phi}\frac{\partial M_{\phi\theta}}{\partial \theta}+\left(M_\phi-M_\theta\right)\cot\phi-RQ_\phi=0\\
&\frac{\partial M_{\phi\theta}}{\partial \phi}+\frac{1}{\sin\phi}\frac{\partial M_\theta}{\partial \theta}+2M_{\phi\theta}\cot\phi-RQ_\theta=0
\end{aligned} \tag{1}$$

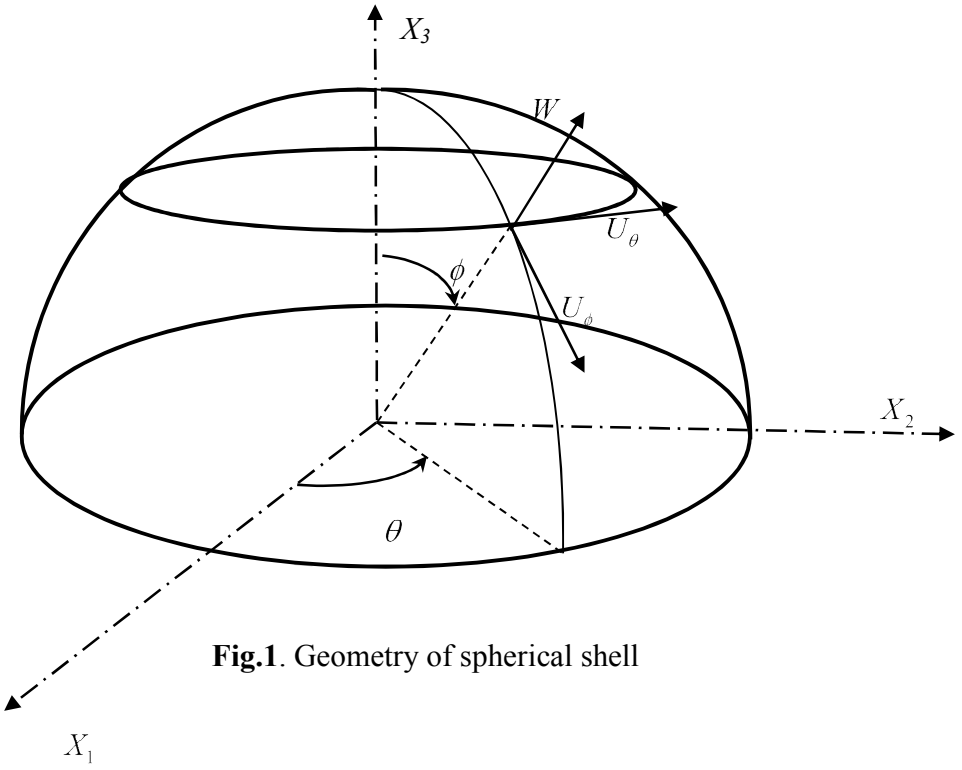

Fig.1. Geometry of spherical shell

where N_ϕ, N_θ, $N_{\phi\theta}$ are membrane stress resultants; M_ϕ, M_θ, $M_{\phi\theta}$ the bending stress resultants and Q_ϕ, Q_θ the shear forces (Fig. 2). The sixth equation, which is an identity equation for spherical shells, is not presented here.

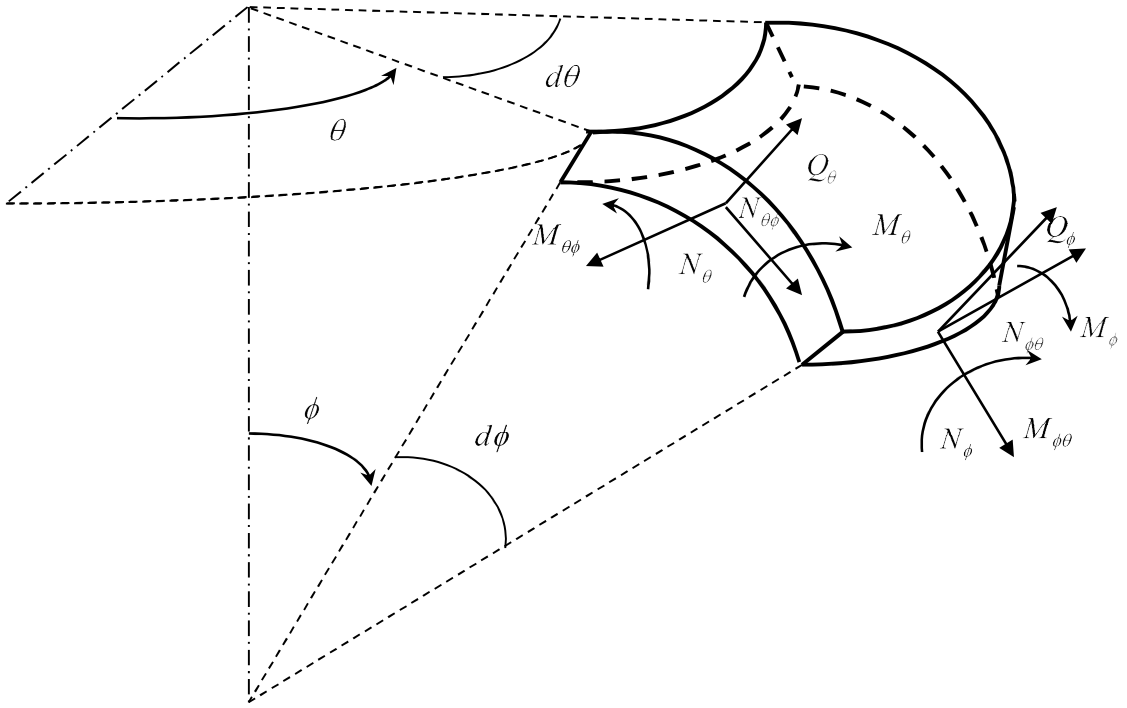

Fig.2. Stress resultants and stress couples

Strain and displacements for three displacements in axial U_ϕ, radial W and circumferential U_θ are related as follows:

$$\{\varepsilon\}=\begin{Bmatrix}\varepsilon_\phi\\ \varepsilon_\theta\\ 2\varepsilon_{\phi\theta}\\ \kappa_\phi\\ \kappa_\theta\\ 2\kappa_{\phi\theta}\end{Bmatrix}=\begin{Bmatrix}\frac{1}{R}\left(\frac{\partial U_\phi}{\partial\phi}+W\right)\\ \frac{1}{R}\left(\frac{1}{\sin\phi}\frac{\partial U_\theta}{\partial\theta}+U_\phi\cot\phi+W\right)\\ \frac{1}{R}\left(\frac{\partial U_\theta}{\partial\phi}+\frac{1}{\sin\phi}\frac{\partial U_\phi}{\partial\theta}-U_\theta\cot\phi\right)\\ \frac{1}{R^2}\left(\frac{\partial U_\phi}{\partial\phi}-\frac{\partial^2 W}{\partial\phi^2}\right)\\ \frac{1}{R^2}\left(\frac{1}{\sin\phi}\frac{\partial U_\theta}{\partial\theta}+U_\phi\cot\phi-\frac{1}{\sin^2\phi}\frac{\partial^2 W}{\partial\theta^2}-\cot\phi\frac{\partial W}{\partial\phi}\right)\\ \frac{1}{R^2}\left(\frac{\partial U_\theta}{\partial\phi}+\frac{1}{\sin\phi}\frac{\partial U_\phi}{\partial\theta}-U_\theta\cot\phi+2\frac{1}{\sin\phi}\cot\phi\frac{\partial W}{\partial\theta}-2\frac{1}{\sin\phi}\frac{\partial^2 W}{\partial\phi\partial\theta}\right)\end{Bmatrix} \tag{2}$$

Displacements U, W and V in the global Cartesian coordinate system are related to displacements $U_{\phi i}$, W_i and $U_{\theta i}$ indicated in Fig 3. by:

$$\begin{Bmatrix}U\\ W\\ V\end{Bmatrix}=\begin{bmatrix}\sin\phi_i & -\cos\phi_i & 0\\ \cos\phi_i & \sin\phi_i & 0\\ 0 & 0 & 1\end{bmatrix}\begin{Bmatrix}U_{\phi i}\\ W_i\\ U_{\theta i}\end{Bmatrix} \tag{3}$$

The stress vector $\{\sigma\}$ is expressed as function of strain $\{\varepsilon\}$ by:

$$\{\sigma\}=[P]\{\varepsilon\} \tag{4}$$

where $[P]$ is the elasticity matrix for an anisotropic shell given by:

$$[P]=\begin{bmatrix}P_{11} & P_{12} & 0 & P_{14} & P_{15} & 0\\ P_{21} & P_{22} & 0 & P_{24} & P_{25} & 0\\ 0 & 0 & P_{33} & 0 & 0 & 0\\ P_{41} & P_{42} & 0 & P_{44} & P_{45} & 0\\ P_{51} & P_{52} & 0 & P_{54} & P_{55} & 0\\ 0 & 0 & P_{36} & 0 & 0 & P_{66}\end{bmatrix} \tag{5}$$

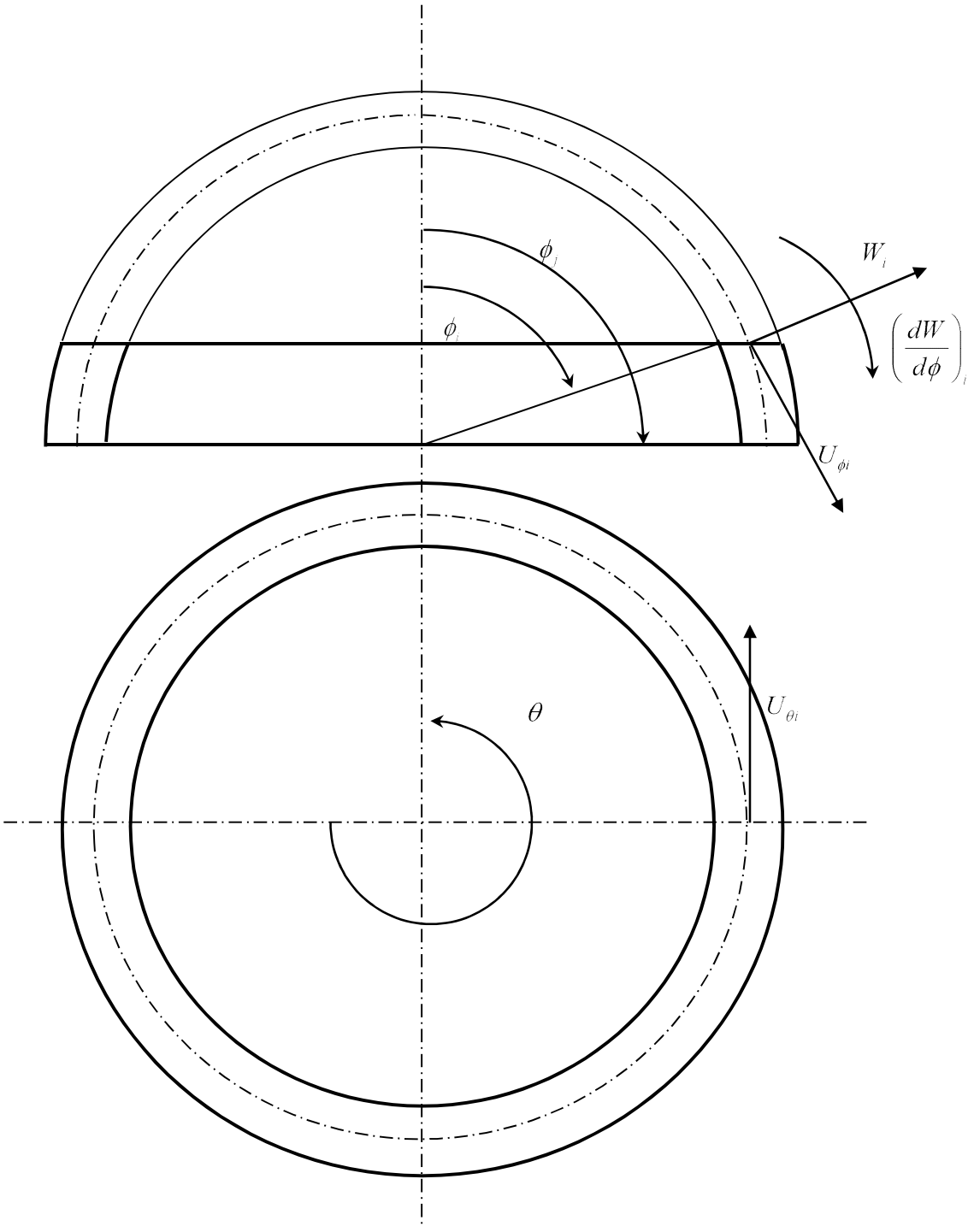

Fig. 3. Spherical frustum element

Upon substitution of equations (2), (4) and (5) into equations (1), a system of equilibrium equations can be obtained as a function of displacements:

$$\begin{aligned} L_1\left(U_\phi, W, U_\theta, P_{ij}\right) &= 0 \\ L_2\left(U_\phi, W, U_\theta, P_{ij}\right) &= 0 \\ L_3\left(U_\phi, W, U_\theta, P_{ij}\right) &= 0 \end{aligned} \tag{6}$$

These three linear partial differentials operators L_1, L_2 and L_3 are given in the Appendix, and P_{ij} are elements of the elasticity matrix, which, for an isotropic thin shell with thickness *h* is given by:

$$[P] = \begin{bmatrix} D & \nu D & 0 & 0 & 0 & 0 \\ \nu D & D & 0 & 0 & 0 & 0 \\ 0 & 0 & \dfrac{(1-\nu)D}{2} & 0 & 0 & 0 \\ 0 & 0 & 0 & K & \nu K & 0 \\ 0 & 0 & 0 & \nu K & K & 0 \\ 0 & 0 & 0 & 0 & 0 & \dfrac{(1-\nu)K}{2} \end{bmatrix} \tag{7}$$

where $D = \dfrac{Et}{1-\nu^2}$ is the membrane stiffness and $K = \dfrac{Et^3}{12\left(1-\nu^2\right)}$ is the bending stiffness.

The element is a circumferential spherical frustum shown in Fig. 3. It has two nodal circles with four degrees of freedom; axial, radial, circumferential and rotation at each node. This element type makes it possible to use thin shell equations easily to find the exact solution of displacement functions rather than an approximation with polynomial functions as done in classical finite element method. For motions associated with the *n*th circumferential wave number we may write:

$$\begin{Bmatrix} U_\phi(\phi,\theta) \\ W(\phi,\theta) \\ U_\theta(\phi,\theta) \end{Bmatrix} = \begin{bmatrix} \cos n\theta & 0 & 0 \\ 0 & \cos n\theta & 0 \\ 0 & 0 & \sin n\theta \end{bmatrix} \begin{Bmatrix} u_{\phi n}(\phi) \\ w_n(\phi) \\ u_{\theta n}(\phi) \end{Bmatrix} = [T] \begin{Bmatrix} u_{\phi n}(\phi) \\ w_n(\phi) \\ u_{\theta n}(\phi) \end{Bmatrix} \tag{8}$$

The transversal displacement $w_n(\phi)$ can be expressed as:

$$w_n(\phi) = \sum_{i=1}^{3} w_i^n \tag{9}$$

where

$$w_i^n = A_i P_{\mu_i}^n(\cos\phi) + B_i Q_{\mu_i}^n(\cos\phi) \tag{10}$$

and where $P_{\mu_i}^n(\cos\phi), Q_{\mu_i}^n(\cos\phi)$ are the associated Legendre functions of the first and second kinds respectively of order *n* and degree μ_i.

The expression of the axial displacement $u_{\phi n}(\phi)$ is:

$$u_{\phi n}(\phi) = \sum_{i=1}^{3} E_i \frac{dw_i^n}{d\phi} - \frac{n^2}{2\sin\phi}\psi(\phi) \tag{11}$$

where the coefficient E_i is given by:

$$E_i = \frac{\lambda_i + k(1+\nu) - (1-\nu)}{(1+k)(\lambda_i - 1 + \nu)} \tag{12}$$

The auxiliary function ψ is given by the expression:

$$\psi(\phi) = A_4 P_1^n(\cos\phi) + B_4 Q_1^n(\cos\phi) \tag{13}$$

Finally the circumferential displacement $u_{\theta n}(\phi)$ can be expressed as:

$$u_{\theta n}(\phi) = -n\sum_{i=1}^{3} \frac{1}{\sin\phi} E_i w_i^n + \frac{n}{2}\frac{d\psi}{d\phi} \tag{14}$$

The degree μ_i is obtained from the expression

$$\mu_i = \left(\frac{1}{4} + \lambda_i\right)^{1/2} - \frac{1}{2} \tag{15}$$

where λ_i is one the roots of the cubic equation:

$$\lambda^3 - h_1\lambda^2 + h_2\lambda - h_3 = 0 \tag{16}$$

where

$$\begin{aligned} h_1 &= 4 \\ h_2 &= 4 + (1+k)(1-\nu^2) \\ h_3 &= 2(1+k)(1-\nu^2) \end{aligned} \tag{17}$$

with $k = 12\dfrac{R^2}{h^2}$

The above equation has three roots with one root is real and two other are complex conjugate roots.

The Legendre functions $P^n_{\mu_1}$, $P^{n-1}_{\mu_1}, Q^n_{\mu_1}$ and $Q^{n-1}_{\mu_1}$ are a real functions whereas $P^n_{\mu_i}$, $P^{n-1}_{\mu_i}, Q^n_{\mu_i}$ and $Q^{n-1}_{\mu_i}$ (i = 2,3) are complex functions so we can put:

$$\begin{aligned} P^n_{\mu_2} &= \mathrm{Re}(P^n_{\mu_2}) + i\,\mathrm{Im}(P^n_{\mu_2}) \\ P^n_{\mu_3} &= \mathrm{Re}(P^n_{\mu_2}) - i\,\mathrm{Im}(P^n_{\mu_2}) \\ Q^n_{\mu_2} &= \mathrm{Re}(Q^n_{\mu_2}) + i\,\mathrm{Im}(Q^n_{\mu_2}) \\ Q^n_{\mu_3} &= \mathrm{Re}(Q^n_{\mu_2}) - i\,\mathrm{Im}(Q^n_{\mu_2}) \\ P^{n-1}_{\mu_2} &= \mathrm{Re}(P^{n-1}_{\mu_2}) + i\,\mathrm{Im}(P^{n-1}_{\mu_2}) \\ P^{n-1}_{\mu_3} &= \mathrm{Re}(P^{n-1}_{\mu_2}) - i\,\mathrm{Im}(P^{n-1}_{\mu_2}) \\ Q^{n-1}_{\mu_2} &= \mathrm{Re}(Q^{n-1}_{\mu_2}) + i\,\mathrm{Im}(Q^{n-1}_{\mu_2}) \\ Q^{n-1}_{\mu_3} &= \mathrm{Re}(P^{n-1}_{\mu_2}) - i\,\mathrm{Im}(Q^{n-1}_{\mu_2}) \end{aligned} \tag{18}$$

Setting

$$\begin{aligned} (n-\mu_1-1)\left(n+\mu_1\right) &= c_1 \\ (n-\mu_2-1)\left(n+\mu_2\right) &= c_2 + ic_3 \\ (n-\mu_3-1)\left(n+\mu_3\right) &= c_2 - ic_3 \end{aligned} \tag{19}$$

$$\begin{aligned} E_1 &= e_1 \\ E_2 &= e_2 - ie_3 \\ E_3 &= e_2 + ie_3 \end{aligned} \tag{20}$$

Substituting equations (18), (19) and (20) in equations (9), (11) and (14) we have:

$$
\begin{aligned}
u_{n\phi}(\phi) &= \left(-ne_1\cot\phi P^n_{\mu_1} + e_1c_1P^{n-1}_{\mu_1}\right)A_1 \\
&+\left[-ne_2\cot\phi\,\mathrm{Re}(P^n_{\mu_2}) - ne_3\cot\phi\,\mathrm{Im}(P^n_{\mu_2}) + (e_2c_2+e_3c_3)\,\mathrm{Re}(P^{n-1}_{\mu_2}) + (e_3c_2-e_2c_3)\,\mathrm{Im}(P^{n-1}_{\mu_2})\right](A_2+A_3) \\
&+\left[\ ne_3\cot\phi\,\mathrm{Re}(P^n_{\mu_2}) - ne_2\cot\phi\,\mathrm{Im}(P^n_{\mu_2}) - (e_3c_2-e_2c_3)\,\mathrm{Re}(P^{n-1}_{\mu_2}) + (e_2c_2+e_3c_3)\,\mathrm{Im}(P^{n-1}_{\mu_2})\right]i(A_2-A_3) \\
&+\left[-\frac{n^2}{2\sin\phi}P^n_1\right]A_4 \\
&+\left(-ne_1\cot\phi Q^n_{\mu_1} + e_1c_1Q^{n-1}_{\mu_1}\right)B_1 \\
&+\left[-ne_2\cot\phi\,\mathrm{Re}(Q^n_{\mu_2}) - ne_3\cot\phi\,\mathrm{Im}(Q^n_{\mu_2}) + (e_2c_2+e_3c_3)\,\mathrm{Re}(Q^{n-1}_{\mu_2}) + (e_3c_2-e_2c_3)\,\mathrm{Im}(Q^{n-1}_{\mu_2})\right](B_2+B_3) \\
&+\left[\ ne_3\cot\phi\,\mathrm{Re}(Q^n_{\mu_2}) - ne_2\cot\phi\,\mathrm{Im}(Q^n_{\mu_2}) - (e_3c_2-e_2c_3)\,\mathrm{Re}(Q^{n-1}_{\mu_2}) + (e_2c_2+e_3c_3)\,\mathrm{Im}(Q^{n-1}_{\mu_2})\right]i(B_2-B_3) \\
&+\left[-\frac{n^2}{2\sin\phi}Q^n_1\right]B_4 \\
w_n(\phi) &= P^n_{\mu_1}A_1 + \mathrm{Re}(P^n_{\mu_2})(A_2+A_3) + \mathrm{Im}(P^n_{\mu_2})i(A_2-A_3) + Q^n_{\mu_1}B_1 + \mathrm{Re}(Q^n_{\mu_2})(B_2+B_3) + \mathrm{Im}(Q^n_{\mu_2})i(B_2-B_3)
\end{aligned}
$$

$$
\begin{aligned}
u_{n\theta}(\phi) &= -ne_1P^n_{\mu_1}\frac{1}{\sin\phi}A_1 \\
&-\left[ne_2\frac{1}{\sin\phi}\mathrm{Re}(P^n_{\mu_2}) + ne_3\frac{1}{\sin\phi}\mathrm{Im}(P^n_{\mu_2})\right](A_2+A_3) + \left[ne_3\frac{1}{\sin\phi}\mathrm{Re}(P^n_{\mu_2}) - ne_2\frac{1}{\sin\phi}\mathrm{Im}(P^n_{\mu_2})\right]i(A_2-A_3) \\
&+\left[-\frac{n^2}{2}\cot\phi P^n_1 + \frac{n}{2}(n-2)(n+1)P^{n-1}_1\right]A_4 \\
&-ne_1Q^n_{\mu_1}\frac{1}{\sin\phi}B_1 \\
&-\left[ne_2\frac{1}{\sin\phi}\mathrm{Re}(Q^n_{\mu_2}) + ne_3\frac{1}{\sin\phi}\mathrm{Im}(Q^n_{\mu_2})\right](B_2+B_3) + \left[ne_3\frac{1}{\sin\phi}\mathrm{Re}(Q^n_{\mu_2}) - ne_2\frac{1}{\sin\phi}\mathrm{Im}(Q^n_{\mu_2})\right]i(B_2-B_3) \\
&+\left[-\frac{n^2}{2}\cot\phi Q^n_1 + \frac{n}{2}(n-2)(n+1)Q^{n-1}_1\right]B_4
\end{aligned}
\tag{21}
$$

In deriving the above relation we used the recursive relations:

$$
\begin{aligned}
\frac{dP^n_{\mu_i}}{d\phi} &= -n\cot\phi P^n_{\mu_i} + (n-\mu_i-1)(n+\mu_i)P^{n-1}_{\mu_i} \\
\frac{dQ^n_{\mu_i}}{d\phi} &= -n\cot\phi Q^n_{\mu_i} + (n-\mu_i-1)(n+\mu_i)Q^{n-1}_{\mu_i}
\end{aligned}
\tag{22}
$$

Using matrix formulation, the displacement functions can be expressed as follows:

$$\begin{Bmatrix} U_\phi(\phi,\theta) \\ W(\phi,\theta) \\ U_\theta(\phi,\theta) \end{Bmatrix} = [T] \begin{Bmatrix} u_{\phi n}(\phi) \\ w_n(\phi) \\ u_{\theta n}(\phi) \end{Bmatrix} = [T][R]\{C\} \tag{23}$$

The vector $\{C\}$ is given by the expression:

$$\{C\}^T = \begin{Bmatrix} A_1 & A_2 + A_3 & i(A_2 - A_3) & A_4 & B_1 & B_2 + B_3 & i(B_2 - B_3) & B_4 \end{Bmatrix} \tag{24}$$

The elements of matrix $[R]$ are given in the Appendix.

In the finite element method, the vector C is eliminated in favor of displacements at elements nodes. At each finite element node, the three displacements (axial, transversal and circumferential) and the rotation are applied. The displacement of node *i* are defined by the vector:

$$\{\delta_i\} = \begin{Bmatrix} u^i_{\phi n} & w^i_n & \left(\frac{dw_n}{dx}\right)^i & u^i_{\theta n} \end{Bmatrix}^T \tag{25}$$

The element in Fig. 3 with two nodal lines (*i* and *j*) and eight degrees of freedom will have the following nodal displacement vector:

$$\begin{Bmatrix} \delta_i \\ \delta_j \end{Bmatrix} = \begin{Bmatrix} u^i_{\phi n} & w^i_n & \left(\frac{dw_n}{d\phi}\right)^i & u^i_{\theta n} & u^j_{\phi n} & w^j_n & \left(\frac{dw_n}{d\phi}\right)^j & u^j_{\theta n} \end{Bmatrix}^T = [A]\{C\} \tag{26}$$

with

$$\begin{aligned} \frac{dw_n}{d\phi} = {} & \left(-n\cot\phi P^n_{\mu_1} + c_1 P^{n-1}_{\mu_1}\right) A_1 + \left[-n\cot\phi \,\mathrm{Re}(P^n_{\mu_2}) + c_2\,\mathrm{Re}(P^{n-1}_{\mu_2}) - c_3\,\mathrm{Im}(P^{n-1}_{\mu_2})\right](A_2 + A_3) \\ & + \left[-n\cot\phi \,\mathrm{Im}(P^n_{\mu_2}) + c_3\,\mathrm{Re}(P^{n-1}_{\mu_2}) + c_2\,\mathrm{Im}(P^{n-1}_{\mu_2})\right] i(A_2 - A_3) + \left(-n\cot\phi Q^n_{\mu_1} + c_1 Q^{n-1}_{\mu_1}\right) B_1 \\ & + \left[-n\cot\phi \,\mathrm{Re}(Q^n_{\mu_2}) + c_2\,\mathrm{Re}(Q^{n-1}_{\mu_2}) - c_3\,\mathrm{Im}(Q^{n-1}_{\mu_2})\right](B_2 + B_3) \\ & + \left[-n\cot\phi \,\mathrm{Im}(Q^n_{\mu_2}) + c_3\,\mathrm{Re}(Q^{n-1}_{\mu_2}) + c_2\,\mathrm{Im}(Q^{n-1}_{\mu_2})\right] i(B_2 - B_3) \end{aligned} \tag{27}$$

The terms of matrix $[A]$, obtained from the values of matrix $[R]$ and $\frac{dw_n}{dx}$, are given in the appendix. Now, pre-multiplying by $[A]^{-1}$ equation (26) one obtains the matrix of the constant C_i as a function of the degree of freedom:

$$\{C\} = [A]^{-1} \begin{Bmatrix} \delta_i \\ \delta_j \end{Bmatrix} \tag{28}$$

Finally, one substitutes the vector $\{C\}$ into equation and obtains the displacement functions as follows:

$$\begin{Bmatrix} U_\phi(\phi,\theta) \\ W(\phi,\theta) \\ U_\theta(\phi,\theta) \end{Bmatrix} = [T][R][A]^{-1} \begin{Bmatrix} \delta_i \\ \delta_j \end{Bmatrix} = [N] \begin{Bmatrix} \delta_i \\ \delta_j \end{Bmatrix} \tag{29}$$

The strain vector $\{\varepsilon\}$ can be determined from the displacement functions U_ϕ, U_θ, W and the deformation –displacement as:

$$\{\varepsilon\} = \begin{bmatrix} [T] & [0] \\ [0] & [T] \end{bmatrix} [Q]\{C\} = \begin{bmatrix} [T] & [0] \\ [0] & [T] \end{bmatrix} [Q][A]^{-1} \begin{Bmatrix} \delta_i \\ \delta_j \end{Bmatrix} = [B] \begin{Bmatrix} \delta_i \\ \delta_j \end{Bmatrix} \tag{30}$$

where matrix $[Q]$ is given in the appendix.

This relation can be used to find the stress vector, equation (4), in terms of the nodal degrees of freedom vector:

$$\{\sigma\} = [P][B] \begin{Bmatrix} \delta_i \\ \delta_j \end{Bmatrix} \tag{31}$$

Based on the finite element formulation, the local stiffness and mass matrices are:

$$[k]_{loc} = \iint_A [B]^T [P][B] dA$$
$$[m]_{loc} = \rho\, h \iint_A [N]^T [N] dA \tag{32}$$

where ρ is the density and h is the thickness of shell.

The surface element of the shell wall is $dA = R^2 \sin\phi d\phi d\theta$. After integrating over θ, the preceding equations become

$$[k]_{loc} = \left[A^{-1}\right]^T \left(\pi R^2 \int_{\phi_i}^{\phi_j} [Q]^T [P][Q] \sin\phi d\phi \right) \left[A^{-1}\right] = \left[A^{-1}\right]^T [G] \left[A^{-1}\right]$$
$$[m]_{loc} = \rho h \left[A^{-1}\right]^T \left(\pi R^2 \int_{\phi_i}^{\phi_j} [R]^T [R] \sin\phi d\phi \right) \left[A^{-1}\right] = \rho h \left[A^{-1}\right]^T [S] \left[A^{-1}\right] \tag{33}$$

In the global system the element stiffness and mass matrices are

$$[k] = [LG]^T \left[A^{-1}\right]^T [G] \left[A^{-1}\right] [LG]$$
$$[m] = \rho h [LG]^T \left[A^{-1}\right]^T [S] \left[A^{-1}\right] [LG] \tag{34}$$

where

$$[LG] = \begin{bmatrix} \sin\phi_i & -\cos\phi_i & 0 & 0 & 0 & 0 & 0 & 0 \\ \cos\phi_i & \sin\phi_i & 0 & 0 & 0 & 0 & 0 & 0 \\ 0 & 0 & 1 & 0 & 0 & 0 & 0 & 0 \\ 0 & 0 & 0 & 1 & 0 & 0 & 0 & 0 \\ 0 & 0 & 0 & 0 & \sin\phi_j & -\cos\phi_j & 0 & 0 \\ 0 & 0 & 0 & 0 & \cos\phi_j & \sin\phi_j & 0 & 0 \\ 0 & 0 & 0 & 0 & 0 & 0 & 1 & 0 \\ 0 & 0 & 0 & 0 & 0 & 0 & 0 & 1 \end{bmatrix} \tag{35}$$

From these equations, one can assemble the mass and stiffness matrix for each element to obtain the mass and stiffness matrices for the whole shell: $[M]$ and $[K]$. Each elementary matrix is 8x8,

therefore the final dimensions of $[M]$ and $[K]$ will be 4*(N+1) where N is the number of elements of the shell.

2.2 Aerodynamic Modeling

Piston theory, introduced by Ashley and Zartarian [3], is a powerful tool for aeroelasticity modeling. In this study the fluid-structure effect due to external pressure loading can be taken into account using linearized first-order potential theory. This pressure is expressed as:

$$P_a = -\frac{\gamma P_\infty M^2}{\left(M^2-1\right)^{1/2}}\left[\frac{\partial W}{R\partial\phi}+\frac{M^2-2}{M^2-1}\frac{1}{U_\infty}\frac{\partial W}{\partial t}-\frac{W}{2R_m\left(M^2-1\right)^{1/2}}\right] \tag{36}$$

where P_∞, U_∞, M and γ are the freestream static pressure, freestream velocity, Mach number and adiabatic exponent of air respectively. If the Mach number is sufficiently high ($\left(M \geq 2\right)$, and curvature term, $W \Big/ 2R_m\left(M^2-1\right)^{1/2}$ is neglected, the result is the so-called piston theory:

$$P_a = -\gamma P_\infty\left[\frac{M}{R}\frac{\partial W}{\partial\phi}+\frac{1}{a_\infty}\frac{\partial W}{\partial t}\right] \tag{37}$$

where a_∞ is the freestream speed of sound.

Finally, the aerodynamic pressure in terms of radial displacement is written:

$$P_a = -\frac{\rho_\infty U_\infty^2}{\left(M^2-1\right)^{1/2}}\sum_{j=1}^{3}\left[\frac{1}{U_\infty}\frac{M^2-2}{M^2-1}\dot{W}_j+\frac{1}{R}\frac{dW_j}{d\phi}-\frac{1}{2\left(M^2-1\right)^{1/2}R_m}W_j\right] \tag{38}$$

And the pressure loading in terms of nodal degrees of freedom is written as:

$$\{P_a\}=\begin{Bmatrix}0\\P_r\\0\end{Bmatrix}=-\frac{\rho_\infty U_\infty^2}{\left(M^2-1\right)^{1/2}}\frac{1}{U_\infty}\frac{M^2-2}{M^2-1}[T]\left[R_1^a\right]\left[A^{-1}\right]\begin{Bmatrix}\dot{\delta}_i\\\dot{\delta}_j\end{Bmatrix}-\frac{\rho_\infty U_\infty^2}{\left(M^2-1\right)^{1/2}}\frac{1}{R}[T]\left[R_2^a\right]\left[A^{-1}\right]\begin{Bmatrix}\delta_i\\\delta_j\end{Bmatrix}$$
$$+\frac{\rho_\infty U_\infty^2}{\left(M^2-1\right)^{1/2}}\frac{1}{2\left(M^2-1\right)^{1/2}R_m}[T]\left[R_1^a\right]\left[A^{-1}\right]\begin{Bmatrix}\delta_i\\\delta_j\end{Bmatrix}$$

where ρ_∞ is the freestream air density and R_m is the median radius for each element. Based on thermodynamic relations the freestream pressure and velocity can be linked together using the following relations:

$$U_\infty = Ma_\infty \tag{39}$$

$$a_\infty=\sqrt{\gamma\frac{P_\infty}{\rho_\infty}} \tag{40}$$

The matrix $\left[R_1^a\right]$ is given by:

$$\left[R_1^a\right]=\begin{bmatrix}0 & 0 & 0 & 0 & 0 & 0 & 0 & 0\\ P_{\mu_1}^n & \mathrm{Re}(P_{\mu_2}^n) & \mathrm{Im}(P_{\mu_2}^n) & 0 & Q_{\mu_1}^n & \mathrm{Re}(Q_{\mu_2}^n) & \mathrm{Im}(Q_{\mu_2}^n) & 0\\ 0 & 0 & 0 & 0 & 0 & 0 & 0 & 0\end{bmatrix} \tag{41}$$

The matrix $\left[R_2^a\right]$ is given by:

$$\left[R_2^a\right]=-n\cot\phi\begin{bmatrix}0 & 0 & 0 & 0 & 0 & 0 & 0 & 0\\ P_{\mu_1}^n & \mathrm{Re}(P_{\mu_2}^n) & \mathrm{Im}(P_{\mu_2}^n) & 0 & Q_{\mu_1}^n & \mathrm{Re}(Q_{\mu_2}^n) & \mathrm{Im}(Q_{\mu_2}^n) & 0\\ 0 & 0 & 0 & 0 & 0 & 0 & 0 & 0\end{bmatrix}$$
$$+\begin{bmatrix}0 & 0 & 0 & 0 & 0 & 0 & 0 & 0\\ P_{\mu_1}^{n-1} & \mathrm{Re}(P_{\mu_2}^{n-1}) & \mathrm{Im}(P_{\mu_2}^{n-1}) & 0 & Q_{\mu_1}^{n-1} & \mathrm{Re}(Q_{\mu_2}^{n-1}) & \mathrm{Im}(Q_{\mu_2}^{n-1}) & 0\\ 0 & 0 & 0 & 0 & 0 & 0 & 0 & 0\end{bmatrix}[C] \tag{42}$$

where matrix $[C]$ is given by:

$$[C]=\begin{bmatrix} c_1 & 0 & 0 & 0 & 0 & 0 & 0 & 0 \\ 0 & c_2 & c_3 & 0 & 0 & 0 & 0 & 0 \\ 0 & -c_3 & c_2 & 0 & 0 & 0 & 0 & 0 \\ 0 & 0 & 0 & 0 & 0 & 0 & 0 & 0 \\ 0 & 0 & 0 & 0 & c_1 & 0 & 0 & 0 \\ 0 & 0 & 0 & 0 & 0 & c_2 & c_3 & 0 \\ 0 & 0 & 0 & 0 & 0 & -c_3 & c_2 & 0 \\ 0 & 0 & 0 & 0 & 0 & 0 & 0 & 0 \end{bmatrix} \tag{43}$$

The general force vector due to a pressure field is written as:

$$\left\{F_p\right\}=\iint_A \left[N\right]^T \left\{P_a\right\} dA \tag{44}$$

The local damping matrix is given by:

$$\left[c_f\right]_{loc} = -\frac{\rho_\infty U_\infty^2}{\left(M^2-1\right)^{1/2}}\frac{1}{U_\infty}\frac{M^2-2}{M^2-1}\left[A^{-1}\right]^T\left(\pi R^2\int_{\phi_i}^{\phi_j}\left[R\right]^T\left[R_1^a\right]\sin\phi d\phi\right)\left[A^{-1}\right] = -\frac{\rho_\infty U_\infty^2}{\left(M^2-1\right)^{1/2}}\frac{1}{U_\infty}\frac{M^2-2}{M^2-1}\left[A^{-1}\right]^T\left[D_f\right]\left[A^{-1}\right] \tag{45}$$

Finally the local stiffness matrix is given by:

$$\left[k_f\right]_{loc} = -\frac{\rho_\infty U_\infty^2}{\left(M^2-1\right)^{1/2}}\left[A^{-1}\right]^T\left(\pi R^2\int_{\phi_i}^{\phi_j}\left[R\right]^T\left[R_2^a\right]\sin\phi d\phi -\right)\left[A^{-1}\right]$$

$$+\frac{\rho_\infty U_\infty^2}{\left(M^2-1\right)^{1/2}}\frac{1}{2\left(M^2-1\right)^{1/2}R_m}\left[A^{-1}\right]^T\pi R^2\int_{\phi_i}^{\phi_j}\left[R\right]^T\left[R_1^a\right]\sin\phi d\phi\left[A^{-1}\right] = \text{ In the global system}$$

$$= -\frac{\rho_\infty U_\infty^2}{\left(M^2-1\right)^{1/2}}\left[A^{-1}\right]^T\left[G_f\right]\left[A^{-1}\right]$$

the element damping and stiffness matrices are

$$\left[c_f\right] = -\frac{\rho_\infty U_\infty^2}{\left(M^2-1\right)^{1/2}} \frac{1}{U_\infty} \frac{M^2-2}{M^2-1} \left[LG\right]^T \left[A^{-1}\right]^T \left[D_f\right] \left[A^{-1}\right] \left[LG\right]$$

$$\left[k_f\right] = -\frac{\rho_\infty U_\infty^2}{\left(M^2-1\right)^{1/2}} \left[LG\right]^T \left[A^{-1}\right]^T \left[G_f\right] \left[A^{-1}\right] \left[LG\right] \tag{46}$$

From these equations, one can assemble the damping and stiffness matrices for each element to obtain the mass and stiffness matrices for the whole shell: $\left[C_f\right]$ and $\left[K_f\right]$.

The governing equation which accounts for fluid-shell interaction in the presence of axial in the presence of internal pressure is derived as:

$$\left[M_s\right]\left\{\ddot{\delta}\right\} - \left[C_f\right]\left\{\dot{\delta}\right\} + \left[\left[K_s\right] - \left[K_f\right]\right]\left\{\delta\right\} = 0 \tag{47}$$

where subscripts *s* and *f* refer to shells in vacuo and fluid respectively.

3. Eigenvalue problem

The global fluid matrices mentioned in equation (47) may be obtained, respectively by superimposing the damping and stiffness matrices for each individual fluid finite element. After applying the boundary conditions the global matrices are reduced to squares matrices of order $4(N+1)-J$, where N is the number of finite elements in the shell and J is the number of constraints applied. Finally, the eigenvalue problem is solved by means of the equation reduction technique. Equation may be rewritten as follows:

$$\begin{bmatrix} [0] & [M_s] \\ [M_s] & -[C_f] \end{bmatrix} \begin{Bmatrix} \{\ddot{\delta}\} \\ \{\dot{\delta}\} \end{Bmatrix} + \begin{bmatrix} -[M_s] & [0] \\ [0] & [K] \end{bmatrix} \begin{Bmatrix} \{\dot{\delta}\} \\ \{\delta\} \end{Bmatrix} = \{0\} \tag{48}$$

where

$$\left[K\right] = \left[K_s\right] - \left[K_f\right]$$

$\{\delta\}$ is the global displacement vector. $\left[C_f\right]$ and $\left[K_f\right]$ represent the Coriolis and centrifugal forces induced by the flowing fluid. The eigenvalue problem is given by :

$$\left[\left[DD\right]-\Lambda\left[I\right]\right]=\left[0\right] \tag{49}$$

where

$$\left[DD\right]=\begin{bmatrix}\left[0\right] & \left[I\right]\\ \left[K\right]^{-1}\left[M_s\right] & -\left[K\right]^{-1}\left[C_f\right]\end{bmatrix}$$

$\Lambda=\dfrac{1}{\omega^2}$ and $\left[I\right]$ is the identity matrix.

An in house computer code was developed as part of this work to establish the structural matrices of each element based on equations developed using the theoretical approach. The calculations for each finite element are performed in two stages: the first dealing with solid shell and the second with the effect of the flowing fluid.

4. Results and discussion

In this section numerical results are presented and compared with existing experimental, analytical and numerical data.

4.1 Validation and comparison

For the cases investigated in the present paper, the predicted dimensionless frequencies are expressed by the following relation:

$$\Omega=\omega R\left(\frac{\rho}{E}\right)^{\frac{1}{2}}$$

where:

ω is the natural angular frequency,

R is the radius of the reference surface,

ρ is the density,

E is the modulus of elasticity.

Results for different boundary conditions, geometries, flow parameters and radius to thickness ratios compared to experimental, theoretical and numerical analyses are presented

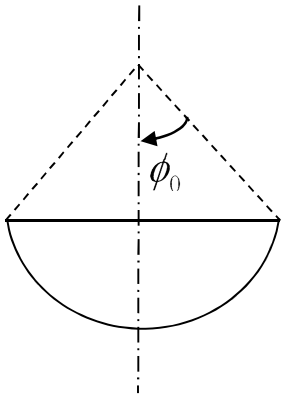

Fig.4. Definition of angle ϕ_0

The problem treated for validation is the flutter boundary of a simply–supported spherical shell subjected to external supersonic airflow. As there is no information available for flutter of spherical shell, this case has been compared with simply-supported cone studied by various authors. The conical shell has the following data: Young's Modulus, E=6.5 10^6 ln-in^{-2}, Poisson's ratio, ν=0.29, material mass density, ρ=8.33 10^{-4} lb-s^2-in^{-4}, shell thickness, h=0.051 in, cone semi-vertex angle α= 5°. The supersonic airflow has freestream Mach number, M_∞ = 3, stagnation temperature, T_∞ = 288.15 K. The results are shown in Table 1 where Λ the dynamic pressure parameter is defined as:

$$\Lambda = \frac{\rho_\infty U_\infty^2 R^3}{K\sqrt{(M_\infty^2 - 1)}}$$

where $K = \dfrac{Et^3}{12\left(1-\nu^2\right)}$ is the bending stiffness.

Table 1. : Comparison of critical dynamical pressure parameter

Present	Dixon and Hudson [15]	Udea et al. [14]	Pidaparti and Yang Henri[21]	Shulman [13]	Bismark-Nasr[17]
520(5)	590(5)	609(5)	576(5)	669(6)	702(6)

When results are summarized and compared with other finite element and analytical solutions, this method shows good convergence using only 15 elements with small disagreements. It should be noted that the previous analytical methods [13, 15] use Donnel-Mushtari simplified shell theory while [14] uses Novozhilov's thin shell with the different method of application of finite element solution. On the other hand, a complete form of the linear piston theory is used by [21] as in the present study and the results are so close to each other; but the expression used by Dixon and Hudson[15], Ueda and al.[14] for the piston theory has not a curvature term which has caused greater differences in the results.

4.2 Flutter boundary

The complex frequencies only for the first and second modes versus freestream dynamic pressure are plotted in Fig. 5. Aerodynamic pressure is evaluated using equation (36). In Fig. 5a the real part of the complex frequency increases for the first mode while for the second mode it decreases as the freestream dynamic pressure parameter Λ increases. For higher values of dynamic pressure these real parts, representing the oscillation frequency, eventually coalesce into a single mode. Further increasing the dynamic pressure of the flow causes the shell to lose its stability at $\Lambda = 410$. This instability is due to coupled-mode flutter where the imaginary part of complex frequency (representing the damping term of the aeroelastic system) becomes zero for certain critical pressure (Fig. 5b).

The same behaviour is observed by real and imaginary parts as the static pressure increases is observed in Fig. 6 but the onset of flutter is at $\Lambda = 450$ where the freestream static pressure is evaluated using equation (37). Prediction of the critical freestream static pressure using equation (36) provides the approximately the same results when evaluating the pressure field using equation (37). As expected, the piston theory with the correction term to account for shell

curvature produces a better approximation for the pressure loading acting on a curved shell exposed to supersonic flow.

(a)

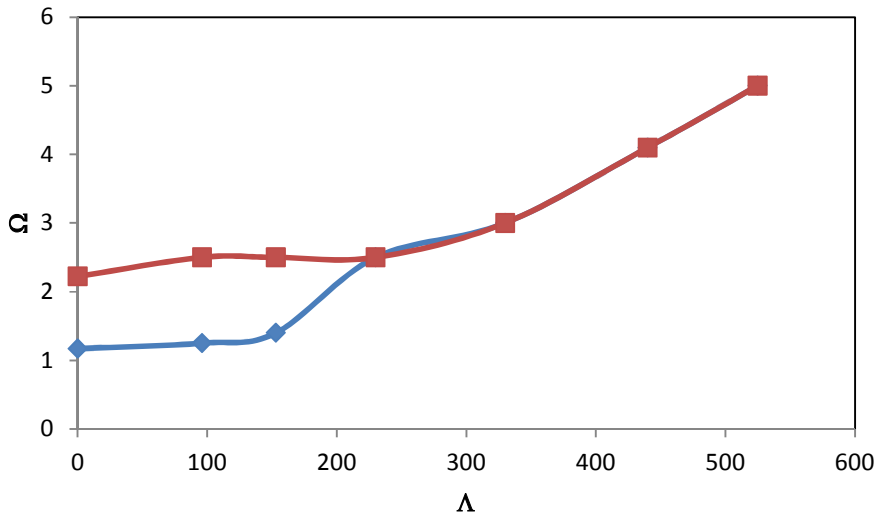

(b)

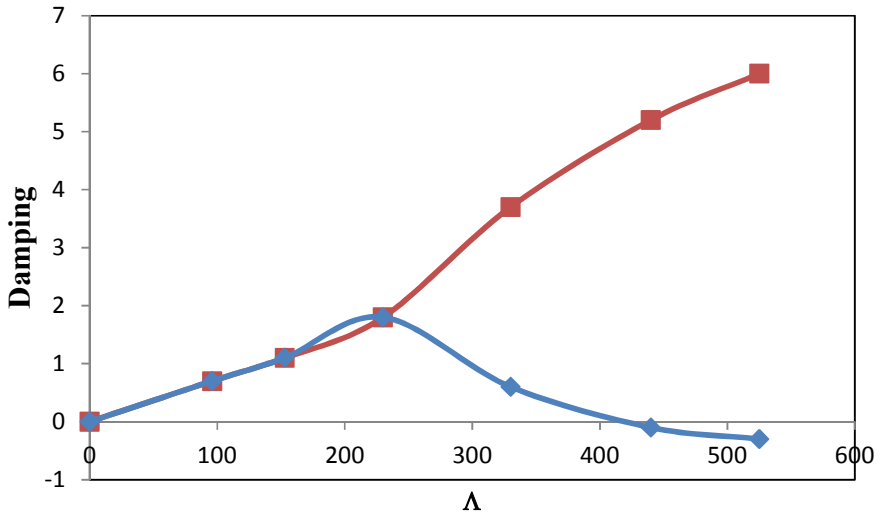

Fig. 5. (a) Real part and (b) Imaginary part of the complex frequencies versus freestream static pressure parameter, static pressure evaluated by Eq. (36)

(a)

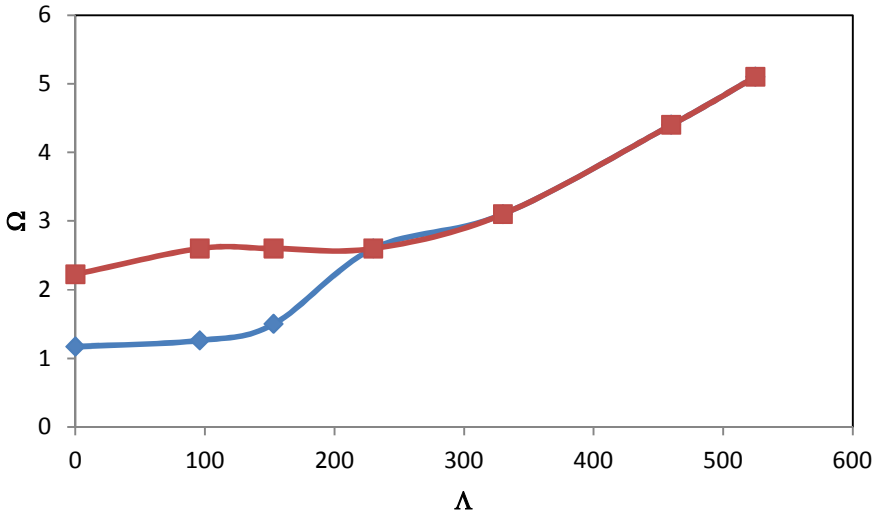

(b)

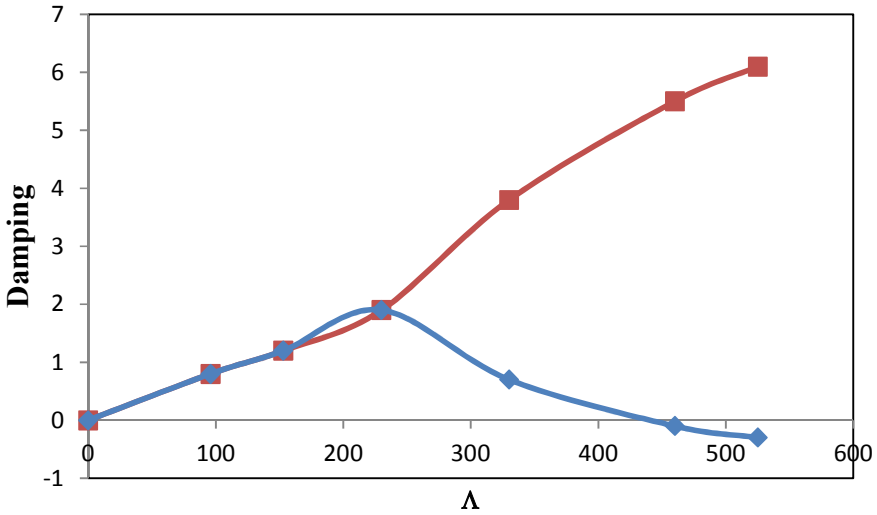

Fig. 6. (a) Real part and (b) Imaginary part of the complex frequencies versus freestream static pressure parameter, static pressure evaluated by Eq. (37)

In Figure 7 the onset of flutter for different angles is plotted, by increasing the angle ϕ_0, flutter instability occurs at lower pressure. This degreases in Λ with ϕ_0 is attributed to the fact that the natural frequencies always decrease with increasing the angle ϕ_0.

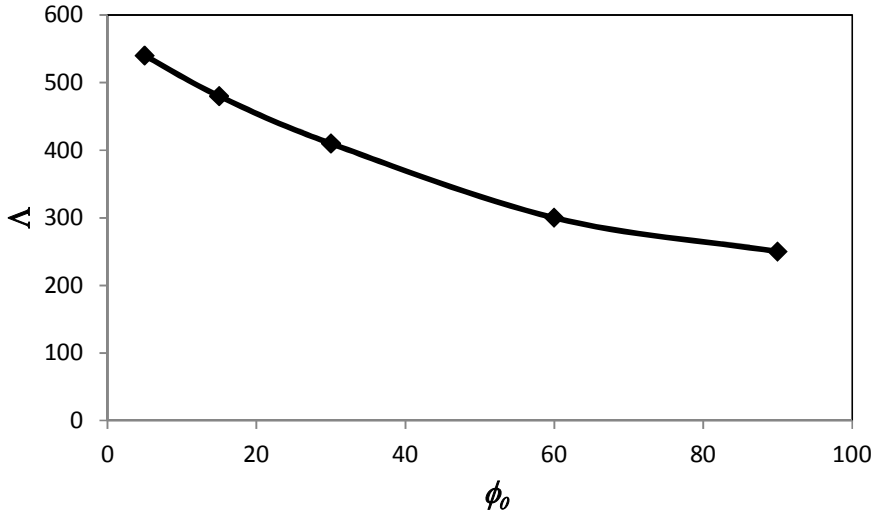

Fig.7. Variation of freestream static pressure parameter with angle ϕ_0

The effect of radius to thickness ratio *R/h* is presented in Fig. 8. This figure shows an increase of Λ with an increase of radius to thickness ratio.

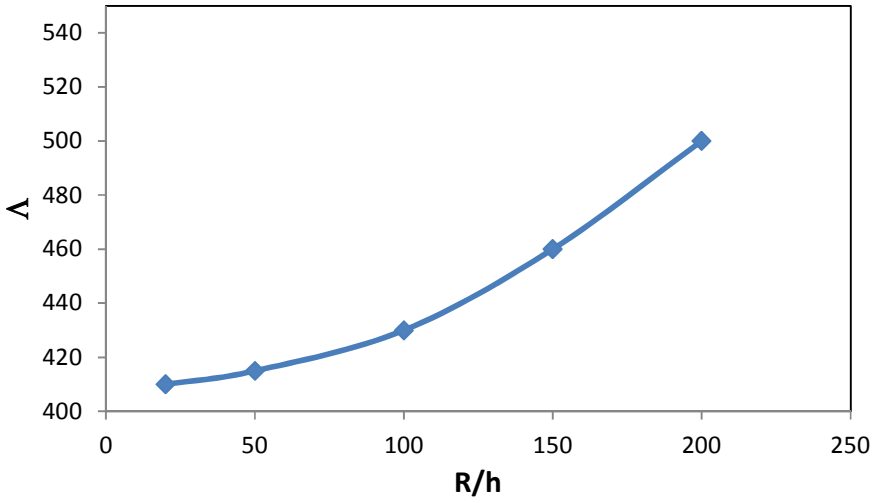

Fig. 8. Variation of freestream static pressure parameter with R/h

The effect of boundary conditions on the flutter onset is presented in table 2. It is seen that for freely simply supported ends, $v = w=0$, flutter onset occurs at $\Lambda = 510.5$ which indicates more flutter resistance compared to simply supported or clamped ends. It is indicated that is no difference for flutter onset when the shell is either clamped or simply supported.

Table 2. : Critical freestream pressure parameter for different boundary conditions.

Boundary conditions	Λ	Mode no.
Freely simply supported ($v=w=0$)	510.5	Coupled 1st and 2nd
Simply supported*(u=v=w=0)*	410	Coupled 1st and 2nd
Clamped	410	Coupled 1st and 2nd

5. Conclusion

An efficient hybrid finite element method is presented to investigate the aeroelastic stability of an empty spherical shell subjected to external supersonic flow. Linear shell theory is coupled with first order piston theory to account for aerodynamic pressure. The effect of curvature correction in piston theory was analyzed. The study has been done for shells with various geometries, radius to thickness ratios and boundary conditions. In all study cases one type of instability is found; coupled-mode flutter in the first and second mode. Increasing the radius to thickness ratio leads the onset of flutter to occur at higher dynamic pressure. Decreasing the angle ϕ_0 of the spherical shell causes the flutter boundary to occur at lower dynamic pressure. The proposed hybrid finite element formulation can gives reliable results at less computational cost compared to commercial software since the latter imposes some restrictions when such analysis is done.

Appendix

$$
\begin{aligned}
L_1(U_\phi,U_\theta,W) &= \left(\frac{P_{11}}{R}+\frac{P_{41}}{R^2}\right)\left[\frac{\partial}{\partial\phi}\left(\frac{\partial U_\phi}{\partial\phi}+W\right)+\left(\frac{\partial U_\phi}{\partial\phi}+W\right)\cot(\phi)\right] \\
&+\left(\frac{P_{12}}{R}+\frac{P_{42}}{R^2}\right)\left[\frac{\partial}{\partial\phi}\left(\frac{1}{\sin(\phi)}\frac{\partial U_\theta}{\partial\theta}+U_\phi\cot(\phi)+W\right)+\left(\frac{1}{\sin(\phi)}\frac{\partial U_\theta}{\partial\theta}+U_\phi\cot(\phi)+W\right)\cot(\phi)\right] \\
&+\frac{1}{R}\left(\frac{P_{14}}{R}+\frac{P_{44}}{R^2}\right)\left[\frac{\partial}{\partial\phi}\left(\frac{\partial U_\phi}{\partial\phi}-\frac{\partial^2 W}{\partial\phi^2}\right)+\left(\frac{\partial U_\phi}{\partial\phi}-\frac{\partial^2 W}{\partial\phi^2}\right)\cot(\phi)\right] \\
&+\frac{1}{R}\left(\frac{P_{15}}{R}+\frac{P_{45}}{R^2}\right)\left[\frac{\partial}{\partial\phi}\left(\frac{1}{\sin(\phi)}\frac{\partial U_\theta}{\partial\theta}+U_\phi\cot(\phi)-\frac{1}{\sin^2(\phi)}\frac{\partial^2 W}{\partial\theta^2}-\frac{\partial W}{\partial\phi}\cot(\phi)\right)+\left(\frac{1}{\sin(\phi)}\frac{\partial U_\theta}{\partial\theta}+U_\phi\cot(\phi)-\frac{1}{\sin^2(\phi)}\frac{\partial^2 W}{\partial\theta^2}-\frac{\partial W}{\partial\phi}\cot(\phi)\right)\cot(\phi)\right] \\
&-\left(\frac{P_{21}}{R}+\frac{P_{51}}{R^2}\right)\left(\frac{\partial U_\phi}{\partial\phi}+W\right)\cot(\phi) \\
&-\left(\frac{P_{22}}{R}+\frac{P_{52}}{R^2}\right)\left(\frac{1}{\sin(\phi)}\frac{\partial U_\theta}{\partial\theta}+U_\phi\cot(\phi)+W\right)\cot(\phi) \\
&-\frac{1}{R}\left(\frac{P_{24}}{R}+\frac{P_{54}}{R^2}\right)\left(\frac{\partial U_\phi}{\partial\phi}-\frac{\partial^2 W}{\partial\phi^2}\right)\cot(\phi) \\
&-\frac{1}{R}\left(\frac{P_{25}}{R}+\frac{P_{55}}{R^2}\right)\left(\frac{1}{\sin(\phi)}\frac{\partial U_\theta}{\partial\theta}+U_\phi\cot(\phi)-\frac{1}{\sin^2(\phi)}\frac{\partial^2 W}{\partial\theta^2}-\frac{\partial W}{\partial\phi}\cot(\phi)\right)\cot(\phi) \\
&+\left(\frac{P_{33}}{R}+\frac{P_{63}}{R^2}\right)\frac{1}{\sin(\phi)}\frac{\partial}{\partial\theta}\left(\frac{\partial U_\theta}{\partial\phi}+\frac{1}{\sin(\phi)}\frac{\partial U_\varphi}{\partial\theta}-U_\theta\cot(\phi)\right) \\
&+\frac{1}{R}\left(\frac{P_{36}}{R}+\frac{P_{66}}{R^2}\right)\frac{1}{\sin(\phi)}\frac{\partial}{\partial\theta}\left(\frac{\partial U_\theta}{\partial\phi}+\frac{1}{\sin(\phi)}\frac{\partial U_\varphi}{\partial\theta}-U_\theta\cot(\phi)+2\frac{\cot(\phi)}{\sin(\phi)}\frac{\partial W}{\partial\theta}-\frac{2}{\sin(\phi)}\frac{\partial^2 W}{\partial\phi\,\partial\theta}\right)
\end{aligned}
$$

$$
\begin{aligned}
L_2(U_\phi,U_\theta,W) &= \left(\frac{P_{21}}{R}+\frac{P_{51}}{R^2}\right)\frac{1}{\sin(\phi)}\frac{\partial}{\partial\theta}\left(\frac{\partial U_\phi}{\partial\phi}+W\right) \\
&+\left(\frac{P_{22}}{R}+\frac{P_{52}}{R^2}\right)\frac{1}{\sin(\phi)}\frac{\partial}{\partial\theta}\left(\frac{1}{\sin(\phi)}\frac{\partial U_\theta}{\partial\theta}+U_\phi\cot(\phi)+W\right) \\
&+\frac{1}{R}\left(\frac{P_{24}}{R}+\frac{P_{54}}{R^2}\right)\frac{1}{\sin(\phi)}\frac{\partial}{\partial\theta}\left(\frac{\partial U_\phi}{\partial\phi}-\frac{\partial^2 W}{\partial\phi^2}\right) \\
&+\frac{1}{R}\left(\frac{P_{25}}{R}+\frac{P_{55}}{R^2}\right)\frac{1}{\sin(\phi)}\frac{\partial}{\partial\theta}\left(\frac{1}{\sin(\phi)}\frac{\partial U_\theta}{\partial\theta}+U_\phi\cot(\phi)-\frac{1}{\sin^2(\phi)}\frac{\partial^2 W}{\partial\theta^2}-\frac{\partial W}{\partial\phi}\cot(\phi)\right) \\
&+\left(\frac{P_{33}}{R}+\frac{P_{63}}{R^2}\right)\left[\frac{\partial}{\partial\phi}\left(\frac{\partial U_\theta}{\partial\phi}+\frac{1}{\sin(\phi)}\frac{\partial U_\varphi}{\partial\theta}-U_\theta\cot(\phi)\right)+2\left(\frac{\partial U_\theta}{\partial\phi}+\frac{1}{\sin(\phi)}\frac{\partial U_\varphi}{\partial\theta}-U_\theta\cot(\phi)\right)\cot(\phi)\right] \\
&+\frac{1}{R}\left(\frac{P_{36}}{R}+\frac{P_{66}}{R^2}\right)\left[\frac{\partial}{\partial\phi}\left(\frac{\partial U_\theta}{\partial\phi}+\frac{1}{\sin(\phi)}\frac{\partial U_\varphi}{\partial\theta}-U_\theta\cot(\phi)+2\frac{\cot(\phi)}{\sin(\phi)}\frac{\partial W}{\partial\theta}-\frac{2}{\sin(\phi)}\frac{\partial^2 W}{\partial\phi\,\partial\theta}\right)+2\left(\frac{\partial U_\theta}{\partial\phi}+\frac{1}{\sin(\phi)}\frac{\partial U_\varphi}{\partial\theta}-U_\theta\cot(\phi)+2\frac{\cot(\phi)}{\sin(\phi)}\frac{\partial W}{\partial\theta}-\frac{2}{\sin(\phi)}\frac{\partial^2 W}{\partial\phi\,\partial\theta}\right)\cot t(\phi)\right]
\end{aligned}
$$

$$
\begin{aligned}
L_3(U_\phi, U_\theta, W) = &-\left(\frac{P_{11}}{R}+\frac{P_{21}}{R}\right)\left(\frac{\partial U_\phi}{\partial \phi}+W\right)\\
&-\left(\frac{P_{12}}{R}+\frac{P_{22}}{R}\right)\left(\frac{1}{\sin(\phi)}\frac{\partial U_\theta}{\partial \theta}+U_\phi\cot(\phi)+W\right)\\
&-\left(\frac{P_{14}}{R^2}+\frac{P_{24}}{R^2}\right)\left(\frac{\partial U_\phi}{\partial \phi}-\frac{\partial^2 W}{\partial \phi^2}\right)\\
&-\left(\frac{P_{15}}{R^2}+\frac{P_{25}}{R^2}\right)\left(\frac{1}{\sin(\phi)}\frac{\partial U_\theta}{\partial \theta}+U_\phi\cot(\phi)-\frac{1}{\sin^2(\phi)}\frac{\partial^2 W}{\partial \theta^2}-\frac{\partial W}{\partial \phi}\cot(\phi)\right)\\
&+\frac{P_{41}-P_{51}}{R^2}\left(\cot(\phi)\frac{\partial}{\partial \phi}\left(\frac{\partial U_\phi}{\partial \phi}+W\right)-\left(\frac{\partial U_\phi}{\partial \phi}+W\right)\right)\\
&+\frac{1}{R^2\sin(\phi)}\left[P_{41}\frac{\partial}{\partial \phi}\left(\sin(\phi)\frac{\partial}{\partial \phi}\left(\frac{\partial U_\phi}{\partial \phi}+W\right)\right)+P_{51}\frac{\partial}{\partial \theta}\left(\frac{\partial U_\phi}{\partial \phi}+W\right)\right]\\
&+\frac{P_{42}-P_{52}}{R^2}\left(\cot(\phi)\frac{\partial}{\partial \phi}\left(\frac{1}{\sin(\phi)}\frac{\partial U_\theta}{\partial \theta}+U_\phi\cot(\phi)+W\right)-\left(\frac{1}{\sin(\phi)}\frac{\partial U_\theta}{\partial \theta}+U_\phi\cot(\phi)+W\right)\right)\\
&+\frac{1}{R^2\sin(\phi)}\left[P_{42}\frac{\partial}{\partial \phi}\left(\sin(\phi)\frac{\partial}{\partial \phi}\left(\frac{1}{\sin(\phi)}\frac{\partial U_\theta}{\partial \theta}+U_\phi\cot(\phi)+W\right)\right)+P_{52}\frac{\partial}{\partial \theta}\left(\frac{1}{\sin(\phi)}\frac{\partial U_\theta}{\partial \theta}+U_\phi\cot(\phi)+W\right)\right]\\
&+\frac{P_{44}-P_{54}}{R^3}\left(\cot(\phi)\frac{\partial}{\partial \phi}\left(\frac{\partial U_\phi}{\partial \phi}-\frac{\partial^2 W}{\partial \phi^2}\right)-\left(\frac{\partial U_\phi}{\partial \phi}-\frac{\partial^2 W}{\partial \phi^2}\right)\right)\\
&+\frac{1}{R^3\sin(\phi)}\left[P_{44}\frac{\partial}{\partial \phi}\left(\sin(\phi)\frac{\partial}{\partial \phi}\left(\frac{\partial U_\phi}{\partial \phi}-\frac{\partial^2 W}{\partial \phi^2}\right)\right)+P_{54}\frac{\partial}{\partial \theta}\left(\frac{\partial U_\phi}{\partial \phi}-\frac{\partial^2 W}{\partial \phi^2}\right)\right]\\
&+\frac{P_{45}-P_{55}}{R^3}\left(\cot(\phi)\frac{\partial}{\partial \phi}\left(\frac{1}{\sin(\phi)}\frac{\partial U_\theta}{\partial \theta}+U_\phi\cot(\phi)-\frac{1}{\sin^2(\phi)}\frac{\partial^2 W}{\partial \theta^2}-\frac{\partial W}{\partial \phi}\cot(\phi)\right)-\left(\frac{1}{\sin(\phi)}\frac{\partial U_\theta}{\partial \theta}+U_\phi\cot(\phi)-\frac{1}{\sin^2(\phi)}\frac{\partial^2 W}{\partial \theta^2}-\frac{\partial W}{\partial \phi}\cot(\phi)\right)\right)\\
&+\frac{1}{R^3\sin(\phi)}\left[P_{45}\frac{\partial}{\partial \phi}\left(\sin(\phi)\frac{\partial}{\partial \phi}\left(\frac{1}{\sin(\phi)}\frac{\partial U_\theta}{\partial \theta}+U_\phi\cot(\phi)-\frac{1}{\sin^2(\phi)}\frac{\partial^2 W}{\partial \theta^2}-\frac{\partial W}{\partial \phi}\cot(\phi)\right)\right)+P_{55}\frac{\partial}{\partial \theta}\left(\frac{1}{\sin(\phi)}\frac{\partial U_\theta}{\partial \theta}+U_\phi\cot(\phi)-\frac{1}{\sin^2(\phi)}\frac{\partial^2 W}{\partial \theta^2}-\frac{\partial W}{\partial \phi}\cot(\phi)\right)\right]\\
&+\frac{P_{63}}{R^2\sin(\phi)}\left[\frac{\partial^2}{\partial \phi\partial \theta}\left(\frac{\partial U_\theta}{\partial \phi}+\frac{1}{\sin(\phi)}\frac{\partial U_\varphi}{\partial \theta}-U_\theta\cot(\phi)\right)+3\cot(\phi)\left(\frac{\partial}{\partial \theta}\frac{\partial U_\theta}{\partial \phi}+\frac{1}{\sin(\phi)}\frac{\partial U_\varphi}{\partial \theta}-U_\theta\cot(\phi)\right)\right]\\
&+\frac{P_{66}}{R^3\sin(\phi)}\left[\frac{\partial^2}{\partial \phi\partial \theta}\left(\frac{\partial U_\theta}{\partial \phi}+\frac{1}{\sin(\phi)}\frac{\partial U_\varphi}{\partial \theta}-U_\theta\cot(\phi)+2\frac{\cot(\phi)}{\sin(\phi)}\frac{\partial W}{\partial \theta}-\frac{2}{\sin(\phi)}\frac{\partial^2 W}{\partial \phi\,\partial \theta}\right)+3\cot(\phi)\left(\frac{\partial U_\theta}{\partial \phi}+\frac{1}{\sin(\phi)}\frac{\partial U_\varphi}{\partial \theta}-U_\theta\cot(\phi)+2\frac{\cot(\phi)}{\sin(\phi)}\frac{\partial W}{\partial \theta}-\frac{2}{\sin(\phi)}\frac{\partial^2 W}{\partial \phi\,\partial \theta}\right)\right]
\end{aligned}
$$

$$R(1,1) = \left(-e_1 n \cot\phi P^n_{\mu_1} + e_1 c_1 P^{n-1}_{\mu_1}\right)$$

$$R(1,2) = -ne_2 \cot\phi \,\mathrm{Re}(P^n_{\mu_2}) - ne_3 \cot\phi \,\mathrm{Im}(P^n_{\mu_2}) + (e_2c_2 + e_3c_3)\,\mathrm{Re}(P^{n-1}_{\mu_2}) + (e_3c_2 - e_2c_3)\,\mathrm{Im}(P^{n-1}_{\mu_2})$$

$$R(1,3) = ne_3 \cot\phi \,\mathrm{Re}(P^n_{\mu_2}) - ne_2 \cot\phi \,\mathrm{Im}(P^n_{\mu_2}) - (e_3c_2 - e_2c_3)\,\mathrm{Re}(P^{n-1}_{\mu_2}) + (e_2c_2 + e_3c_3)\,\mathrm{Im}(P^{n-1}_{\mu_2})$$

$$R(1,4) = -\frac{n^2}{2\sin\phi} P^n_1$$

$$R(1,5) = \left(-e_1 n \cot\phi Q^n_{\mu_1} + e_1 c_1 Q^{n-1}_{\mu_1}\right)$$

$$R(1,6) = -ne_2 \cot\phi \,\mathrm{Re}(Q^n_{\mu_2}) - ne_3 \cot\phi \,\mathrm{Im}(Q^n_{\mu_2}) + (e_2c_2 + e_3c_3)\,\mathrm{Re}(Q^{n-1}_{\mu_2}) + (e_3c_2 - e_2c_3)\,\mathrm{Im}(Q^{n-1}_{\mu_2})$$

$$R(1,7) = ne_3 \cot\phi \,\mathrm{Re}(Q^n_{\mu_2}) - ne_2 \cot\phi \,\mathrm{Im}(Q^n_{\mu_2}) - (e_3c_2 - e_2c_3)\,\mathrm{Re}(Q^{n-1}_{\mu_2}) + (e_2c_2 + e_3c_3)\,\mathrm{Im}(Q^{n-1}_{\mu_2})$$

$$R(1,8) = -\frac{n^2}{2\sin\phi} Q^n_1$$

$$R(2,1) = P^n_{\mu_1}$$

$$R(2,2) = \mathrm{Re}(P^n_{\mu_2})$$

$$R\left(2,3\right) = \mathrm{Im}(P^n_{\mu_2})$$

$$R\left(2,4\right) = 0$$

$$R(2,5) = Q^n_{\mu_1}$$

$$R(2,6) = \mathrm{Re}(Q^n_{\mu_2})$$

$$R\left(2,7\right) = \mathrm{Im}(Q^n_{\mu_2})$$

$$R\left(2,8\right) = 0$$

$$R\left(3,1\right) = -ne_1 \frac{1}{\sin\phi} P^n_{\mu_1}$$

$$R(3,2) = -ne_2 \frac{1}{\sin\phi}\mathrm{Re}(P^n_{\mu_2}) - ne_3 \frac{1}{\sin\phi}\mathrm{Im}(P^n_{\mu_2})$$

$$R(3,3) = ne_3 \frac{1}{\sin\phi}\mathrm{Re}(P^n_{\mu_2}) - ne_2 \frac{1}{\sin\phi}\mathrm{Im}(P^n_{\mu_2})$$

$$R(3,4) = -\frac{n^2}{2}\cot\phi P^n_1 + \frac{n}{2}(n-2)(n+1)P^{n-1}_1$$

$$R(3,5) = -ne_1 \frac{1}{\sin\phi} Q^n_{\mu_1}$$

$$R(3,6) = -ne_2 \frac{1}{\sin\phi}\mathrm{Re}(Q^n_{\mu_2}) - ne_3 \frac{1}{\sin\phi}\mathrm{Im}(Q^n_{\mu_2})$$

$$R(3,7) = ne_3 \frac{1}{\sin\phi}\mathrm{Re}(Q^n_{\mu_2}) - ne_2 \frac{1}{\sin\phi}\mathrm{Im}(Q^n_{\mu_2})$$

$$R(3,8) = -\frac{n^2}{2}\cot\phi Q^n_1 + \frac{n}{2}(n-2)(n+1)Q^{n-1}_1$$

$$A(1,j) = R(1,j),\quad A(2,j) = R(2,j),\quad A(3,j) = \frac{dw_n}{d\phi}(j),\quad A(4,j) = R(3,j) \text{ with } \phi = \phi_i$$

$$A(5,j) = R(1,j),\ A(6,j) = R(2,j)\ ;\ A(7,j) = \frac{dw_n}{d\phi}(j),\ A(8,j) = R(3,j) \text{ with } \phi = \phi_j$$

j=1,…, 8

$$Q(1,1)=\frac{1}{R}\left[e_1c_1+ne_1(\frac{1}{\sin^2\phi}+n\cot^2\phi)+1\right]P_{\mu_1}^n-\frac{e_1}{r}c_1\cot\phi P_{\mu_1}^{n-1}$$

$$Q(1,2)=\frac{1}{R}\left[\left(e_2c_2+e_3c_3\right)+ne_2(\frac{1}{\sin^2\phi}+n\cot^2\phi)+1\right]\mathrm{Re}(P_{\mu_2}^n)$$
$$+\frac{1}{R}\left[\left(e_3c_2-e_2c_3\right)+ne_3(\frac{1}{\sin^2\phi}+n\cot^2\phi)\right]\mathrm{Im}(P_{\mu_2}^n)$$
$$-\frac{1}{R}\left(e_2c_2+e_3c_3\right)\cot\phi\,\mathrm{Re}(P_{\mu_2}^{n-1})-\frac{1}{R}\left(e_3c_2-e_2c_3\right)\cot\phi\,\mathrm{Im}(P_{\mu_2}^{n-1})$$

$$Q(1,3)=-\frac{1}{R}\left[\left(e_3c_2-e_2c_3\right)+ne_3(\frac{1}{\sin^2\phi}+n\cot^2\phi)\right]\mathrm{Re}(P_{\mu_2}^n)$$
$$+\frac{1}{R}\left[\left(e_2c_2+e_3c_3\right)+ne_2(\frac{1}{\sin^2\phi}+n\cot^2\phi)+1\right]\mathrm{Im}(P_{\mu_2}^n)$$
$$+\frac{1}{R}\left(e_3c_2-e_2c_3\right)\cot\phi\,\mathrm{Re}(P_{\mu_2}^{n-1})-\frac{1}{R}\left(e_2c_2+e_3c_3\right)\cot\phi\,\mathrm{Im}(P_{\mu_2}^{n-1})$$

$$Q(1,4)=\frac{n^2}{2R}(n+1)\frac{1}{\sin\phi}\cot\phi P_1^n-\frac{n^2}{2R}(n-2)(n+1)\frac{1}{\sin\phi}P_1^{n-1}$$

$$Q(1,5)=\frac{1}{R}\left[e_1c_1+ne_1(\frac{1}{\sin^2\phi}+n\cot^2\phi)+1\right]Q_{\mu_1}^n-\frac{e_1}{r}c_1\cot\phi Q_{\mu_1}^{n-1}$$

$$Q(1,6)=\frac{1}{R}\left[\left(e_2c_2+e_3c_3\right)+ne_2(\frac{1}{\sin^2\phi}+n\cot^2\phi)+1\right]\mathrm{Re}(Q_{\mu_2}^n)$$
$$+\frac{1}{R}\left[\left(e_3c_2-e_2c_3\right)+ne_3(\frac{1}{\sin^2\phi}+n\cot^2\phi)\right]\mathrm{Im}(Q_{\mu_2}^n)$$
$$-\frac{1}{R}\left(e_2c_2+e_3c_3\right)\cot\phi\,\mathrm{Re}(Q_{\mu_2}^{n-1})-\frac{1}{R}\left(e_3c_2-e_2c_3\right)\cot\phi\,\mathrm{Im}(Q_{\mu_2}^{n-1})$$

$$Q(1,7)=-\frac{1}{R}\left[\left(e_3c_2-e_2c_3\right)+ne_3(\frac{1}{\sin^2\phi}+n\cot^2\phi)\right]\mathrm{Re}(Q_{\mu_2}^n)$$
$$+\frac{1}{R}\left[\left(e_2c_2+e_3c_3\right)+ne_2(\frac{1}{\sin^2\phi}+n\cot^2\phi)+1\right]\mathrm{Im}(Q_{\mu_2}^n)$$
$$+\frac{1}{R}\left(e_3c_2-e_2c_3\right)\cot\phi\,\mathrm{Re}(Q_{\mu_2}^{n-1})-\frac{1}{R}\left(e_2c_2+e_3c_3\right)\cot\phi\,\mathrm{Im}(Q_{\mu_2}^{n-1})$$

$$Q(1,8)=\frac{n^2}{2R}(n+1)\frac{1}{\sin\phi}\cot\phi Q_1^n-\frac{n^2}{2R}(n-2)(n+1)\frac{1}{\sin\phi}Q_1^{n-1}$$

$$Q(2,1)=\frac{1}{R}\left[1-ne_1(n\frac{1}{\sin^2\phi}+\cot^2\phi)\right]P_{\mu_1}^n+\frac{e_1}{r}c_1\cot\phi P_{\mu_1}^{n-1}$$

$$Q(2,2)=\frac{1}{R}\left[1-ne_2(n\frac{1}{\sin^2\phi}+\cot^2\phi)\right]\mathrm{Re}(P_{\mu_2}^n)-\frac{ne_3}{R}(n\frac{1}{\sin^2\phi}+\cot^2\phi)\,\mathrm{Im}(P_{\mu_2}^n)$$
$$+\frac{1}{R}(e_2c_2+e_3c_3)\cot\phi\,\mathrm{Re}(P_{\mu_2}^{n-1})+\frac{1}{R}(e_3c_2-e_2c_3)\cot\phi\,\mathrm{Im}(P_{\mu_2}^{n-1})$$

$$Q(2,3)=\frac{ne_3}{R}(n\frac{1}{\sin^2\phi}+\cot^2\phi)\,\mathrm{Re}(P_{\mu_2}^n)+\frac{1}{R}\left[1-ne_2(n\frac{1}{\sin^2\phi}+\cot^2\phi)\right]\mathrm{Im}(P_{\mu_2}^n)$$
$$-\frac{1}{R}(e_3c_2-e_2c_3)\cot\phi\,\mathrm{Re}(P_{\mu_2}^{n-1})+\frac{1}{R}(e_2c_2+e_3c_3)\cot\phi\,\mathrm{Im}(P_{\mu_2}^{n-1})$$

$$Q(2,4)=-\frac{n^2}{2R}(n+1)\frac{1}{\sin\phi}\cot\phi P_1^n+\frac{n^2}{2R}(n-2)(n+1)\frac{1}{\sin\phi}P_1^{n-1}$$

$$Q(2,5)=\frac{1}{R}\left[1-ne_1(\frac{1}{\sin^2\phi}+n\cot^2\phi)\right]Q_{\mu_1}^n+\frac{e_1}{r}c_1\cot\phi Q_{\mu_1}^{n-1}$$

$$Q(2,6)=\frac{1}{R}\left[1-ne_2(n\frac{1}{\sin^2\phi}+\cot^2\phi)\right]\mathrm{Re}(Q_{\mu_2}^n)-\frac{ne_3}{R}(n\frac{1}{\sin^2\phi}+\cot^2\phi)\,\mathrm{Im}(Q_{\mu_2}^n)$$
$$+\frac{1}{R}(e_2c_2+e_3c_3)\cot\phi\,\mathrm{Re}(Q_{\mu_2}^{n-1})+\frac{1}{R}(e_3c_2-e_2c_3)\cot\phi\,\mathrm{Im}(Q_{\mu_2}^{n-1})$$

$$Q(2,7)=\frac{ne_3}{R}(n\frac{1}{\sin^2\phi}+\cot^2\phi)\,\mathrm{Re}(Q_{\mu_2}^n)+\frac{1}{R}\left[1-ne_2(n\frac{1}{\sin^2\phi}+\cot^2\phi)\right]\mathrm{Im}(Q_{\mu_2}^n)$$
$$-\frac{1}{R}(e_3c_2-e_2c_3)\cot\phi\,\mathrm{Re}(Q_{\mu_2}^{n-1})+\frac{1}{R}(e_2c_2+e_3c_3)\cot\phi\,\mathrm{Im}(Q_{\mu_2}^{n-1})$$

$$Q(2,8)=-\frac{n^2}{2R}(n+1)\frac{1}{\sin\phi}\cot\phi Q_1^n+\frac{n^2}{2R}(n-2)(n+1)\frac{1}{\sin\phi}Q_1^{n-1}$$

$$Q(3,1)=\frac{2n}{R}e_1(n+1)\frac{1}{\sin\phi}\cot\phi P_{\mu_1}^{n}-\frac{2n}{R}e_1c_1\frac{1}{\sin\phi}P_{\mu_1}^{n-1}$$

$$Q(3,2)=\frac{2n}{R}e_2(n+1)\frac{1}{\sin\phi}\cot\phi\,\mathrm{Re}(P_{\mu_2}^{n})+\frac{2n}{R}e_3(n+1)\frac{1}{\sin\phi}\cot\phi\,\mathrm{Im}(P_{\mu_2}^{n})$$
$$-\frac{2n}{R}(e_2c_2+e_3c_3)\frac{1}{\sin\phi}\mathrm{Re}(P_{\mu_2}^{n-1})-\frac{2n}{R}(e_3c_2-e_2c_3)\frac{1}{\sin\phi}\mathrm{Im}(P_{\mu_2}^{n-1})$$

$$Q(3,3)=-\frac{2n}{R}e_3(n+1)\frac{1}{\sin\phi}\cot\phi\,\mathrm{Re}(P_{\mu_2}^{n})+\frac{2n}{R}e_2(n+1)\frac{1}{\sin\phi}\cot\phi\,\mathrm{Im}(P_{\mu_2}^{n})$$
$$+\frac{2n}{R}(e_3c_2-e_2c_3)\frac{1}{\sin\phi}\mathrm{Re}(P_{\mu_2}^{n-1})-\frac{2n}{R}(e_2c_2+e_3c_3)\frac{1}{\sin\phi}\mathrm{Im}(P_{\mu_2}^{n-1})$$

$$Q(3,4)=\frac{n}{2R}(n+1)\left[(n-2)+n\left(\frac{1}{\sin^2\phi}+\cot^2\phi\right)\right]P_1^{n}-\frac{n}{R}(n-2)(n+1)\cot\phi P_1^{n-1}$$

$$Q(3,5)=\frac{2n}{R}e_1(n+1)\frac{1}{\sin\phi}\cot\phi Q_{\mu_1}^{n}-\frac{2n}{R}c_1\frac{1}{\sin\phi}Q_{\mu_1}^{n-1}$$

$$Q(3,6)=\frac{2n}{R}e_2(n+1)\frac{1}{\sin\phi}\cot\phi\,\mathrm{Re}(Q_{\mu_2}^{n})+\frac{2n}{R}e_3(n+1)\frac{1}{\sin\phi}\cot\phi\,\mathrm{Im}(Q_{\mu_2}^{n})$$
$$-\frac{2n}{R}(e_2c_2+e_3c_3)\frac{1}{\sin\phi}\mathrm{Re}(Q_{\mu_2}^{n-1})-\frac{2n}{R}(e_3c_2-e_2c_3)\frac{1}{\sin\phi}\mathrm{Im}(Q_{\mu_2}^{n-1})$$

$$Q(3,7)=-\frac{2n}{R}e_3(n+1)\frac{1}{\sin\phi}\cot\phi\,\mathrm{Re}(Q_{\mu_2}^{n})+\frac{2n}{R}e_2(n+1)\frac{1}{\sin\phi}\cot\phi\,\mathrm{Im}(Q_{\mu_2}^{n})$$
$$+\frac{2n}{R}(e_3c_2-e_2c_3)\frac{1}{\sin\phi}\mathrm{Re}(Q_{\mu_2}^{n-1})-\frac{2n}{R}(e_2c_2+e_3c_3)\frac{1}{\sin\phi}\mathrm{Im}(Q_{\mu_2}^{n-1})$$

$$Q(3,8)=\frac{n}{2R}(n+1)\left[(n-2)+n\left(\frac{1}{\sin^2\phi}+\cot^2\phi\right)\right]Q_1^{n}-\frac{n}{R}(n-2)(n+1)\cot\phi Q_1^{n-1}$$

$$Q(4,1)=\frac{1}{R^2}\left[\left(e_1-1\right)c_1+n\left(e_1-1\right)\left(\frac{1}{\sin^2\phi}+n\cot^2\phi\right)\right]P_{\mu_1}^n-\frac{e_1-1}{R^2}c_1\cot\phi P_{\mu_1}^{n-1}$$

$$\begin{aligned}Q(4,2)=&\frac{1}{R^2}\left[\left(e_2-1\right)c_2+e_3c_3+n\left(e_2-1\right)\left(\frac{1}{\sin^2\phi}+n\cot^2\phi\right)\right]\mathrm{Re}\left(P_{\mu_2}^n\right)\\&+\frac{1}{R^2}\left[e_3c_2-\left(e_2-1\right)c_3+ne_3\left(\frac{1}{\sin^2\phi}+n\cot^2\phi\right)\right]\mathrm{Im}\left(P_{\mu_2}^n\right)\\&-\frac{1}{R^2}\left[\left(e_2-1\right)c_2+e_3c_3\right]\cot\phi\,\mathrm{Re}\left(P_{\mu_2}^{n-1}\right)-\frac{1}{R^2}\left[e_3c_2-\left(e_2-1\right)c_3\right]\cot\phi\,\mathrm{Im}\left(P_{\mu_2}^{n-1}\right)\end{aligned}$$

$$\begin{aligned}Q(4,3)=&-\frac{1}{R^2}\left[e_3c_2-\left(e_2-1\right)c_3+ne_3\left(\frac{1}{\sin^2\phi}+n\cot^2\phi\right)\right]\mathrm{Re}\left(P_{\mu_2}^n\right)\\&+\frac{1}{R^2}\left[\left(e_2-1\right)c_2+e_3c_3+n\left(e_2-1\right)\left(\frac{1}{\sin^2\phi}+n\cot^2\phi\right)\right]\mathrm{Im}\left(P_{\mu_2}^n\right)\\&+\frac{1}{R^2}\left[e_3c_2-\left(e_2-1\right)c_3\right]\cot\phi\,\mathrm{Re}\left(P_{\mu_2}^{n-1}\right)-\frac{1}{R^2}\left[\left(e_2-1\right)c_2+e_3c_3\right]\cot\phi\,\mathrm{Im}\left(P_{\mu_2}^{n-1}\right)\end{aligned}$$

$$Q(4,4)=\frac{n^2}{2R^2}\left(n+1\right)\frac{1}{\sin\phi}\cot\phi P_1^n-\frac{n^2}{2R^2}(n-2)(n+1)\frac{1}{\sin\phi}P_1^{n-1}$$

$$Q(4,5)=\frac{1}{R^2}\left[\left(e_1-1\right)c_1+n\left(e_1-1\right)\left(\frac{1}{\sin^2\phi}+n\cot^2\phi\right)\right]Q_{\mu_1}^n-\frac{e_1-1}{R^2}c_1\cot\phi Q_{\mu_1}^{n-1}$$

$$\begin{aligned}Q(4,6)=&\frac{1}{R^2}\left[\left(e_2-1\right)c_2+e_3c_3+n\left(e_2-1\right)\left(\frac{1}{\sin^2\phi}+n\cot^2\phi\right)\right]\mathrm{Re}\left(Q_{\mu_2}^n\right)\\&+\frac{1}{R^2}\left[e_3c_2-\left(e_2-1\right)c_3+ne_3\left(\frac{1}{\sin^2\phi}+n\cot^2\phi\right)\right]\mathrm{Im}\left(Q_{\mu_2}^n\right)\\&-\frac{1}{R^2}\left[\left(e_2-1\right)c_2+e_3c_3\right]\cot\phi\,\mathrm{Re}\left(Q_{\mu_2}^{n-1}\right)-\frac{1}{R^2}\left[e_3c_2-\left(e_2-1\right)c_3\right]\cot\phi\,\mathrm{Im}\left(Q_{\mu_2}^{n-1}\right)\end{aligned}$$

$$\begin{aligned}Q(4,7)=&-\frac{1}{R^2}\left[e_3c_2-\left(e_2-1\right)c_3+ne_3\left(\frac{1}{\sin^2\phi}+n\cot^2\phi\right)\right]\mathrm{Re}\left(Q_{\mu_2}^n\right)\\&+\frac{1}{R^2}\left[\left(e_2-1\right)c_2+e_3c_3+n\left(e_2-1\right)\left(\frac{1}{\sin^2\phi}+n\cot^2\phi\right)\right]\mathrm{Im}\left(Q_{\mu_2}^n\right)\\&+\frac{1}{R^2}\left[e_3c_2-\left(e_2-1\right)c_3\right]\cot\phi\,\mathrm{Re}\left(Q_{\mu_2}^{n-1}\right)-\frac{1}{R^2}\left[\left(e_2-1\right)c_2+e_3c_3\right]\cot\phi\,\mathrm{Im}\left(Q_{\mu_2}^{n-1}\right)\end{aligned}$$

$$Q(4,8)=\frac{n^2}{2R^2}\left(n+1\right)\frac{1}{\sin\phi}\cot\phi Q_1^n-\frac{n^2}{2R^2}(n-2)(n+1)\frac{1}{\sin\phi}Q_1^{n-1}$$

$$Q(5,1)=\frac{n}{R^2}(1-e_1)\left(\cot^2\phi+n\frac{1}{\sin^2\phi}\right)P_{\mu_1}^n+\frac{(e_1-1)}{R^2}c_1\cot\phi P_{\mu_1}^{n-1}$$

$$Q(5,2)=\frac{n}{R^2}(1-e_2)\left(\cot^2\phi+n\frac{1}{\sin^2\phi}\right)\mathrm{Re}\left(P_{\mu_2}^n\right)-\frac{ne_3}{R^2}\left(\cot^2\phi+n\frac{1}{\sin^2\phi}\right)\mathrm{Im}\left(P_{\mu_2}^n\right)$$
$$+\frac{1}{R^2}\left[(e_2-1)c_2+e_3c_3\right]\cot\phi\,\mathrm{Re}\left(P_{\mu_2}^{n-1}\right)+\frac{1}{R^2}\left[e_3c_2-(e_2-1)c_3\right]\cot\phi\,\mathrm{Im}\left(P_{\mu_2}^{n-1}\right)$$

$$Q(5,3)=\frac{ne_3}{R^2}\left(\cot^2\phi+n\frac{1}{\sin^2\phi}\right)\mathrm{Re}\left(P_{\mu_2}^n\right)+\frac{n}{R^2}(1-e_2)\left(\cot^2\phi+n\frac{1}{\sin^2\phi}\right)\mathrm{Im}\left(P_{\mu_2}^n\right)$$
$$-\frac{1}{R^2}\left[e_3c_2-(e_2-1)c_3\right]\cot\phi\,\mathrm{Re}\left(P_{\mu_2}^{n-1}\right)+\frac{1}{R^2}\left[(e_2-1)c_2+e_3c_3\right]\cot\phi\,\mathrm{Im}\left(P_{\mu_2}^{n-1}\right)$$

$$Q(5,4)=-\frac{n}{2R^2}(n+1)\frac{1}{\sin\phi}\cot\phi P_1^n+\frac{n}{2R^2}(n-2)(n+1)\frac{1}{\sin\phi}P_1^{n-1}$$

$$Q(5,5)=\frac{n}{R^2}(1-e_1)\left(\cot^2\phi+n\frac{1}{\sin^2\phi}\right)Q_{\mu_1}^n+\frac{(e_1-1)}{R^2}c_1\cot\phi Q_{\mu_1}^{n-1}$$

$$Q(5,6)=\frac{n}{R^2}(1-e_2)\left(\cot^2\phi+n\frac{1}{\sin^2\phi}\right)\mathrm{Re}\left(Q_{\mu_2}^n\right)-\frac{ne_3}{R^2}\left(\cot^2\phi+n\frac{1}{\sin^2\phi}\right)\mathrm{Im}\left(Q_{\mu_2}^n\right)$$
$$+\frac{1}{R^2}\left[(e_2-1)c_2+e_3c_3\right]\cot\phi\,\mathrm{Re}\left(Q_{\mu_2}^{n-1}\right)+\frac{1}{R^2}\left[e_3c_2-(e_2-1)c_3\right]\cot\phi\,\mathrm{Im}\left(Q_{\mu_2}^{n-1}\right)$$

$$Q(5,7)=\frac{ne_3}{R^2}\left(\cot^2\phi+n\frac{1}{\sin^2\phi}\right)\mathrm{Re}\left(Q_{\mu_2}^n\right)+\frac{n}{R^2}(1-e_2)\left(\cot^2\phi+n\frac{1}{\sin^2\phi}\right)\mathrm{Im}\left(Q_{\mu_2}^n\right)$$
$$-\frac{1}{R^2}\left[e_3c_2-(e_2-1)c_3\right]\cot\phi\,\mathrm{Re}\left(Q_{\mu_2}^{n-1}\right)+\frac{1}{R^2}\left[(e_2-1)c_2+e_3c_3\right]\cot\phi\,\mathrm{Im}\left(Q_{\mu_2}^{n-1}\right)$$

$$Q(5,8)=-\frac{n}{2R^2}(n+1)\frac{1}{\sin\phi}\cot\phi Q_1^n+\frac{n}{2R^2}(n-2)(n+1)\frac{1}{\sin\phi}Q_1^{n-1}$$

$$Q(6,1)=\frac{2n}{R^2}(n+1)(e_1-1)\frac{1}{\sin\phi}\cot\phi P_{\mu_1}^n+\frac{2n}{R^2}(1-e_1)c_1\frac{1}{\sin\phi}P_{\mu_1}^{n-1}$$

$$Q(6,2)=\frac{2n(n+1)}{R^2}(e_2-1)\frac{1}{\sin\phi}\cot\phi\,\mathrm{Re}\left(P_{\mu_2}^n\right)+\frac{2n(n+1)}{R^2}e_3\frac{1}{\sin\phi}\cot\phi\,\mathrm{Im}\left(P_{\mu_2}^n\right)$$
$$-\frac{2n}{R^2}\left[(e_2-1)c_2+e_3c_3\right]\frac{1}{\sin\phi}\mathrm{Re}\left(P_{\mu_2}^{n-1}\right)-\frac{2n}{R^2}\left[e_3c_2-(e_2-1)c_3\right]\frac{1}{\sin\phi}\mathrm{Im}\left(P_{\mu_2}^{n-1}\right)$$

$$Q(6,3)=-\frac{2n(n+1)}{R^2}e_3\frac{1}{\sin\phi}\cot\phi\,\mathrm{Re}\left(P_{\mu_2}^n\right)+\frac{2n(n+1)}{R^2}(e_2-1)\frac{1}{\sin\phi}\cot\phi\,\mathrm{Im}\left(P_{\mu_2}^n\right)$$
$$+\frac{2n}{R^2}\left[e_3c_2-(e_2-1)c_3\right]\frac{1}{\sin\phi}\mathrm{Re}\left(P_{\mu_2}^{n-1}\right)-\frac{2n}{R^2}\left[(e_2-1)c_2+e_3c_3\right]\frac{1}{\sin\phi}\mathrm{Im}\left(P_{\mu_2}^{n-1}\right)$$

$$Q(6,4)=\frac{n}{2R^2}(n+1)\left[(n-2)+n\left(\frac{1}{\sin^2\phi}+\cot^2\phi\right)\right]P_1^n-\frac{n}{R^2}(n-2)(n+1)\cot\phi P_1^{n-1}$$

$$Q(6,5)=\frac{2n}{R^2}(n+1)(e_1-1)\frac{1}{\sin\phi}\cot\phi Q_{\mu_1}^n+\frac{2n}{R^2}(1-e_1)c_1\frac{1}{\sin\phi}Q_{\mu_1}^{n-1}$$

$$Q(6,6)=\frac{2n(n+1)}{R^2}(e_2-1)\frac{1}{\sin\phi}\cot\phi\,\mathrm{Re}\left(Q_{\mu_2}^n\right)+\frac{2n(n+1)}{R^2}e_3\frac{1}{\sin\phi}\cot\phi\,\mathrm{Im}\left(Q_{\mu_2}^n\right)$$
$$-\frac{2n}{R^2}\left[(e_2-1)c_2+e_3c_3\right]\frac{1}{\sin\phi}\mathrm{Re}\left(Q_{\mu_2}^{n-1}\right)-\frac{2n}{R^2}\left[e_3c_2-(e_2-1)c_3\right]\frac{1}{\sin\phi}\mathrm{Im}\left(Q_{\mu_2}^{n-1}\right)$$

$$Q(6,7)=-\frac{2n(n+1)}{R^2}e_3\frac{1}{\sin\phi}\cot\phi\,\mathrm{Re}\left(Q_{\mu_2}^n\right)+\frac{2n(n+1)}{R^2}(e_2-1)\frac{1}{\sin\phi}\cot\phi\,\mathrm{Im}\left(Q_{\mu_2}^n\right)$$
$$+\frac{2n}{R^2}\left[e_3c_2-(e_2-1)c_3\right]\frac{1}{\sin\phi}\mathrm{Re}\left(Q_{\mu_2}^{n-1}\right)-\frac{2n}{R^2}\left[(e_2-1)c_2+e_3c_3\right]\frac{1}{\sin\phi}\mathrm{Im}\left(Q_{\mu_2}^{n-1}\right)$$

$$Q(6,8)=\frac{n}{2R^2}(n+1)\left[(n-2)+n\left(\frac{1}{\sin^2\phi}+\cot^2\phi\right)\right]Q_1^n-\frac{n}{R^2}(n-2)(n+1)\cot\phi Q_1^{n-1}$$

In deriving the above relation we used the recursive relations:

$$\frac{d^2P_\mu^n}{d\phi^2}=\left[(n-\mu-1)(n+\mu)+n\left(\frac{1}{\sin^2\phi}+n\cot^2\phi\right)\right]P_\mu^n-\cot\phi(n-\mu-1)(n+\mu)P_\mu^{n-1}$$

$$\frac{d^2Q_\mu^n}{d\phi^2}=\left[(n-\mu-1)(n+\mu)+n\left(\frac{1}{\sin^2\phi}+n\cot^2\phi\right)\right]Q_\mu^n-\cot\phi(n-\mu-1)(n+\mu)Q_\mu^{n-1}$$

References

[1] Bismarck-Nasr M.N., Finite elements in aeroelasticity of plates and shells, Applied Mechanics Reviews Journal 49 (1996)17–24.

[2] Dowell E.H., *Aeroelasticity of Plates and Shells*, Noordhoff International Publishing, Leyden, 1975.

[3] Ashley H., Zartarian G., Piston theory –new aerodynamic tool for aeroelastician, Journal of the Aeronautical Sciences 23 (1956)1109–1118.

[4] Olson M.D., Fung Y.C., Supersonic flutter of circular cylindrical shells subjected to internal pressure and axial compression, AIAA Journal 5 (1966) 858-864.

[5] Olson M.D., Fung Y.C., Comparing theory and experiment for supersonic flutter of circular cylindrical shells, AIAA Journal 5 (1967) 1849-1856.

[6] Evensen D.A., Olson M.D., Nonlinear flutter of a circular cylindrical shell in supersonic flow, NASA TN D-4265 (1967).

[7] Evensen D.A., Olson M.D., Circumferentially traveling wave flutter of circular cylindrical shell, AIAA Journal 6 (1968) 1522-1527.

[8] Dowell E.H., Flutter of infinitely long plates and shells. Part II, AIAA Journal 4 (1966) 1510-1518.

[9] Carter L.L., Stearman R.O., Some aspects of cylindrical panel flutter, AIAA Journal 6 (1968) 37-43.

[10] Amabili M., Pellicano F., Nonlinear supersonic flutter of circular cylindrical shells, AIAA Journal 39 (2001) 564-573.

[11] Bismarck-Nasr M.N., Finite element method applied to the supersonic flutter of circular cylindrical shells, International Journal for Numerical Methods in Engineering 10(1976) 423-435

[12] Ganapathi M., Varadan T.K., Jijen J., Field consistent element applied to flutter analysis of circular cylindrical shells, Journal of Sound and Vibration, 171(1994) 509-527.

[13] ShulmanY., Vibration and flutter of cylindrical and conical shells, MIT ASRL Rept.74—2 OSR Tech.Rept . 59-776(1959).

[14] Ueda T., Kobayashi S., Kihira M., Supersonic flutter of truncated conical shells, Transactions of the Japan Society for Aeronautical and Space Sciences, 20(1977) 13-30.

[15] Dixon S.C., Hudson M.L., Flutter, vibration and buckling of truncated orthotropic conical shells with generalized elastic edge restraint, NASA TN D-5759 (1970).

[16] Miserento R., Dixon S.C., Vibration and flutter tests of a pressurized thin walled truncated conical shell, NASA TN D-6106(1971).

[17] Bismarck-Nasr M.N, Costa Savio H.R., Finite element solution of the supersonic flutter of conical shells, AIAA Journal 17 (1979) 1148-1150.

[18] Sunder P.J., Ramakrishnan V.C., Sengupta S., Finite element analysis of 3-ply laminated conical shell for flutter, International Journal for Numerical Methods in Engineering 19(1983) 1183-1192.

[19] Sunder P.J., Ramakrishnan V.C., Sengupta S., Optimum cone angles in aeroelastic flutter, Computer and Structures 17(1983) 25-29.

[20] Mason D.R, Blotter P.T., Finite element application to rocket nozzle aeroelasticity, Journal of Propulsion and Power 2(1986) 499-507.

[21] Pidaparti R.M.V., Yang Henry T.Y., Supersonic flutter analysis of composite plates and shells, AIAA Journal 31(1993) 1109-1117.

CONCLUSION ET RECOMMANDATIONS

Le but principal de l'analyse présentée dans cette thèse est de déterminer les fréquences naturelles et les formes modales des coques sphériques. L'analyse modale est basée sur une approche hybride combinant la méthode des éléments finis classique et la théorie classique des coques. Cette approche théorique est plus précise que la méthode des éléments finis classique, car les déplacements sont déduits de la solution des équations d'équilibre des coques sphériques. Les matrices masse et rigidité sont déterminées par intégration numérique. Les résultats obtenus pour les coques sphériques avec différentes géométries et différentes conditions aux limites sont comparés aux résultats disponibles dans la littérature. Une très bonne concordance a été trouvée. Cette approche a donné lieu à un élément plus précis qui conduit à une convergence rapide et de moindres difficultés numériques. Du fait qu'elle utilise la théorie classique des coques, cette méthode est mieux adaptée pour tenir compte des effets de l'interaction fluide- structure.

Le problème des vibrations libres des coques sphériques partiellement remplies de fluide a été analysé dans cette thèse. Différents paramètres tels que la géométrie, le taux de remplissage, les conditions aux limites et le rapport rayon-épaisseur ont été pris en considération. Une méthode des éléments finis hybride efficace a été présentée pour analyser le comportement dynamique des coques sphériques remplies de fluide. Les équations des coques sphériques ont été couplées à l'équation de Laplace pour un fluide parfait pour tenir compte de la pression hydrodynamique d'un fluide interne. Cette approche théorique est plus précise que la méthode des éléments finis classique car les fonctions de déplacements sont fournies par la solution exacte des équations d'équilibre des coques sphériques. Les matrices masse, de rigidité et d'amortissement sont déterminées par intégration numérique. Le potentiel de vitesse et l'équation de Bernoulli ont été adoptés pour exprimer la pression du fluide agissant sur la structure, ce qui conduit à trois types de forces : inertielle, centrifuge et de Coriolis, dans le cas d'un écoulement de fluide. Les résultats obtenus pour différents paramètres ont été comparés aux résultats disponibles dans la littérature. Une très bonne concordance a été trouvée. Cette approche résulte en un élément précis qui conduit à une convergence rapide et à moindres difficultés numériques d'un point de vue effort de calcul. La méthode des éléments finis hybride fournit la capacité d'analyser des cas impliquant des conditions aux limites et des chargements complexes pour des coques sphériques.

Une méthode des éléments finis hybride est présentée dans cette thèse pour étudier la stabilité aéroélastique des coques sphériques à vide et soumises à un écoulement externe supersonique. La théorie linéaire des coques sphériques a été couplée avec la théorie du piston du premier ordre. L'effet de la correction de la courbure dans la théorie du piston a été pris en compte. L'analyse a été faite pour des coques avec différentes géométries, différents rapports rayon-épaisseur et différentes conditions aux limites. Dans tous les cas où une instabilité a été trouvée, un flottement est établit par la coalescence des 1^{er} et 2^{e} modes. L'augmentation du rapport rayon-épaisseur de la coque conduit au fait que l'établissement du flottement se produit à des pressions dynamiques de plus en plus grandes. Par contre, le flottement se produit à des basses pressions dynamiques lors de la diminution de l'angle d'ouverture de la coque sphérique. La méthode des éléments finis hybride présentée dans cette thèse peut donner des résultats fiables avec un moindre effort de calcul comparé aux logiciels commerciaux car ces derniers imposent une certaine restriction lorsqu'une telle analyse est accomplie.

Finalement un logiciel basé sur une formulation modale d'éléments finis a été développé. Il est capable de faire l'analyse linéaire d'une coque sphérique à vide ou partiellement remplie de fluide ainsi que l'effet d'un écoulement d'air supersonique sur le flottement de la coque sphérique. Une telle formulation modale est destinée à être un outil de conception pratique pour les coques sphériques, afin de réduire le temps de calcul sans perdre la précision souhaitée dans la méthode des éléments finis.

BIBLIOGRAPHIE

[1] Kalnins A., Free non-symmetric vibrations of shallow spherical shells, Journal of the Acoustical Society of America, 33 (1961) 1102-1107.

[2] Kalnins A., Effect of bending on vibration of spherical shell, Journal of the Acoustical Society of America 36 (1964) 74-81.

[3] Cohen G.A., Computer analysis of asymmetric free vibrations of ring stiffened orthotropic shells of revolution, AIAA Journal 3 (1965) 2305-2312.

[4] Navaratna D. R., Natural Vibration of Deep Spherical Shells, AIAA Journal 4 (1966) 2056-2058.

[5] Webster J.J., Free vibrations of shells of revolution using ring finite elements, International Journal of Mechanical Sciences 9(1967) 559-570.

[6] Kraus H., *Thin elastic shells,* John Wiley and Sons, New York, 1967.

[7] Greene B.E., Jones R.E., Mc Lay R.W. and Strome D.R., Dynamic analysis of shells using doubly curved finite elements, Proceedings of The Second Conference on Matrix methods in Structural Mechanics, TR-68-150(1968) 185-212

[8] Tessler A., Spirichigliozzi L., Resolving membrane and shear locking phenomena in curved deformable axisymmetric shell element, International Journal for Numerical Methods in Engineering, 26(1988) 1071-1080.

[9] Narasimhan M.C., Alwar R.S., Free vibration analysis of laminated orthotropic spherical shell, Journal of Sound and Vibration, 54(1992) 515-529.

[10] Gautham B. P., Ganesan N., Free vibration analysis of thick spherical shells, Computers and Structures Journal, 45(1992) 307-313.

[11] Gautham B. P., Ganesan N., Free vibration characteristics of isotropic and laminated orthotropic shell caps, Journal of Sound and Vibration, 204(1997) 17-40.

[12] Sai Ram K.S., Sreedhar Babu T., Free vibration of composite spherical shell cap with and without a cutout, Computers and Structures Journal, 80(2002) 1749-1756.

[13] Buchanan G.R., Rich B.S., Effect of boundary conditions on free vibrations of thick isotropic spherical shells, Journal of Vibration and Control 8(2002) 389-403.

[14] Ventsel E.S, Naumenko V., Strelnikova E., Yeseleva E., Free vibrations of shells of revolution filled with fluid, Journal of Engineering Analysis with Boundary Elements 34(2010) 856-862.

[15] Rayleigh L., On the vibrations of a gas contained within a rigid spherical envelope, Proceedings of London Math Society 4 (1872) 93-103.

[16] Morse, P.M., Feshbach, H, *Methods of Theoretical Physics Part II*, McGraw-Hill, New York (1953)

[17] Budiansky, B Sloshing of liquids in circular canals an spherical tanks, Journal of Aerospace Sciences 27(1960) 161-173

[18] Stofan, A.J., Armstead A.L, Analytical and experimental investigation of forces and frequencies resulting from liquid sloshing in a spherical tank, NASA TN D-128 (1962).

[19] Chu W. H., Fuel sloshing in a spherical tank filled to an arbitrarily depth, AIAA Journal 2 (1964) 1972-1979.

[20] Karamanos S.P., Patkas L.A., Papaprokopiou D., Numerical analysis of externally induced sloshing in spherical liquid containers, Computational Methods in Applied Sciences 21(2011) 489-512

[21] Rand R., Dimaggio F., Vibrations of fluid–filled spherical and spheroidal shells, Journal of the Acoustical Society of America 42(1967) 1278-1286.

[22] Engin A.E., Liu Y.K., Axisymmetric response of a fluid filled spherical shell in free vibrations. Journal of Biomechanics 3 (1970) 11-22

[23] Advani S.H., Lee Y.C., Free vibrations of fluid filled spherical shells, Journal of Sound and Vibration, 12 (1970) 453-462.

[24] Kana D.D., Nagy A., An experimental Study of axisymmetric modes in various propellant tanks containing liquid N72-14782 (1971)

[25] Guarino J. C., Elger D.F., Modal Analysis of fluid filled elastic shell containing an elastic sphere, Journal of Sound and Vibration, 156(1992) 461-479.

[26] Bai M.R., Wu K., Free vibration of thin spherical shell containing a compressible fluid , Journal of the Acoustical Society of America 95(1994) 3300-3310.

[27] Chen W.Q., Ding H.J., Natural frequencies of a fluid filled anisotropic spherical shell, Journal of the Acoustical Society of America 105(1999) 174-182.

[28] Young P.G., A parametric study on the axisymmetric modes of vibrations of multi layered spherical shells with liquid cores of relevance to head impact modelling , Journal of Sound and Vibration, 256 (2002) 665-680

[29] Samoilov Y.A., Pavolv B.S., The vibrations of a hemispherical shell filled with liquid Journal Izvestiya Vuzov Avias Tekh 3(1964) 79-86

[30] Hwang C., Longitudinal sloshing of a liquid in flexible hemispherical tank, Journal of Applied Mechanics 32(1965) 665-670.

[31] Chung T.J., Rush R.H., Dynamically coupled motion of surface fluid shell system, Journal of Applied Mechanics 43(1976) 507-508.

[32] Komatsu K., Vibration analysis of spherical shells partially filled with a liquid using an added mass coefficient, Transactions of the Japan Society for Aeronautical and Space Sciences 22(1979) 70-79

[33] Komatsu K., Matsuhima M., Some experiments on the vibrations of hemispherical shells partially filled with a liquid, Journal of Sound and Vibration 64(1979) 35-44

[34] Ventsel E.S, Naumenko V., Strelnikova E., Yeseleva E., Free vibrations of shells of revolution filled with fluid, Journal of Engineering Analysis with Boundary Elements 34(2010) 856-862.

[35] Menaa M, Lakis A.A., Hybrid finite element method applied to the analysis of free vibration of a spherical shell. EPM-RT-2013-02.

[36] Bismarck-Nasr M.N., Finite elements in aeroelasticity of plates and shells, Applied Mechanics Reviews Journal 49 (1996)17–24.

[37] Dowell E.H., *Aeroelasticity of Plates and Shells*, Noordhoff International Publishing, Leyden, 1975.

[38] Ashley H., Zartarian G., Piston theory –new aerodynamic tool for aeroelastician, Journal of the Aeronautical Sciences 23 (1956)1109–1118.

[39] Olson M.D., Fung Y.C., Supersonic flutter of circular cylindrical shells subjected to internal pressure and axial compression, AIAA Journal 5 (1966) 858-864.

[40] Olson M.D., Fung Y.C., Comparing theory and experiment for supersonic flutter of circular cylindrical shells, AIAA Journal 5 (1967) 1849-1856.

[41] Evensen D.A., Olson M.D., Nonlinear flutter of a circular cylindrical shell in supersonic flow, NASA TN D-4265 (1967).

[42] Evensen D.A., Olson M.D., Circumferentially traveling wave flutter of circular cylindrical shell, AIAA Journal 6 (1968) 1522-1527.

[43] Dowell E.H., Flutter of infinitely long plates and shells. Part II, AIAA Journal 4 (1966) 1510-1518.

[44] Carter L.L., Stearman R.O., Some aspects of cylindrical panel flutter, AIAA Journal 6 (1968) 37-43.

[45] Amabili M., Pellicano F., Nonlinear supersonic flutter of circular cylindrical shells, AIAA Journal 39 (2001) 564-573.

[46] Bismarck-Nasr M.N., Finite element method applied to the supersonic flutter of circular cylindrical shells, International Journal for Numerical Methods in Engineering 10(1976) 423-435

[47] Ganapathi M., Varadan T.K., Jijen J., Field consistent element applied to flutter analysis of circular cylindrical shells, Journal of Sound and Vibration, 171(1994) 509-527.

[48] ShulmanY., Vibration and flutter of cylindrical and conical shells, MIT ASRL Rept.74—2 OSR Tech.Rept. 59-776(1959).

[49] Ueda T., Kobayashi S., Kihira M., Supersonic flutter of truncated conical shells, Transactions of the Japan Society for Aeronautical and Space Sciences, 20(1977) 13-30.

[50] Dixon S.C., Hudson M.L., Flutter, vibration and buckling of truncated orthotropic conical shells with generalized elastic edge restraint, NASA TN D-5759 (1970).

[51] Miserento R., Dixon S.C., Vibration and flutter tests of a pressurized thin walled truncated conical shell, NASA TN D-6106(1971).

[52] Bismarck-Nasr M.N, Costa Savio H.R., Finite element solution of the supersonic flutter of conical shells, AIAA Journal 17 (1979) 1148-1150.

[53] Sunder P.J., Ramakrishnan V.C., Sengupta S., Finite element analysis of 3-ply laminated conical shell for flutter, International Journal for Numerical Methods in Engineering 19(1983) 1183-1192.

[54] Sunder P.J., Ramakrishnan V.C., Sengupta S., Optimum cone angles in aeroelastic flutter, Computer and Structures 17(1983) 25-29.

[55] Mason D.R, Blotter P.T., Finite element application to rocket nozzle aeroelasticity, Journal of Propulsion and Power 2(1986) 499-507.

[56] Pidaparti R.M.V., Yang Henry T.Y., Supersonic flutter analysis of composite plates and shells, AIAA Journal 31(1994) 1109-1117.